SAR POLARIMETRY And APPLICATIONS

Eric Pottier

IETR – UMR CNRS 6164 - University of Rennes 1
Image and Remote Sensing Dept. – SAPHIR Team
(SAR Polarimetry Holography Interferometry Radargrammetry)

esa POLinSAR 2005

ESA – ESRIN Frascati, 17 – 21 January 2005

© E. Pottier, L. Ferro-Famil (01/2005)

POLARIMETRIC REMOTE SENSING

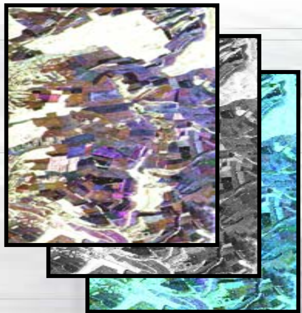

POLARIMETRIC
SAR DATA SET(S)

POLSAR - POLINSAR DATA PROCESSING

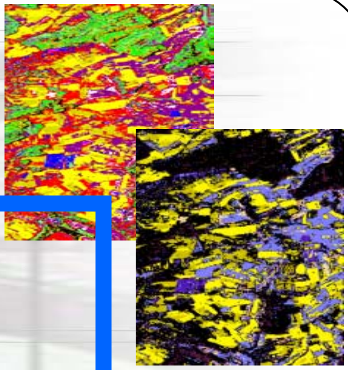

QUALITATIVE ANALYSIS

POLARIMETRIC DESCRIPTORS EXTRACTION

TWO-STEP INVERSION PROCEDURE

MODEL-BASED PHYSICAL PARAMETER INVERSION

BIO and GEO PHYSICAL
PARAMETERS

QUANTITATIVE ANALYSIS

© E. Pottier, L. Ferro-Famil (01/2005)

QUALITATIVE ANALYSIS

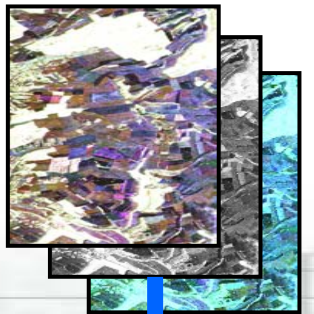

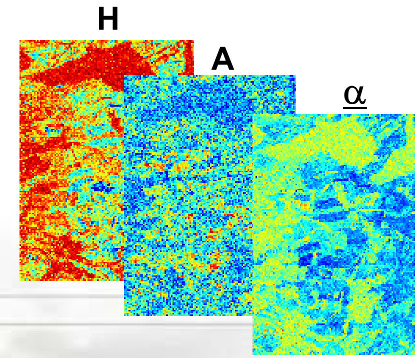

SPECKLE FILTERING

POLARIMETRIC TARGET DECOMPOSITION

WISHART POLARIMETRIC SEGMENTATION
MONO/DUAL FREQUENCY INTERFEROMETRY

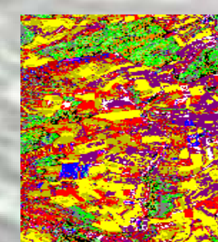

CLUSTER POLARIMETRIC IDENTIFICATION

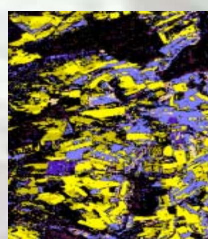

POLARIMETRIC DESCRIPTORS EXTRACTION

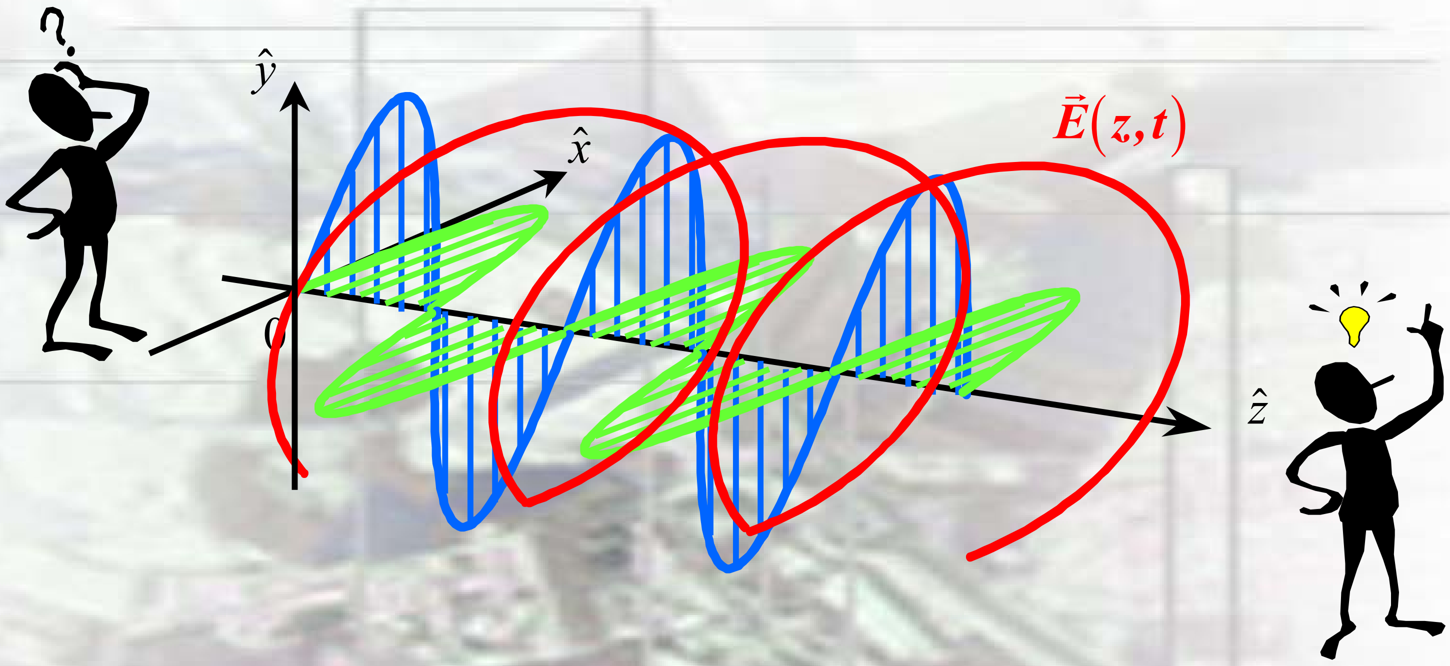

BASIC THEORY

SCATTERING POLARIMETRY

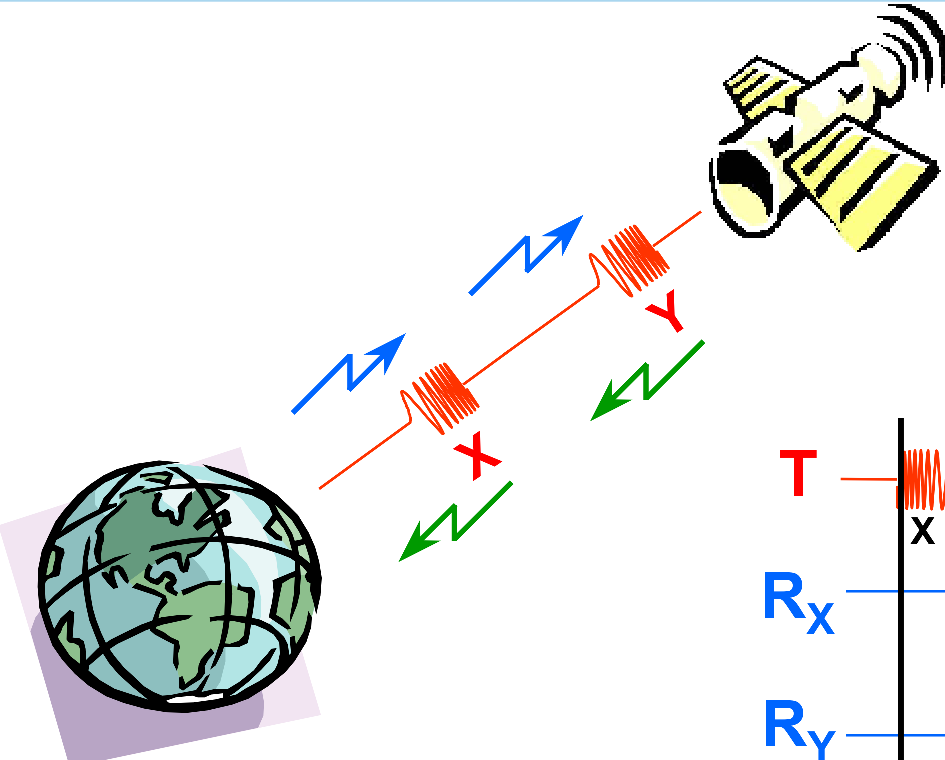

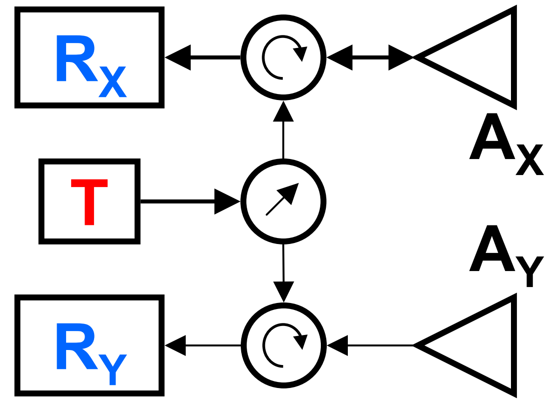

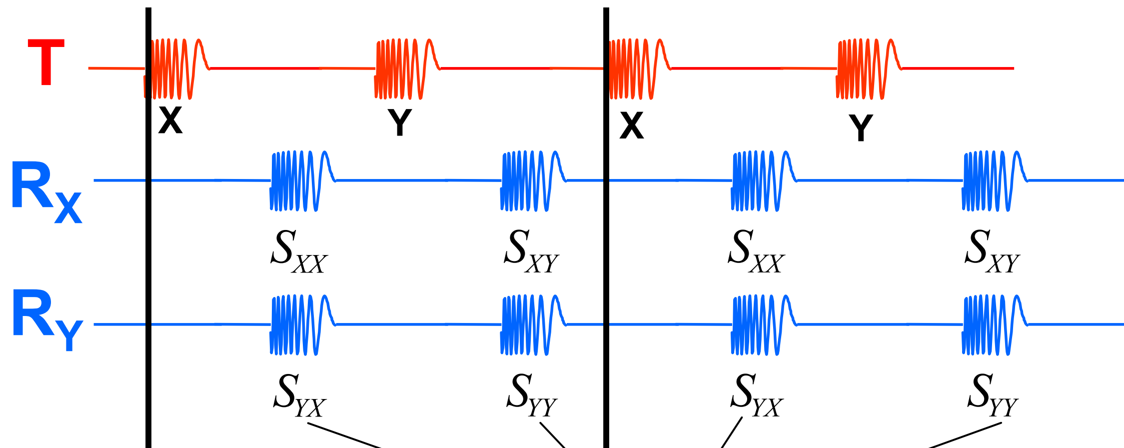

TRANSMITTER: X & Y

RECEIVERS: X & Y

SINCLAIR MATRICES

$$\left\{ [S] = \begin{bmatrix} S_{XX} & S_{XY} \\ S_{YX} & S_{YY} \end{bmatrix} \right\}$$

SCATTERING POLARIMETRY

POLARIMETRIC AIRBORNE SAR SENSORS

AES1
InterMap Technologies (D)
GulfStream Commander
X-Band (HH), P-Band (Quad)

AIRSAR
NASA / JPL (USA)
DC8
P, L, C-Band (Quad)

AuSAR - INGARA
D.S.T.O (Aus)
DC3 (97) KingAir 350 (00) Beach 1900C
X-Band (Quad)

DOSAR
EADS / Dornier GmbH (D)
DO 228 (89), C160 (98), G222 (00)
S, C, X-Band (Quad), Ka-Band (VV)

ESAR
DLR (D)
DO 228
P, L, S-Band (Quad)
C, X-Band (Sngl)

EMISAR
DCRS (DK)
G3 Aircraft
L, C-Band (Quad)

MEMPHIS / AER II-PAMIR
FGAN (D)
Transal C160
Ka, W-Band (Quad) / X-Band (Quad)

STORM
UVSQ / CETP (F)
Merlin IV
C-Band (Quad)

PHARUS
TNO - FEL (NL)
CESSNA – Citation II
C-Band (Quad)

PISAR
NASDA / CRL (J)
GulfStream
L, X-Band (Quad)

RAMSES
ONERA (F)
Transal C160
P, L, S, C, X, Ku, Ka, W-Band (Quad)

SAR580
Environnement Canada (CA)
Convair CV-580
C, X-Band (Quad)

+ CASSAR (China), MIT/Lincoln Lab (USA), P3-SAR (NADC / ERIM -USA), Military Systems …

POLARIMETRIC SPACEBORNE SAR SENSORS

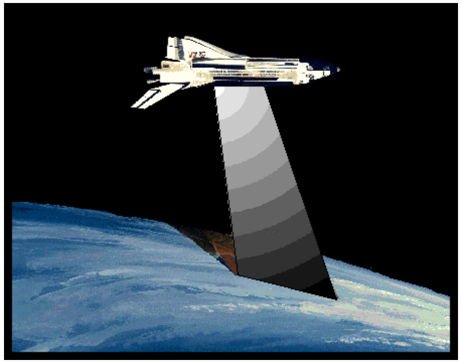

SIR-C
NASA / JPL (USA)
April 1994 (10 days)
October 1994 (10 days)
L, C-Band (Quad)

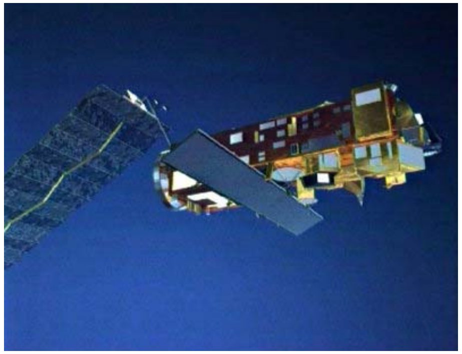

ENVISAT / ASAR
ESA (EU)
2002
C-Band (Sngl / Twin)
HH, VV, (HH,VV),
(HH,HV), (HV,VV)

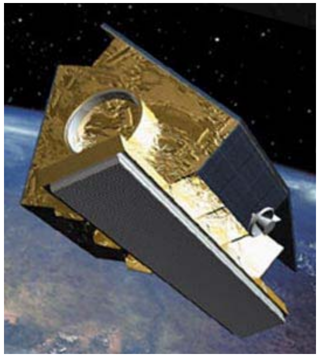

TERRASAR

X-Band (Twin)
(HH,VV), (HH,HV), (HV,VV)
L-Band (Quad)

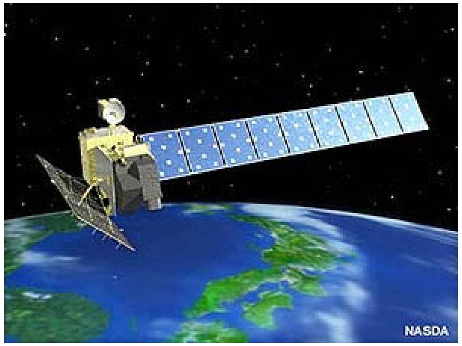

ALOS / PALSAR
JAXA (J)
L-Band
HH,VV, (HH,HV), (VV,VH)

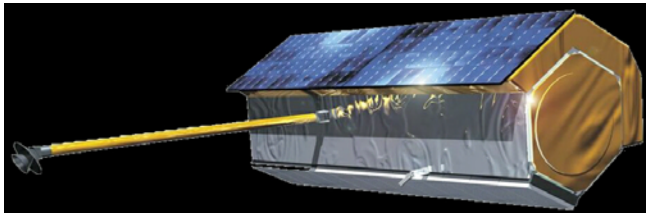

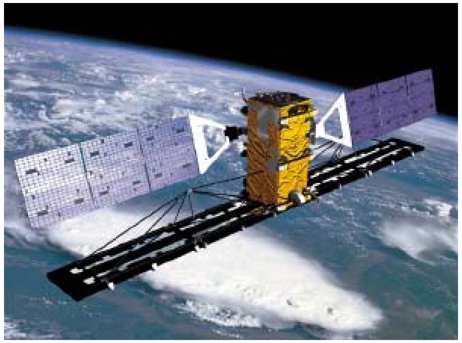

RADARSAT 2
CSA / MDA (CA)
C-Band (Quad)

POLARIMETRIC DESCRIPTORS

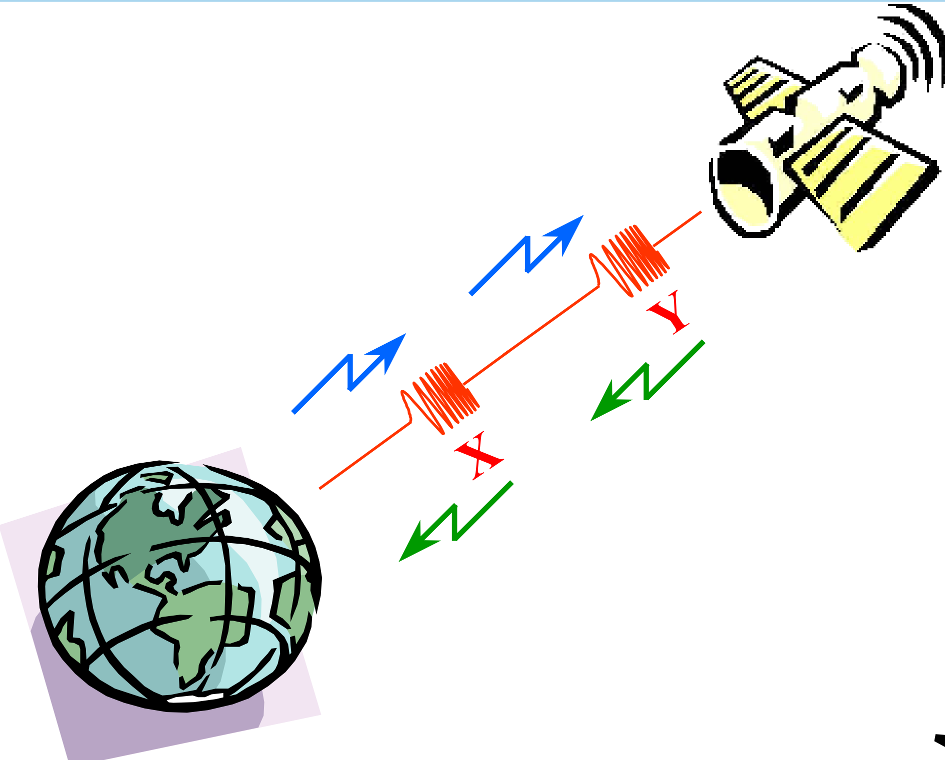

TRANSMITTER: X & Y
RECEIVERS: X & Y

THE DIFFERENT TARGET POLARIMETRIC DESCRIPTORS

[S]	SINCLAIR Matrix
$\underline{k}$, $\underline{\Omega}$	Target Vectors
[K]	KENNAUGH Matrix
[T]	Coherency Matrix
[C]	Covariance Matrix

© E. Pottier, L. Ferro-Famil (01/2005)

TARGET VECTORS

PAULI SCATTERING VECTOR

$$\underline{k} = V([S]) = \frac{1}{2}\mathit{Trace}([S][\psi_P])$$

SET OF 2x2 COMPLEX MATRICES
FROM THE PAULI MATRICES GROUP

$$[\psi_P] = \left\{\sqrt{2}\begin{bmatrix} 1 & 0 \\ 0 & 1 \end{bmatrix}, \sqrt{2}\begin{bmatrix} 1 & 0 \\ 0 & -1 \end{bmatrix}, \sqrt{2}\begin{bmatrix} 0 & 1 \\ 1 & 0 \end{bmatrix}, \sqrt{2}\begin{bmatrix} 0 & -j \\ j & 0 \end{bmatrix}\right\}$$

$$\Downarrow$$

$$\boxed{\underline{k} = \frac{1}{\sqrt{2}}\begin{bmatrix} S_{XX}+S_{YY} & S_{XX}-S_{YY} & S_{XY}+S_{YX} & j(S_{XY}-S_{YX}) \end{bmatrix}^T}$$

Advantage: Closer related to physical properties of the scatterer

Note: Also known as $\underline{k}_{4P}$

COHERENCY MATRIX

BISTATIC CASE

PAULI SCATTERING VECTOR $\underline{k}$

$$\underline{k} = \frac{1}{\sqrt{2}}\left[S_{XX} + S_{YY} \quad S_{XX} - S_{YY} \quad S_{XY} + S_{YX} \quad j\left(S_{XY} - S_{YX}\right)\right]^T$$

$$\Downarrow$$

COHERENCY MATRIX $[T]$

$$[T] = \underline{k} \cdot \underline{k}^{*T} = \begin{bmatrix} 2A_0 & C - jD & H + jG & L - jK \\ C + jD & B_0 + B & E + jF & M - jN \\ H - jG & E - jF & B_0 - B & J + jI \\ L + jK & M + jN & J - jI & 2A \end{bmatrix}$$

HERMITIAN POSITIVE SEMI DEFINITE MATRIX - RANK 1

© IETR SAPHIR E. Pottier, L. Ferro-Famil (01/2005)

MONOSTATIC CASE

PAULI SCATTERING VECTOR $\underline{k}$

$$\underline{k} = \frac{1}{\sqrt{2}}\left[S_{XX} + S_{YY} \quad S_{XX} - S_{YY} \quad 2S_{XY}\right]^T$$

$$\Downarrow$$

COHERENCY MATRIX $[T]$

$$[T] = \underline{k} \cdot \underline{k}^{*T} = \begin{bmatrix} 2A_0 & C - jD & H + jG \\ C + jD & B_0 + B & E + jF \\ H - jG & E - jF & B_0 - B \end{bmatrix}$$

HERMITIAN MATRIX - RANK 1

A0, B0+B, B0-B : HUYNEN TARGET GENERATORS

$[T]$ is closer related to Physical and Geometrical Properties of the Scattering Process, and thus allows a better and direct physical interpretation

PHYSICAL INTERPRETATION

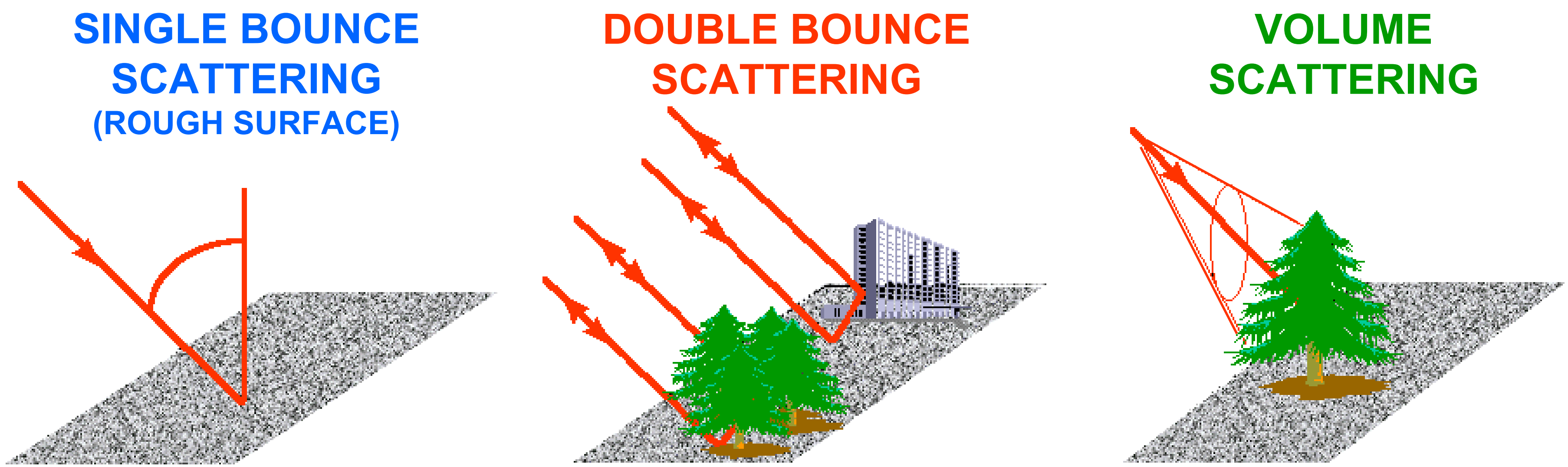

$$T_{11} = 2A_0 = \left|S_{XX} + S_{YY}\right|^2$$

$$T_{33} = B_0 - B = 2\left|S_{XY}\right|^2$$

$$T_{22} = B_0 + B = \left|S_{XX} - S_{YY}\right|^2$$

SAN FRANCISCO BAY

L-band 1988

AIRSAR JPL

DC8

P, L, C-Band (Quad)

TARGET GENERATORS

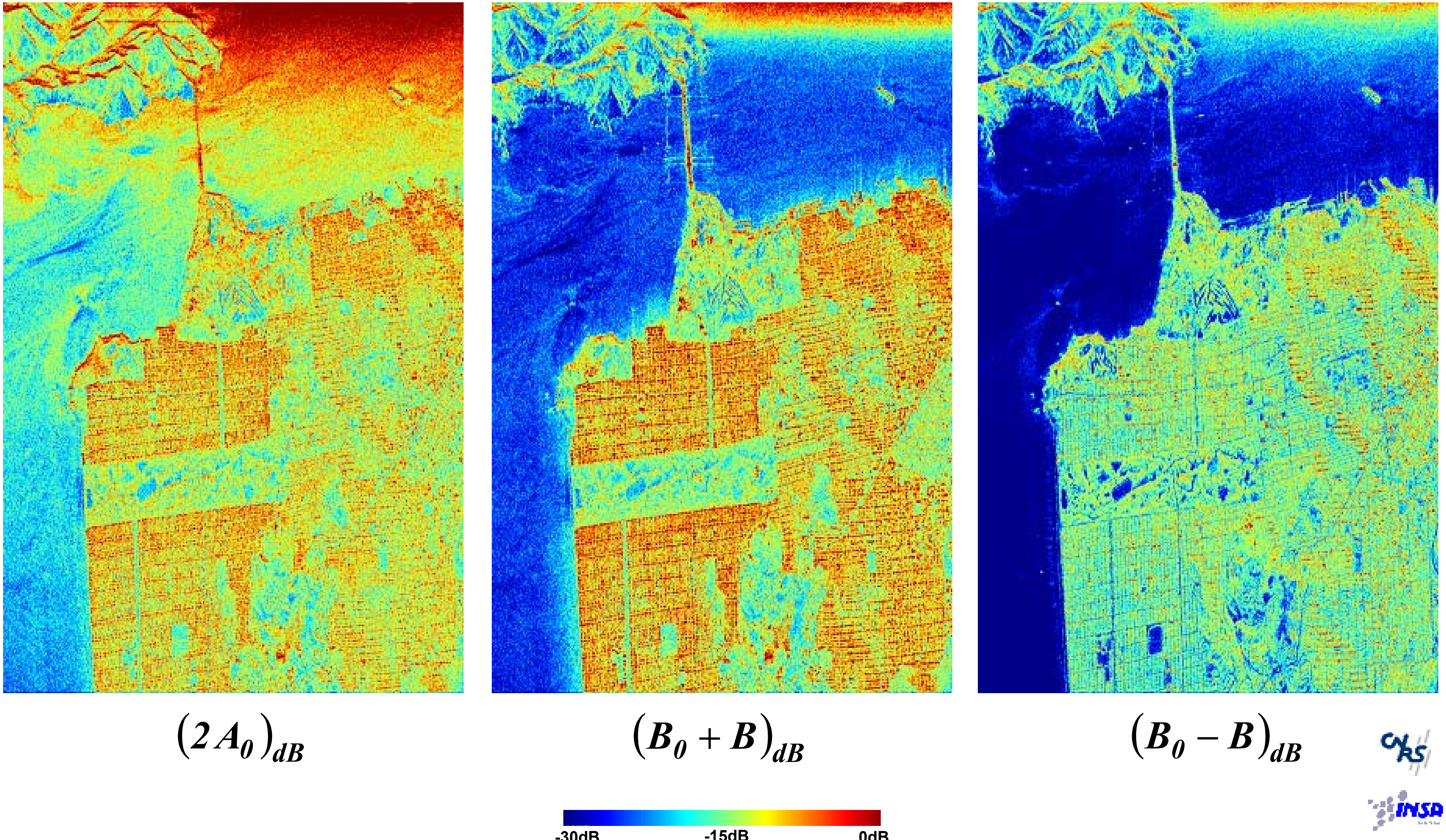

TARGET GENERATORS

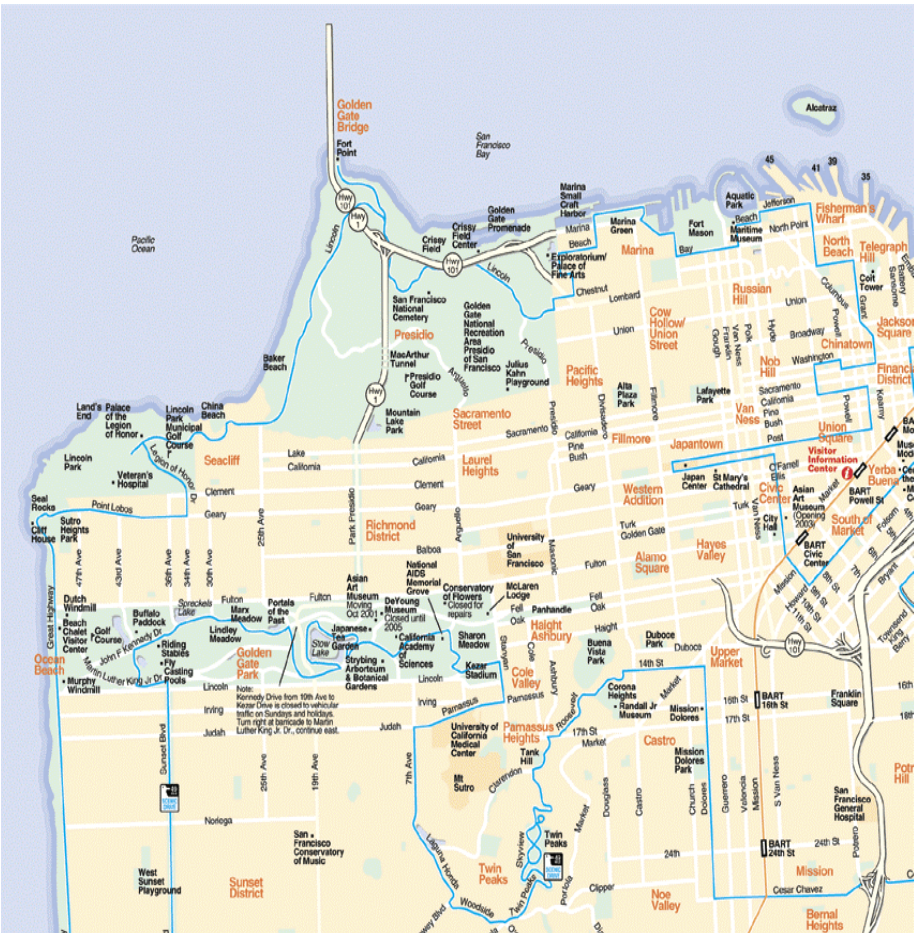

Pauli Color Coding

$|HH+VV|$ $T_{11}=2A_0$

$|HV|$ $T_{33}=B_0-B$

$|HH-VV|$ $T_{22}=B_0+B$

ELLIPTICAL BASIS TRANSFORMATION

Pauli Color Coding (H,V)

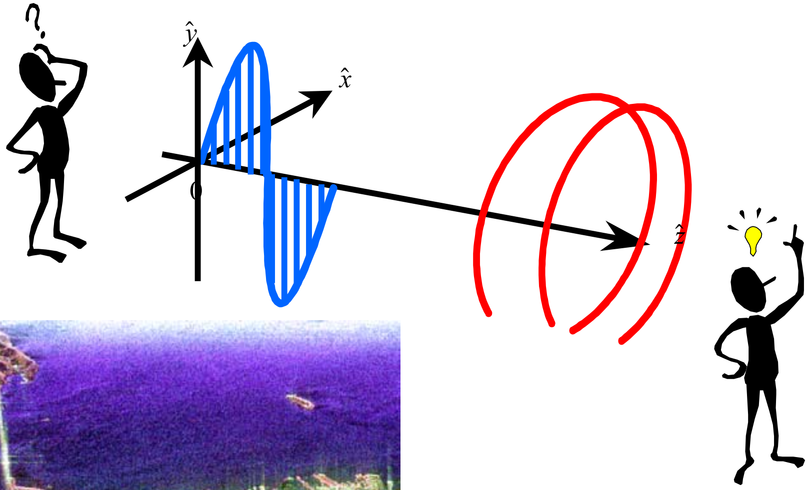

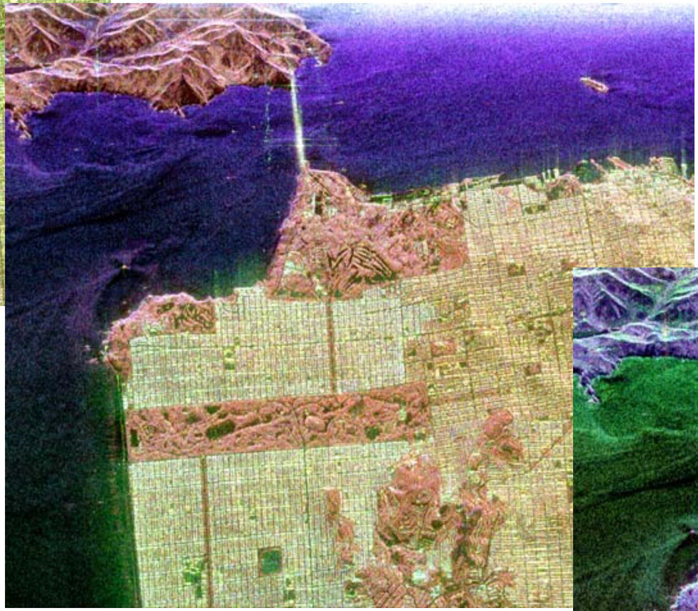

Pauli Color Coding (+45,-45)

Ernst LÜNEBURG
(PIERS95 - Pasadena)

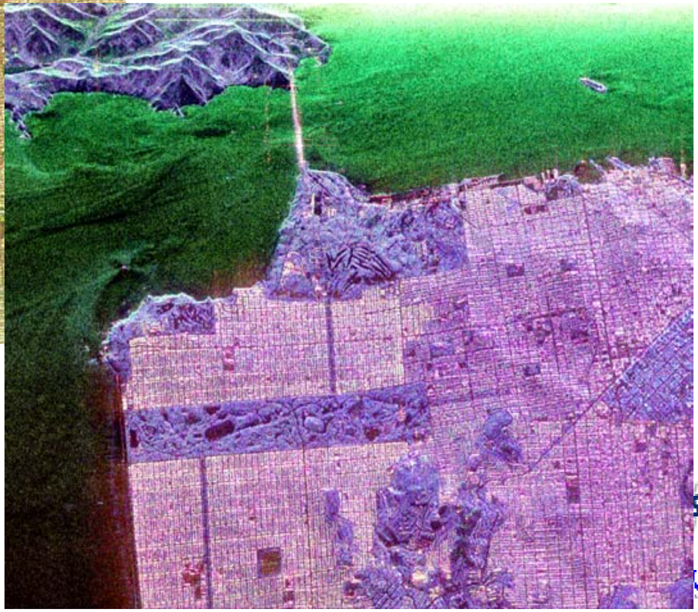

Pauli Color Coding (L,R)

© E. Pottier, L. Ferro-Famil (01/2005)

SAPHIR

SINCLAIR MATRIX

$$\underline{E}^{s}_{(A,A_\perp)} = \left[S_{(A,A_\perp)}\right]\underline{E}^{i}_{(A,A_\perp)} \qquad \underline{E}^{s}_{(B,B_\perp)} = \left[S_{(B,B_\perp)}\right]\underline{E}^{i}_{(B,B_\perp)}$$

$$\left[S_{(B,B_\perp)}\right] = \left[U_{(A,A_\perp)\mapsto(B,B_\perp)}\right]^{T}\left[S_{(A,A_\perp)}\right]\left[U_{(A,A_\perp)\mapsto(B,B_\perp)}\right]$$

CON-SIMILARITY TRANSFORMATION

COHERENCY MATRIX

$$\left[T_{(B,B_\perp)}\right] = \left[U_{3(A,A_\perp)\mapsto(B,B_\perp)}\right]\left[T_{(A,A_\perp)}\right]\left[U_{3(A,A_\perp)\mapsto(B,B_\perp)}\right]^{-1}$$

SIMILARITY TRANSFORMATION

$$\left[U_{3(A,A_\perp)\mapsto(B,B_\perp)}\right]$$

U(3) SPECIAL UNITARY ELLIPTICAL BASIS TRANSFORMATION MATRIX

ELLIPTICAL BASIS TRANSFORMATION

SPECIAL UNITARY SU(2) GROUP

$$[U] = \underbrace{\begin{bmatrix} cos(\phi) & -sin(\phi) \\ sin(\phi) & cos(\phi) \end{bmatrix}}_{[U_2(\phi)]} \underbrace{\begin{bmatrix} cos(\tau) & j\,sin(\tau) \\ j\,sin(\tau) & cos(\tau) \end{bmatrix}}_{[U_2(\tau)]} \underbrace{\begin{bmatrix} e^{-j\alpha} & 0 \\ 0 & e^{j\alpha} \end{bmatrix}}_{[U_2(\alpha)]}$$

SPECIAL UNITARY SU(3) GROUP

$$\underbrace{\begin{bmatrix} 1 & 0 & 0 \\ 0 & cos(2\phi) & sin(2\phi) \\ 0 & -sin(2\phi) & cos(2\phi) \end{bmatrix}}_{[U_3(2\phi)]} \underbrace{\begin{bmatrix} cos(2\tau) & 0 & j\,sin(2\tau) \\ 0 & 1 & 0 \\ j\,sin(2\tau) & 0 & cos(2\tau) \end{bmatrix}}_{[U_3(2\tau)]} \underbrace{\begin{bmatrix} cos(2\alpha) & -j\,sin(2\alpha) & 0 \\ -j\,sin(2\alpha) & cos(2\alpha) & 0 \\ 0 & 0 & 1 \end{bmatrix}}_{[U_3(2\alpha)]}$$

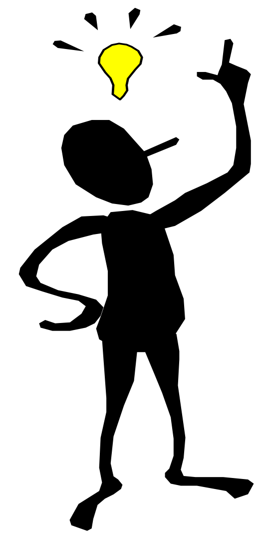

POLARIMETRIC GOLDEN NUMBER

POLARIMETRIC TARGET DIMENSION

$$[S] = \begin{bmatrix} S_{XX} & S_{XY} \\ S_{XY} & S_{YY} \end{bmatrix}$$

5 DEGREES OF FREEDOM

$$|S_{XX}|, |S_{XY}|, |S_{YY}|$$

$$\phi_{XY-XX}, \phi_{YY-XX}$$

COHERENCY MATRIX $[T]$

9 HUYNEN REAL PARAMETERS

(*A0, B0, B, C, D, E, F, G, H*)

TARGET MONOSTATIC POLARIMETRIC « *DIMENSION* »

=

5

9 - 5 = 4 TARGET EQUATIONS

POLARIMETRIC TARGET DIMENSION

PURE TARGET – MONOSTATIC CASE

$$[T] = \underline{k} \cdot \underline{k}^{*T} = \begin{bmatrix} 2A_0 & C - jD & H + jG \\ C + jD & B_0 + B & E + jF \\ H - jG & E - jF & B_0 - B \end{bmatrix}$$

3x3 HERMITIAN MATRIX - RANK 1

↓

9 PRINCIPAL MINORS = 0

$$2A_0(B_0 + B) - C^2 - D^2 = 0 \qquad 2A_0(B_0 - B) - G^2 - H^2 = 0$$

$$-2A_0E + CH - DG = 0 \qquad B_0^2 - B^2 - E^2 - F^2 = 0$$

$$C(B_0 - B) - EH - GF = 0 \qquad -D(B_0 - B) + FH - GE = 0$$

$$2A_0F - CG - DH = 0 \qquad -G(B_0 + B) + FC - ED = 0$$

$$H(B_0 + B) - CE - DF = 0$$

POLARIMETRIC TARGET DIMENSION

$$[S] = \begin{bmatrix} S_{XX} & S_{XY} \\ S_{XY} & S_{YY} \end{bmatrix}$$

5 DEGREES OF FREEDOM

$$|S_{XX}|, |S_{XY}|, |S_{YY}|$$

$$\phi_{XY-XX}, \phi_{YY-XX}$$

COHERENCY MATRIX $[T]$

9 HUYNEN REAL PARAMETERS

(*A0, B0, B, C, D, E, F, G, H*)

TARGET MONOSTATIC POLARIMETRIC « *DIMENSION* »

=

5

9 - 5 = 4 TARGET EQUATIONS

$$2A_0(B_0 + B) = C^2 + D^2$$

$$2A_0(B_0 - B) = G^2 + H^2$$

$$2A_0E = CH - DG$$

$$2A_0F = CG + DH$$

SCATTERING POLARIMETRY

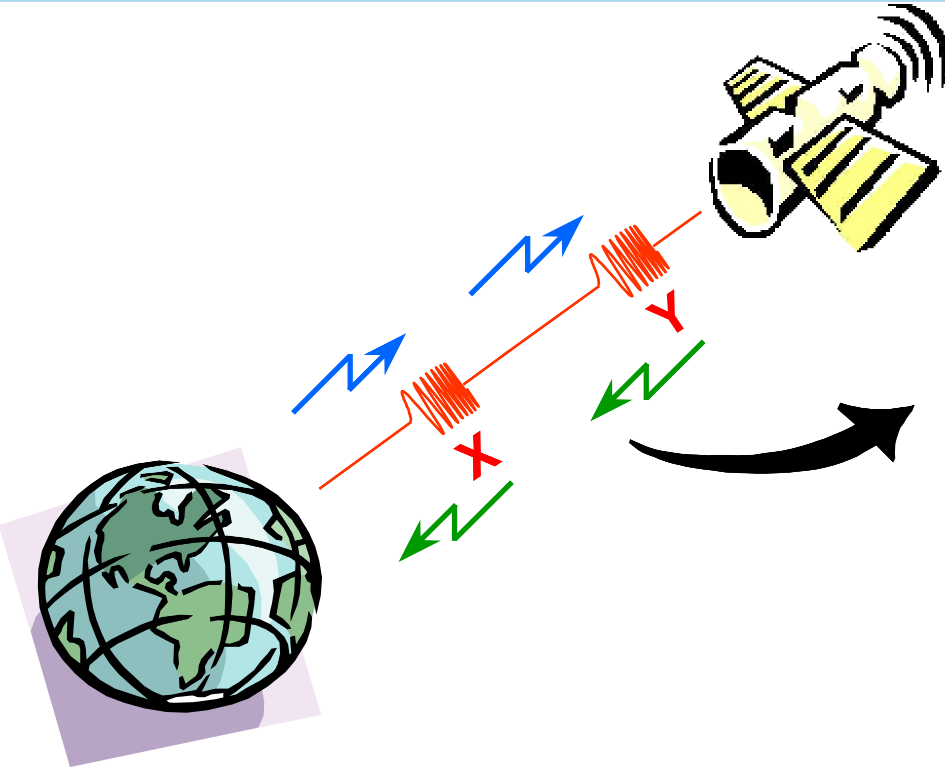

SINCLAIR MATRIX $[S]$

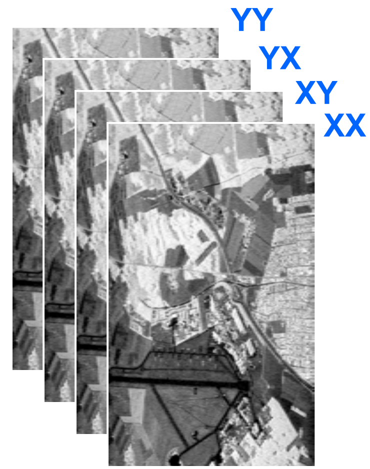

THE DIFFERENT TARGET POLARIMETRIC DESCRIPTORS

[S]	SINCLAIR Matrix
<u>k</u>, <u>Ω</u>	Target Vectors
[K]	KENNAUGH Matrix
[T]	Coherency Matrix
[C]	Covariance Matrix

TRANSMITTER: X & Y

RECEIVERS: X & Y

POLARIMETRIC REMOTE SENSING

© E. Pottier, L. Ferro-Famil (01/2005)

QUALITATIVE ANALYSIS

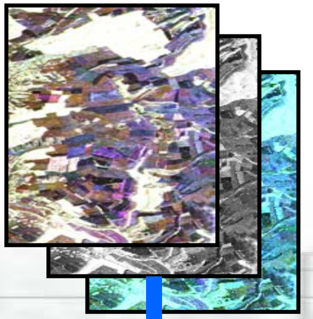

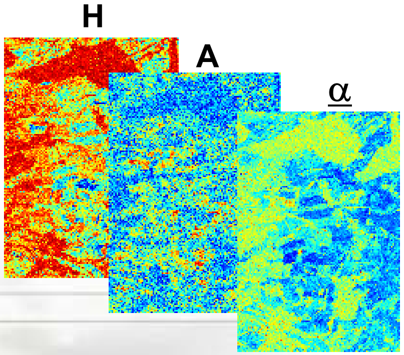

SPECKLE FILTERING

POLARIMETRIC TARGET DECOMPOSITION

WISHART POLARIMETRIC SEGMENTATION
MONO/DUAL FREQUENCY INTERFEROMETRY

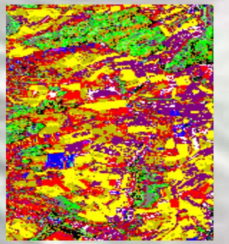

CLUSTER POLARIMETRIC IDENTIFICATION

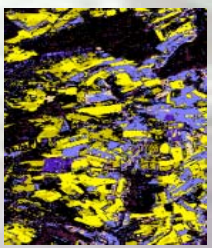

POLARIMETRIC DESCRIPTORS EXTRACTION

SPECKLE FILTERING

SPECKLE PHENOMENON

↓

DISTORTION OF THE INTERPRETATION

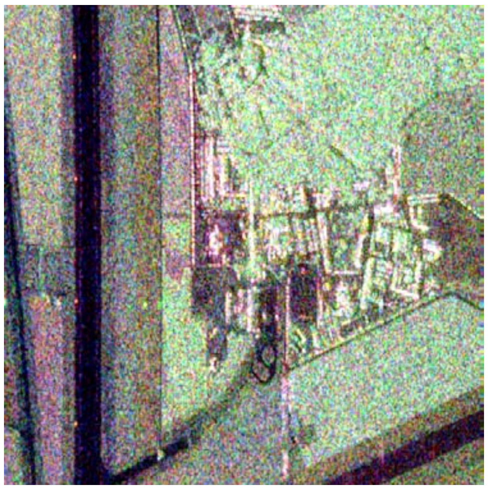

SPECKLE FILTERING

HOMOGENEOUS AREA

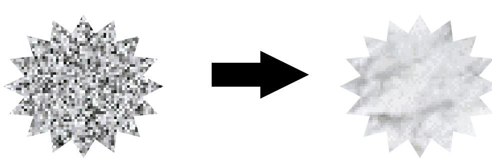

SPECKLE REDUCTION (RADIOMETRIC RESOLUTION)

HETEROGENEOUS AREA

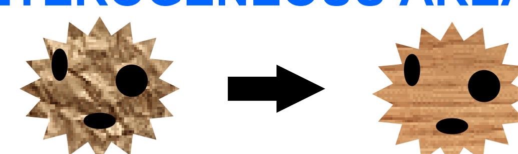

DETAILS PRESERVATION (SPATIAL RESOLUTION)

SPECKLE REDUCTION

MULTI-LOOK SAR PROCESSING (BoxCar)

Averaging Amplitude / Intensity (Not complex images) of neighboring pixels

Good Noise Smoothing

Spatial Resolution Loss - blurring edges - erasing thin lines
Loss of linear or point features …

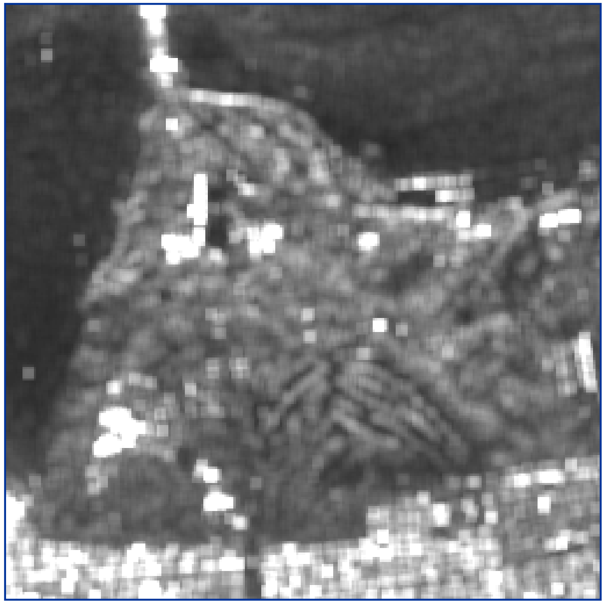

SPECKLE : MULTIPLICATIVE NOISE MODEL

« SPECKLE is a scattering phenomenon and not a noise. However, from the image SAR processing point of vue, the speckle can be modeled as multiplicative noise for extended target » (Lee, IGARSS-98)

$$\underline{y} = \begin{bmatrix} y_{HH} \\ y_{HV} \\ y_{VV} \end{bmatrix} = \begin{bmatrix} n_{HH} & 0 & 0 \\ 0 & n_{HV} & 0 \\ 0 & 0 & n_{VV} \end{bmatrix} \begin{bmatrix} x_{HH} \\ x_{HV} \\ x_{VV} \end{bmatrix} = \begin{bmatrix} x_{HH} n_{HH} \\ x_{HV} n_{HV} \\ x_{VV} n_{VV} \end{bmatrix}$$

SCATTERING FIELD — NOISE — REFLECTIVITY DENSITY

$$Y_{pqpq} = y_{pq} y_{pq}^{*} = X_{pqpq} v_{pqpq}$$ INTENSITY = MULTIPLICATIVE MODEL

$$Y_{pqrs} = y_{pq} y_{rs}^{*} = X_{pqrs} v_{pqrs}$$ NOISE MODEL ????

POLSAR SPECKLE FILTERING

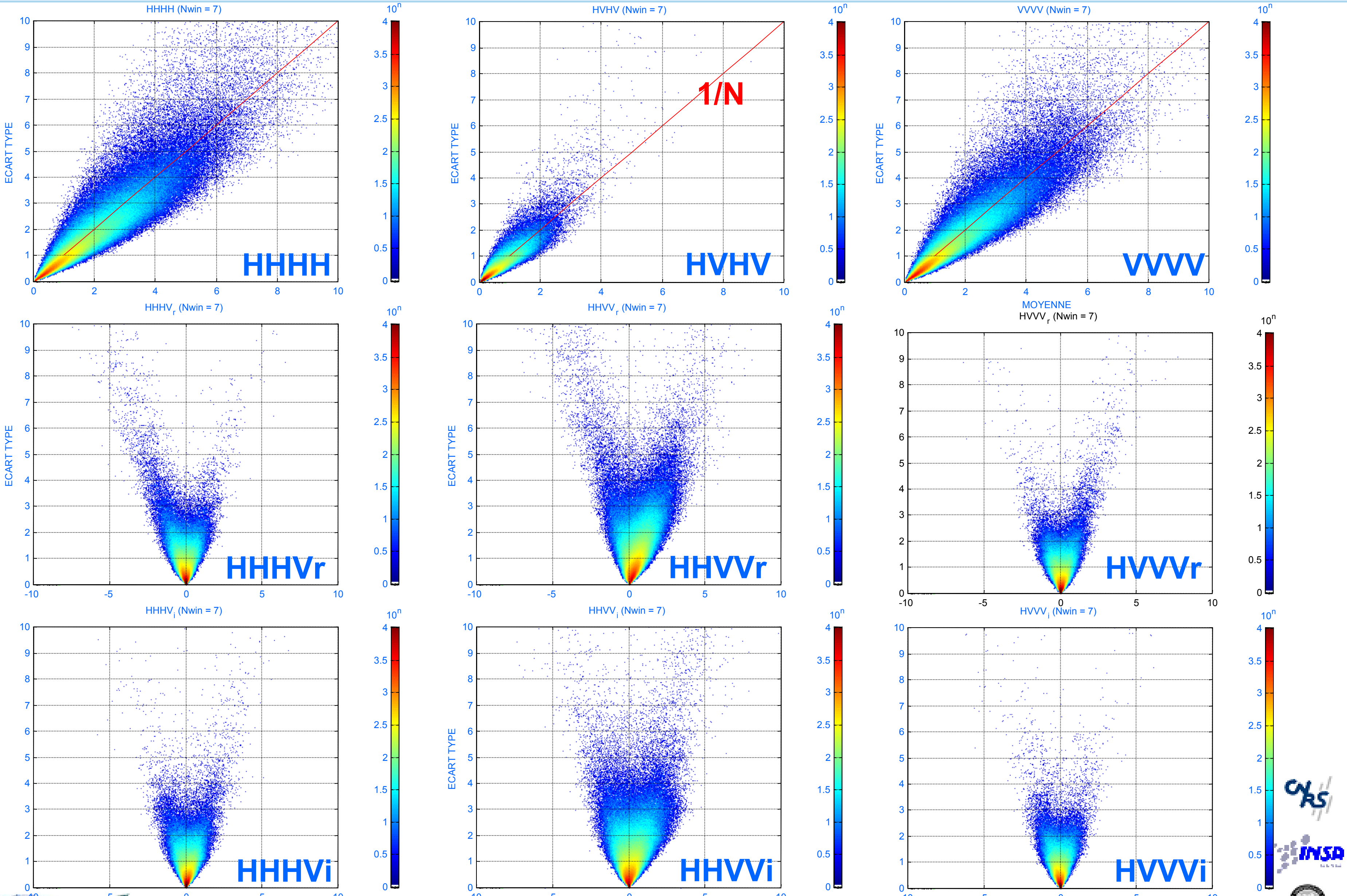

© E. Pottier, L. Ferro-Famil (01/2005)

POLSAR SPECKLE FILTERING

POLARIMETRIC VECTORIAL SPECKLE FILTER

$$\langle [T] \rangle = \frac{1}{N} \sum_{i=1}^{N} \underline{k}_i \underline{k}_i^{*T}$$

$$[\hat{T}] = E([T]) - k\big[E([T]) - [T]\big] \longrightarrow [\hat{T}]$$

SPAN IMAGE

$$S_S = \langle T_{11} \rangle + \langle T_{22} \rangle + \langle T_{33} \rangle$$

LINEAR SCALAR LEE FILTER

$$\hat{S} = E(S_S) - k\big[E(S_S) - S_S\big]$$

$$k = \frac{var(S)}{var(S_S)} = \frac{CV_{S_S}^2 - \sigma_v^2}{CV_{S_S}^2\left[1+\sigma_v^2\right]}$$

J.S. LEE

Homogeneous Areas

$$var(S) \approx 0 \quad \Rightarrow \quad k = 0 \quad \Rightarrow \hat{S} = E(S_S)$$

Highly Inhomogeneous Areas

$$var(S) \mapsto var(S_s) \quad \Rightarrow \quad k = 1 \quad \Rightarrow \hat{S} = S_S$$

REFINED FILTER

SAPHIR

POLARIMETRIC SPECKLE FILTERING IS NOT AN EXACT SCIENCE
SUBJECTIVE, IMAGE DEPENDENT

Quantitative Criteria (J.S. Lee - IGARSS 98)

- Speckle Reduction (E.N.L)
- Edge Sharpness Preservation
- Line and Point Target Contrast Preservation
- Retention of Mean Values in Homogeneous Regions
- Retention of Texture Information
- Retention of Polarimetric Information (co, cross-correlations)
- Computational Efficiency
- Implementation Complexity

$$[\hat{T}] = E([T]) - k[E([T]) - [T]]$$

THE POLARIMETRIC SPECKLE LEE FILTER IS TODAY A GOOD COMPROMISE

POLSAR SPECKLE FILTERING

SAN FRANCISCO BAY JPL - AIRSAR L-band 1988

J.S. Lee, M.R. Grunes and G. De Grandi, "Polarimetric SAR Speckle Filtering and Its Impact on Terrain Classification" *IEEE TGRS*, September 1999

POLSAR SPECKLE FILTERING

SAN FRANCISCO BAY JPL - AIRSAR L-band 1988

J.S. Lee, D.L. Schuler, T.L. Ainsworth, M.R. Grunes, « Scattering Model Based Speckle Filetring of Polarimetric SAR Data" *EUSAR 2004, Ulm, Germany, May 2004*

© *E. Pottier, L. Ferro-Famil (01/2005)*

MULTIPLICATIVE-ADDITIVE NOISE MODEL

$$S_i S_j^* = \underbrace{\psi \bar{z}_n n_m N_c \exp(j\phi_x)}_{\text{Multiplicative term}} + \underbrace{\psi\left(|\rho| - N_c \bar{z}_n\right)\exp(j\phi_x) + \psi\left(n_{ar} + j n_{ai}\right)}_{\text{Additive term}}$$

C. LOPEZ MARTINEZ

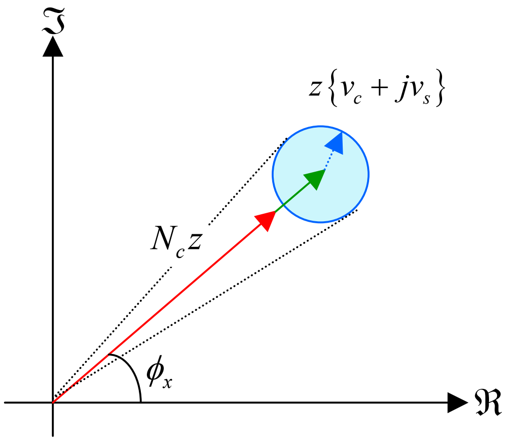

$$E\{n_m\} = 1 \qquad \operatorname{var}\{n_m\} = 1$$

$$E\{n_{c_n}\} = E\{n_{s_n}\} = 0$$

$$\operatorname{var}\{n_{c_n}\} = \operatorname{var}\{n_{s_n}\} = \frac{1}{2}\left(1 - |\rho|^2\right)^{1.3}$$

Diagonal elements

$$\left\{\begin{array}{l} |S_{pq}|^2 = S_{pq} \cdot S_{pq}^* \\ |\rho| = 1 \quad \phi_x = 0 \end{array}\right.$$

$$\Re\{z e^{j\phi_z}\} = \psi n_m \qquad \Im\{z e^{j\phi_z}\} = 0$$

$\longleftarrow$ Speckle Noise Multiplicative model

C. López-Martínez and X. Fàbregas, "Polarimetric SAR Speckle Noise Model," IEEE TGRS, vol. 41, no. 10, pp. 2232 – 2242, Oct. 2003

MULTIPLICATIVE-ADDITIVE NOISE MODEL

$$S_iS_j^* = \underbrace{\psi \bar{z}_n n_m N_c \exp(j\phi_x)}_{Multiplicative\ term} + \underbrace{\psi\left(|\rho| - N_c \bar{z}_n\right)\exp(j\phi_x) + \psi\left(n_{ar} + jn_{ai}\right)}_{Additive\ term}$$

Polarimetric Coherence

Multiplicative speckle component: n_m → High coherence areas
Homogeneous

Additive speckle components: n_{ar}, n_{ai} → Low coherence areas
Non-homogeneous

Final speckle noise behaviour { Combination of multiplicative and additive noise components, determined by ρ

L-band (1.3 GHz) fully PolSAR data. E-SAR system. Oberpfaffenhofen test area (D)

$S_{hh}S_{vv}^*$

$|\rho|$

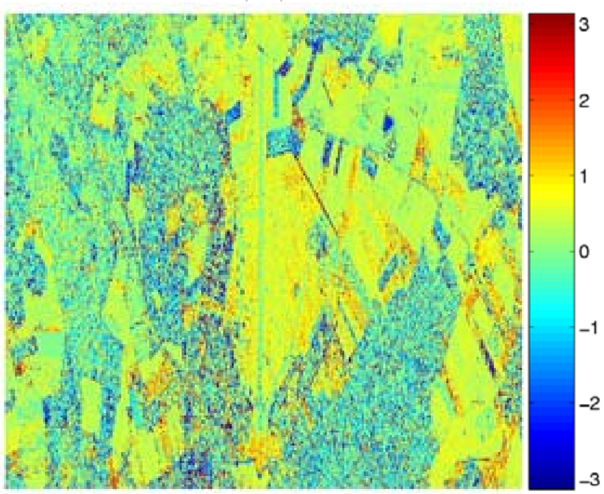

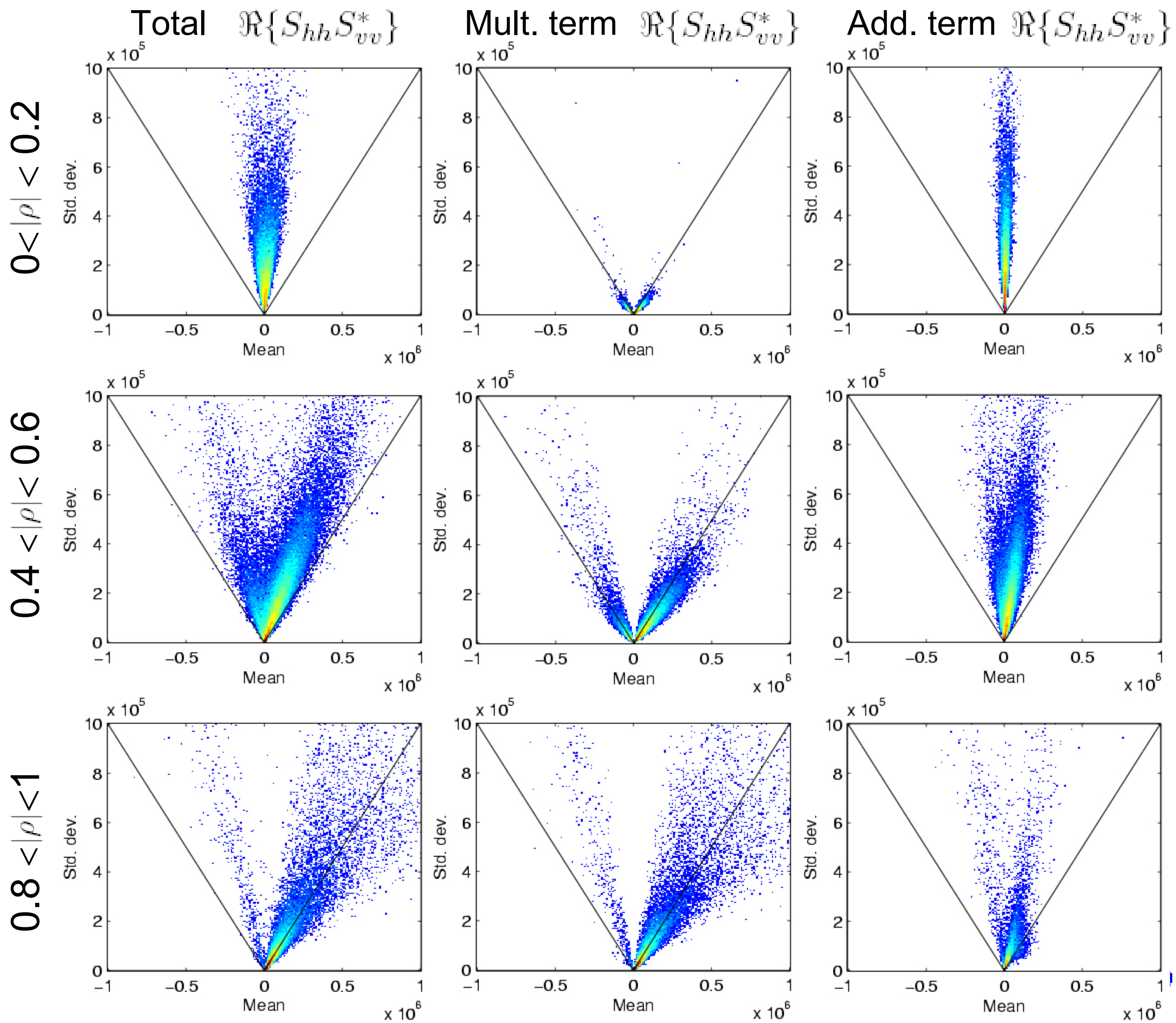

© IETR SAPHIR ϕ_x ıttier, L. Ferro-Famil (01/2005)

$$[T] = \underline{k}\,\underline{k}^{*T} \longrightarrow \boxed{\text{FILTER}} \longrightarrow [\hat{T}] = \underline{\hat{k}}\,\underline{\hat{k}}^{*T}$$

AVERAGING DATA

↓

SECOND ORDER STATISTICS

↓

COHERENCY MATRICES

SMOOTHING AVERAGING

↓

CONCEPT OF THE DISTRIBUTED TARGET

QUALITATIVE ANALYSIS

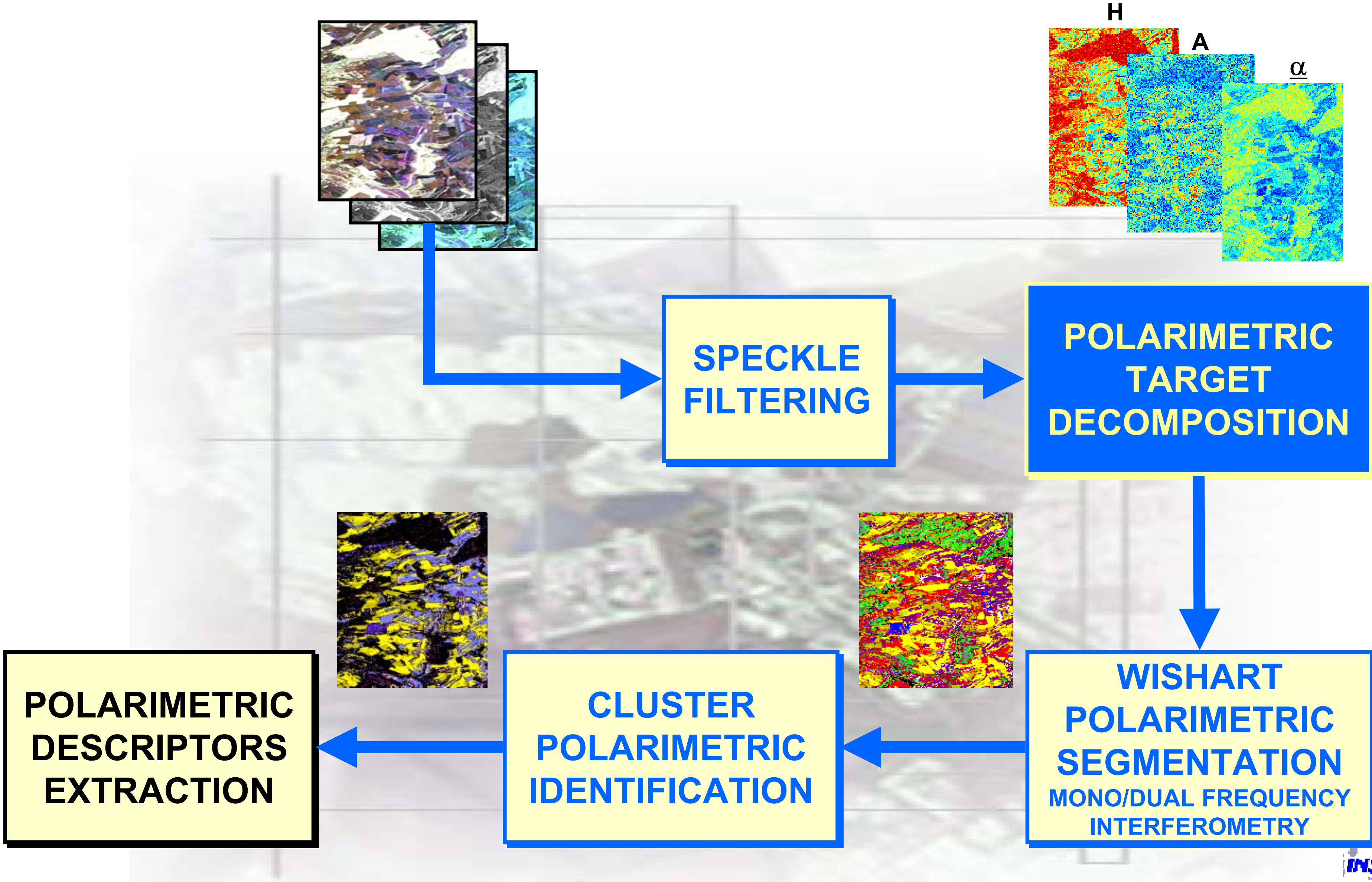

TARGET DECOMPOSITIONS

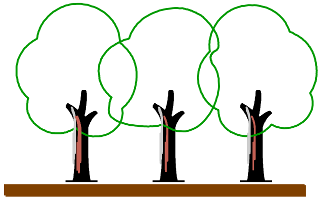

PURE TARGET

COHERENCY MATRIX $[T]$

9 REAL DEPENDANT
HUYNEN PARAMETERS
(A0,B0,B,C,D,E,F,G,H)

POLARIMETRIC DISTRIBUTED
TARGET « *DIMENSION* » = 5

9 - 5 = 4 TARGET EQUATIONS

$$
\begin{aligned}
2A_0(B_0+B) &= C^2+D^2 \\
2A_0(B_0-B) &= G^2+H^2 \\
2A_0E &= CH-DG \\
2A_0F &= CG+DH
\end{aligned}
$$

TARGET DECOMPOSITIONS

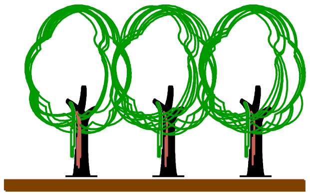

DISTRIBUTED TARGET

COHERENCY MATRIX $<[T]>$

POLARIMETRIC DISTRIBUTED TARGET « *DIMENSION* » = 9

9 REAL INDEPENDANT HUYNEN PARAMETERS
(<A0>,<B0>,<B>,<C>,<D>,<E>,<F>,<G>,<H>)

9 TARGET INEQUATIONS

$$2\langle A_0\rangle\left(\langle B_0\rangle+\langle B\rangle\right)\geq\langle C\rangle^2+\langle D\rangle^2 \qquad \langle H\rangle\left(\langle B_0\rangle+\langle B\rangle\right)\geq\langle C\rangle\langle E\rangle+\langle D\rangle\langle F\rangle$$

$$2\langle A_0\rangle\left(\langle B_0\rangle-\langle B\rangle\right)\geq\langle G\rangle^2+\langle H\rangle^2 \qquad \langle G\rangle\left(\langle B_0\rangle+\langle B\rangle\right)\geq\langle C\rangle\langle F\rangle-\langle D\rangle\langle E\rangle$$

$$2\langle A_0\rangle\langle E\rangle\geq\langle C\rangle\langle H\rangle-\langle D\rangle\langle G\rangle \qquad \langle C\rangle\left(\langle B_0\rangle-\langle B\rangle\right)\geq\langle H\rangle\langle E\rangle+\langle F\rangle\langle G\rangle$$

$$2\langle A_0\rangle\langle F\rangle\geq\langle C\rangle\langle G\rangle+\langle D\rangle\langle H\rangle \qquad \langle D\rangle\left(\langle B_0\rangle-\langle B\rangle\right)\geq\langle F\rangle\langle H\rangle-\langle G\rangle\langle E\rangle$$

$$\langle B_0\rangle^2\geq\langle B\rangle^2+\langle E\rangle^2+\langle F\rangle^2$$

TARGET DECOMPOSITIONS

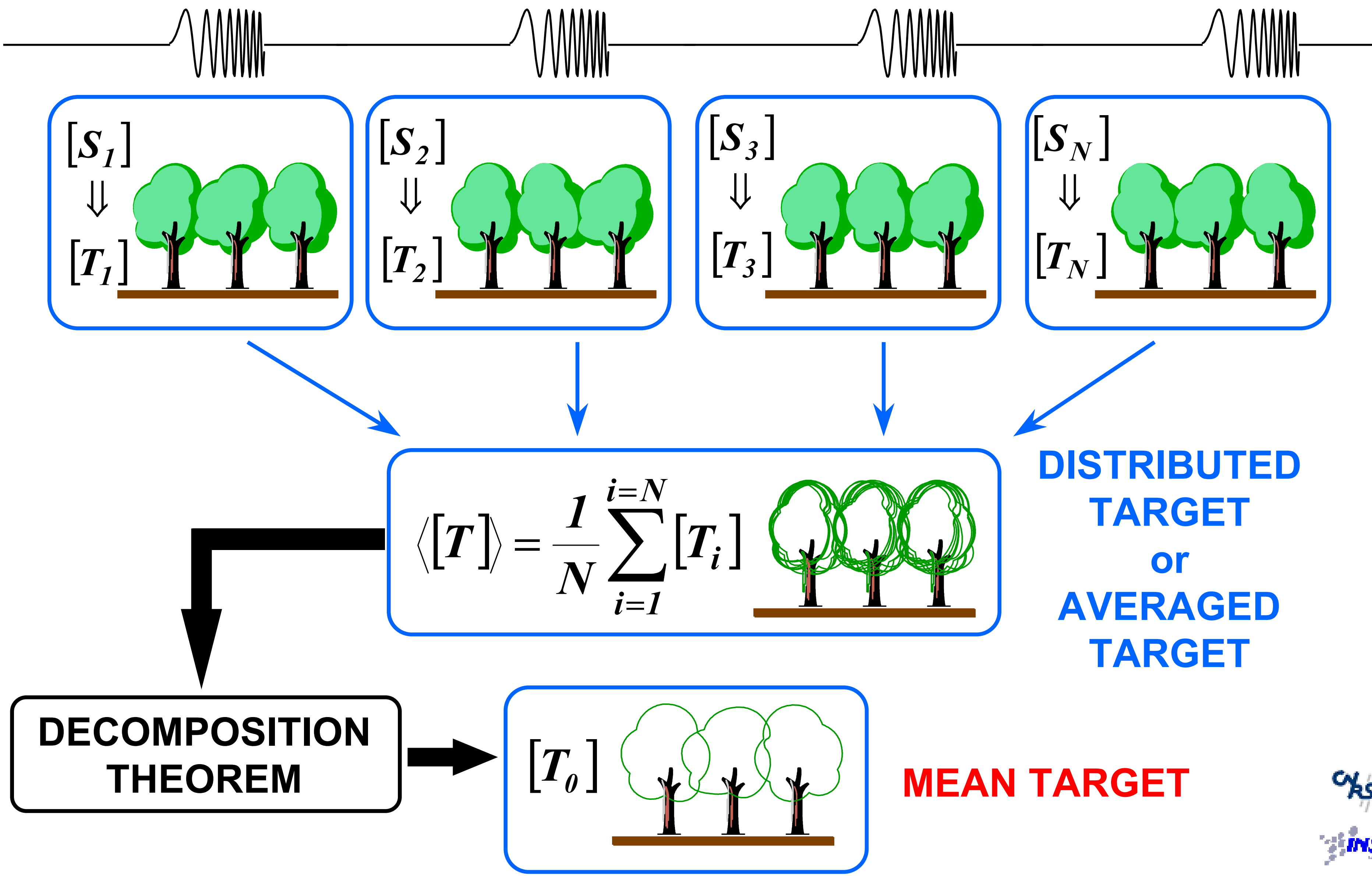

© E. Pottier, L. Ferro-Famil (01/2005)

TARGET DECOMPOSITIONS

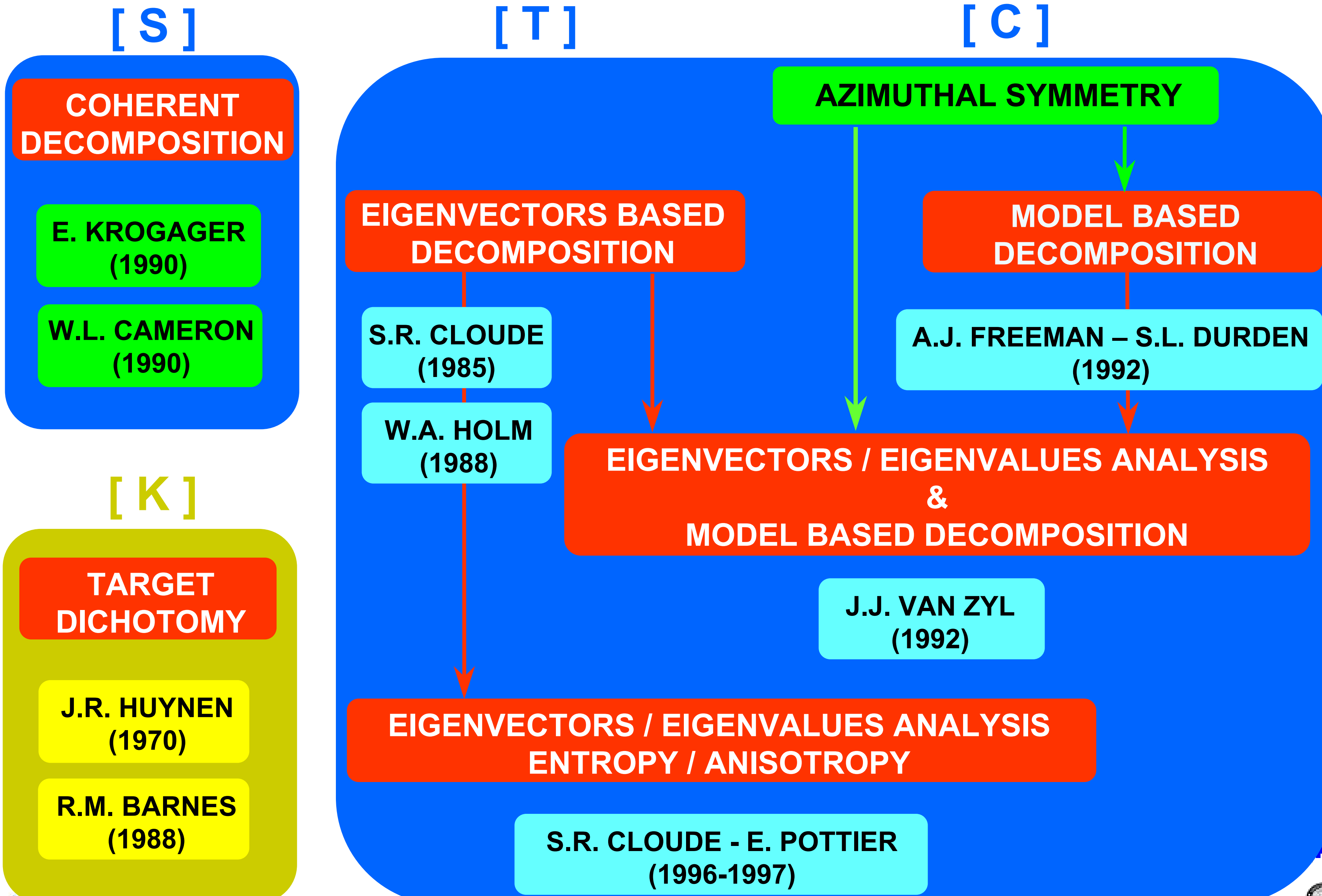

H / A / α DECOMPOSITION

TARGET VECTOR

$$\underline{k} = \frac{1}{\sqrt{2}}\left[S_{XX}+S_{YY} \quad S_{XX}-S_{YY} \quad 2S_{XY}\right]^T$$

LOCAL ESTIMATE OF THE COHERENCY MATRIX

$$\langle [T] \rangle = \frac{1}{N}\sum_{i=1}^{N} \underline{k}_i \cdot \underline{k}_i^{*T} = \frac{1}{N}\sum_{i=1}^{N} [T_i]$$

EIGENVECTORS / EIGENVALUES ANALYSIS

$$\langle [T] \rangle = [U_3][\Sigma][U_3]^{-1} = \begin{bmatrix} \underline{u}_1 & \underline{u}_2 & \underline{u}_3 \end{bmatrix} \begin{bmatrix} \lambda_1 & 0 & 0 \\ 0 & \lambda_2 & 0 \\ 0 & 0 & \lambda_3 \end{bmatrix} \begin{bmatrix} \underline{u}_1 & \underline{u}_2 & \underline{u}_3 \end{bmatrix}^{*T}$$

ORTHOGONAL EIGENVECTORS

REAL EIGENVALUES
$\lambda_1 > \lambda_2 > \lambda_3$

$$\underline{u}_i = \left[\cos\alpha_i \quad \sin\alpha_i \cos\beta_i e^{j\delta_i} \quad \sin\alpha_i \sin\beta_i e^{j\gamma_i}\right]^T$$

$$P_i = \frac{\lambda_i}{\sum_{k=1}^{3}\lambda_k}$$

H / A / $\underline{\alpha}$ DECOMPOSITION

3 ROLL INVARIANT PARAMETERS

ENTROPY

$$H = -\sum_{i=1}^{3} P_i \log_3 (P_i)$$

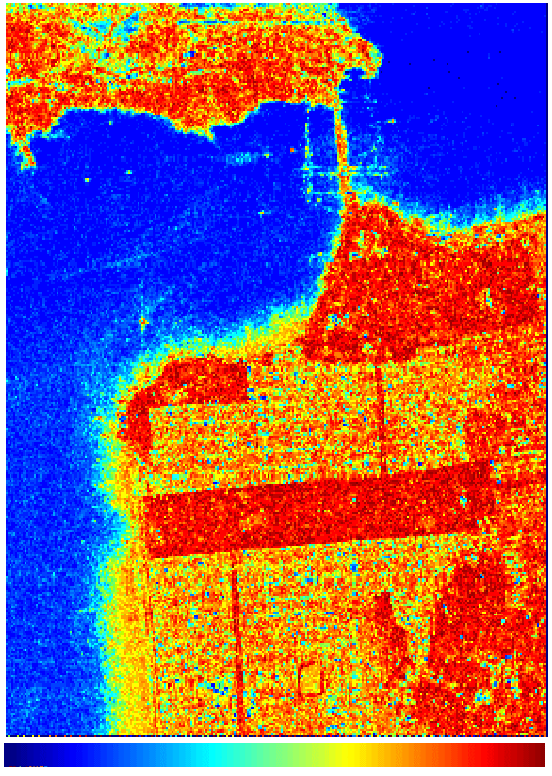

ANISOTROPY

$$A = \frac{\lambda_2 - \lambda_3}{\lambda_2 + \lambda_3}$$

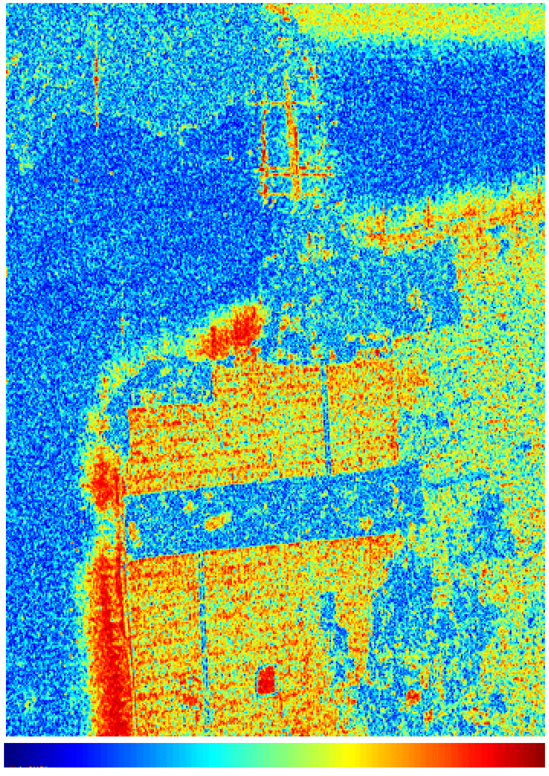

$\underline{\alpha}$ PARAMETER

$$\underline{\alpha} = P_1\alpha_1 + P_2\alpha_2 + P_3\alpha_3$$

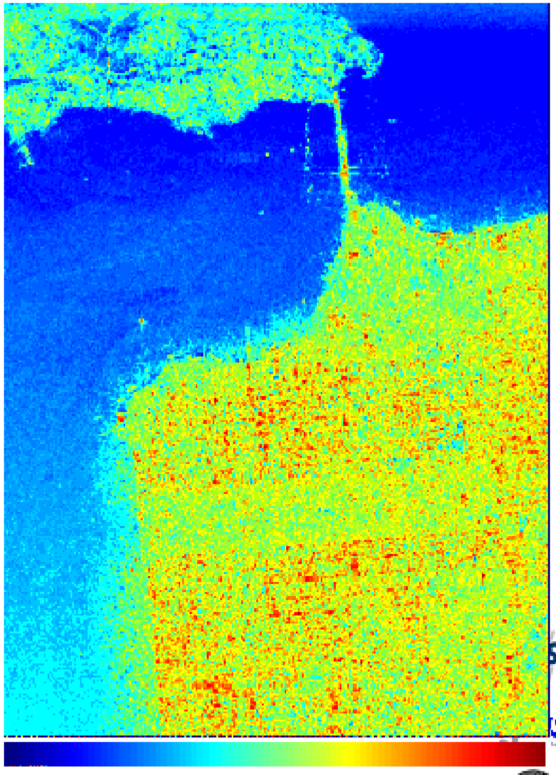

H / A / α DECOMPOSITION

TYPE OF SCATTERING PROCESS

(1-H)(1-A)

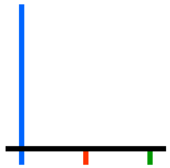

1 MECHANISM

H(1-A)

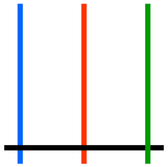

3 MECHANISMS

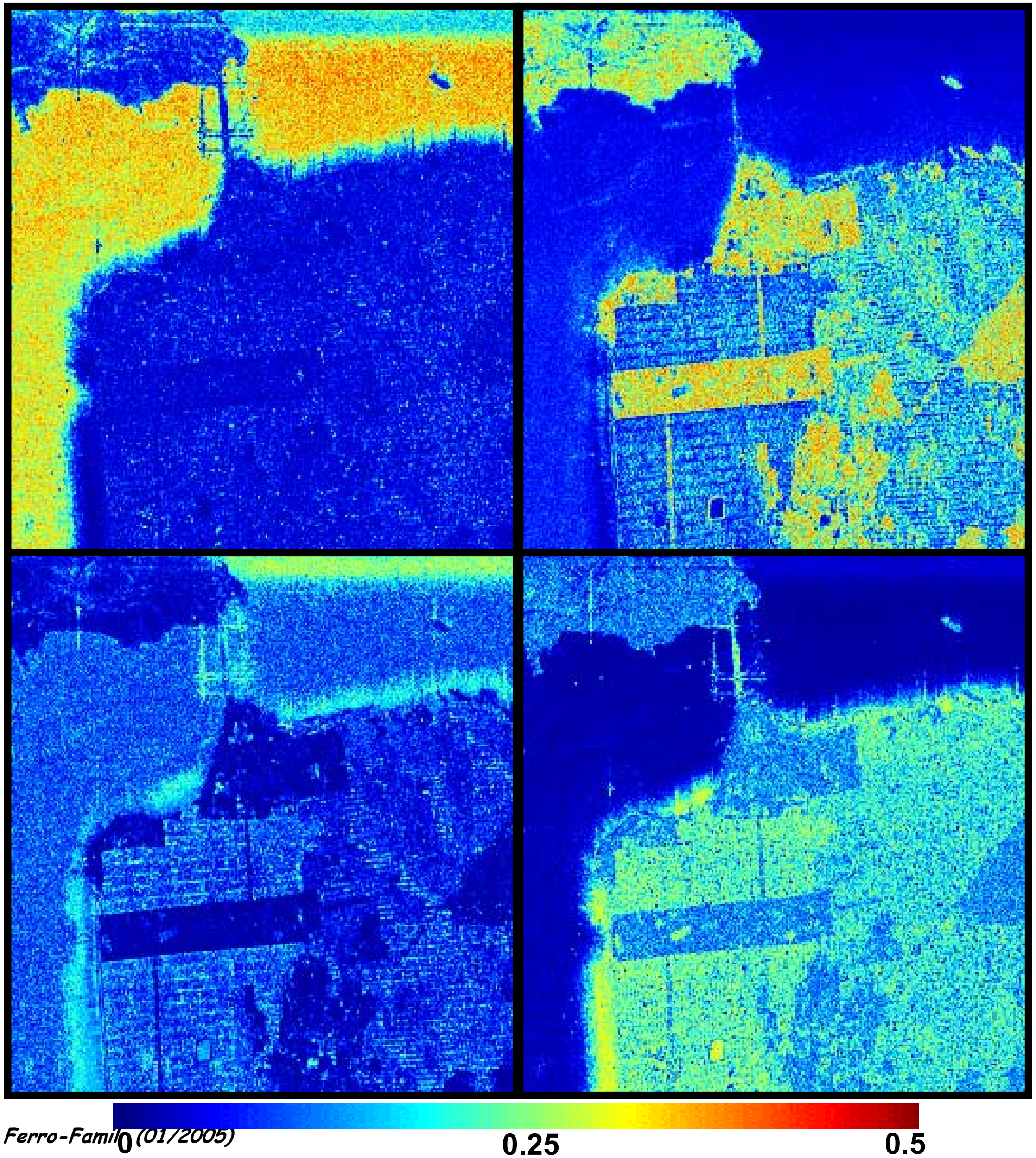

A(1-H)

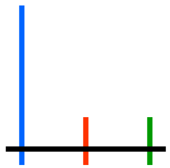

2 MECHANISMS

HA

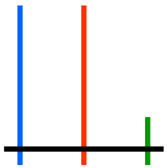

2 MECHANISMS

QUALITATIVE ANALYSIS

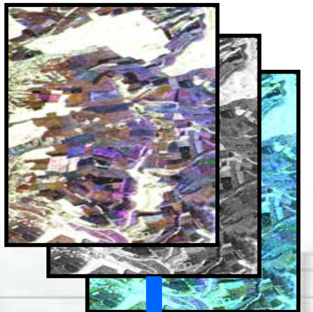

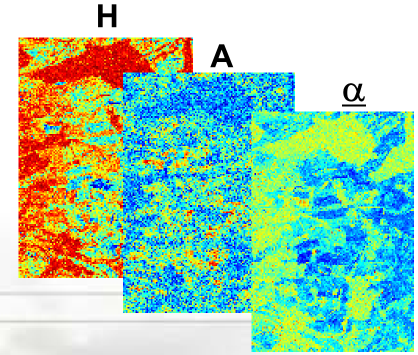

SPECKLE FILTERING

POLARIMETRIC TARGET DECOMPOSITION

WISHART POLARIMETRIC SEGMENTATION
MONO/DUAL FREQUENCY INTERFEROMETRY

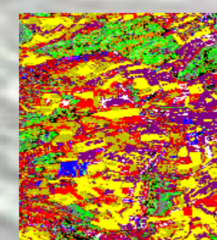

CLUSTER POLARIMETRIC IDENTIFICATION

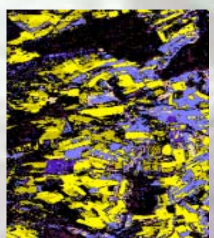

POLARIMETRIC DESCRIPTORS EXTRACTION

Target Vector

$$\underline{X} = \begin{bmatrix} S_{HH} & \sqrt{2}S_{HV} & S_{VV} \end{bmatrix}^T \qquad P(\underline{X}) = \frac{1}{\pi^3 \left|[C]\right|} e^{-\underline{X}^{*T}[C]^{-1}\underline{X}}$$

$$\underline{k} = \frac{1}{\sqrt{2}} \begin{bmatrix} S_{HH} + S_{VV} & S_{HH} - S_{VV} & 2S_{HV} \end{bmatrix}^T \qquad P(\underline{k}) = \frac{1}{\pi^3 \left|[T]\right|} e^{-\underline{k}^{*T}[T]^{-1}\underline{k}}$$

Coherency Matrix

$$\langle [T] \rangle = \frac{1}{N} \sum_{i=1}^{N} \underline{k}_i \cdot \underline{k}_i^{*T} = \frac{1}{N} \sum_{i=1}^{N} [T_i]$$

$$P(\langle [T] \rangle / [T_m]) = \frac{L^{Lp} \left| \langle [T] \rangle \right|^{L-p} e^{-L Tr\left([T_m]^{-1} \langle [T] \rangle\right)}}{\pi^{\frac{p(p-1)}{2}} \Gamma(L) \ldots \Gamma(L-p+1) \left|[T_m]\right|^L}$$

COMPLEX WISHART DISTRIBUTION

L: Number of Look p: Polarimetric Dimension

WISHART CLASSIFIER

$$P\left(\langle[T]\rangle / [T_m]\right) = \frac{L^{Lp} \left|\langle[T]\rangle\right|^{L-p} e^{-LTr\left([T_m]^{-1}\langle[T]\rangle\right)}}{\pi^{\frac{p(p-1)}{2}} \Gamma(L) \ldots \Gamma(L-p+1) \left|[T_m]\right|^{L}}$$

$$\Downarrow$$

SUPERVISED WISHART CLASSIFIER (Lee 1994)

BAYES MAXIMUM LIKELIHOOD CLASSIFICATION PROCEDURE

$$\langle[T]\rangle \in [T_m] \quad \text{if} \quad d_m(\langle[T]\rangle) < d_j(\langle[T]\rangle) \quad \forall\, j \neq m$$

with

$$d_m(\langle[T]\rangle) = LTr\left([T_m]^{-1}\langle[T]\rangle\right) + L\ln\left(\left|[T_m]\right|\right) - \ln\left(P([T_m])\right) + K$$

$[T_m]$: Cluster Center of the class *m*

POLARIMETRIC REMOTE SENSING

WISHART PDF

$$P\left(\langle[T]\rangle/[T_m]\right)=\frac{L^{Lp}\left|\langle[T]\rangle\right|^{L-p}e^{-L\,Tr\left([T_m]^{-1}\langle[T]\rangle\right)}}{\pi^{\frac{p(p-1)}{2}}\Gamma(L)\ldots\Gamma(L-p+1)\left|[T_m]\right|^{L}}$$

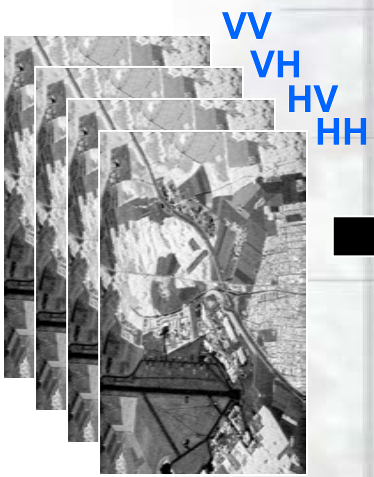

UNSUPERVISED POLSAR CLASSIFICATION

E.POTTIER, J.S LEE (2000)

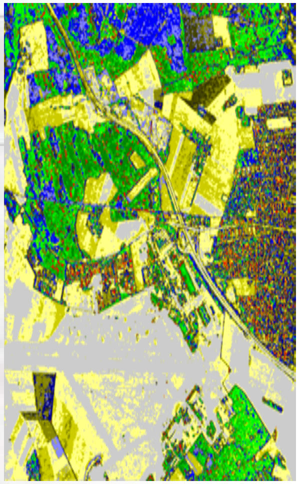

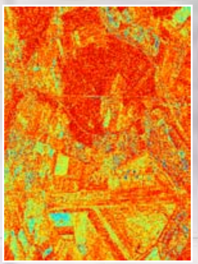
H

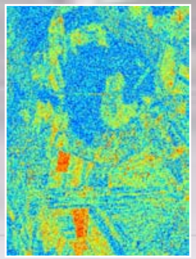
A

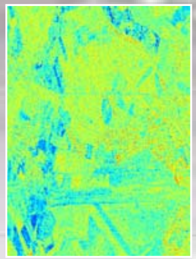
α

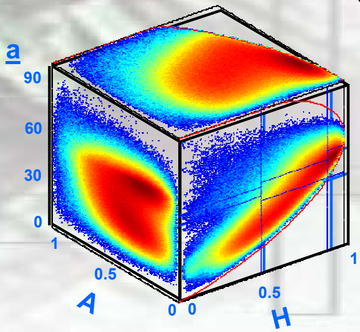

H / A / α DECOMPOSITION THEOREM

© E. Pottier, L. Ferro-Famil (01/2005)

SAPHIR

k - mean CLASSIFICATION PROCEDURE

PROVIDE INITIAL $[T_m]^{(0)}$ FOR EACH CLASS

CLASSIFY THE WHOLE IMAGE WITH THE DISTANCE PROCEDURE

$$\langle[T]\rangle \in [T_m] \quad if \quad d_m(\langle[T]\rangle) < d_j(\langle[T]\rangle) \quad \forall\ j \neq m$$

COMPUTE $[T_m]^{(k+1)}$ FOR EACH CLASS USING THE CLASSIFIED PIXELS OF STEP 2

$$[T_m]^{(k+1)} = \frac{1}{N_m}\sum_{j=1}^{j=N_m}\langle[T]\rangle_j$$

TERMINAISON CRITERION ?

Dr J.S. LEE

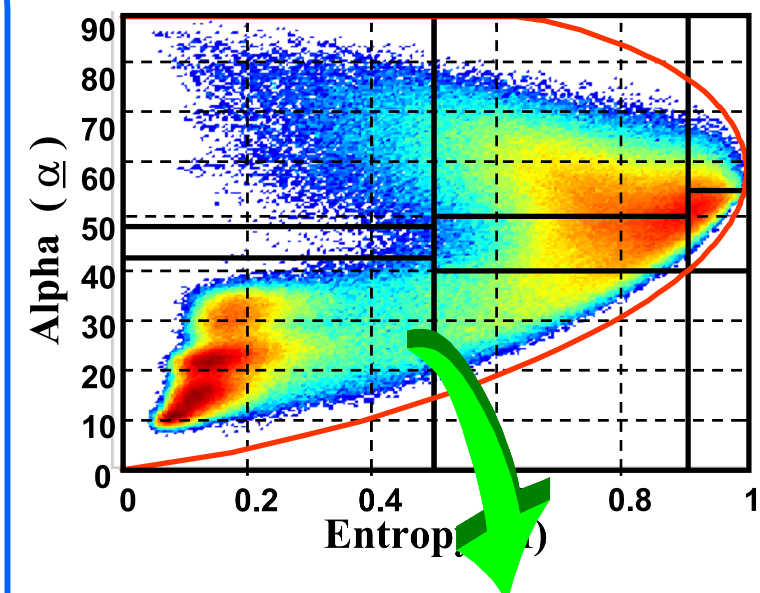

$$[T_m]^{(0)} = \frac{1}{N_m}\sum_{k=1}^{k=N_m}\langle[T]\rangle_k$$

Cluster Center of the class m
(Lee 1998)

H / α - WISHART CLASSIFIER

SAN FRANCISCO BAY JPL - AIRSAR L-band 1988

$2A_0$ B_0+B B_0-B

4th ITERATION

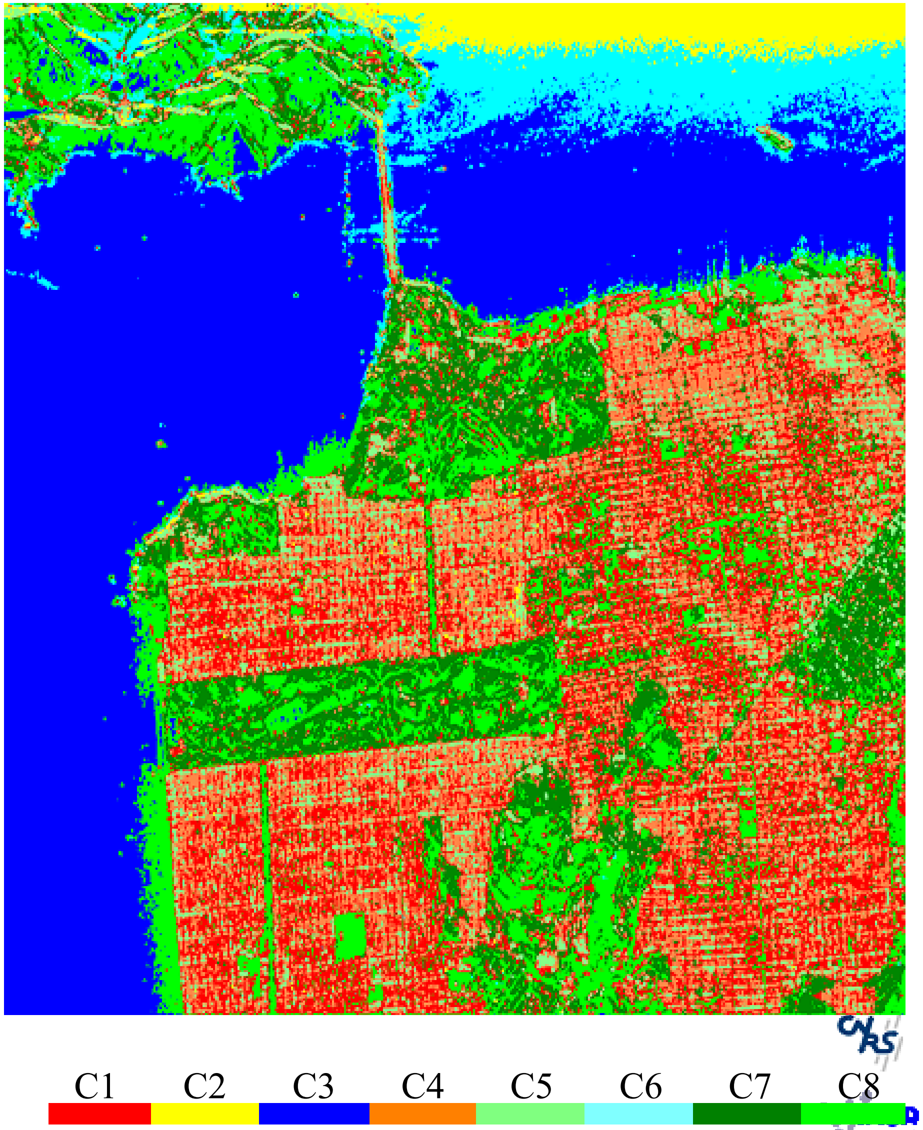

© E. Pottier, L. Ferro-Famil (01/2005)

SAPHIR

2 Successive k - mean Classification procedures

Introduction of the Anisotropy (A) information once the first Classification procedure has met its termination criterion

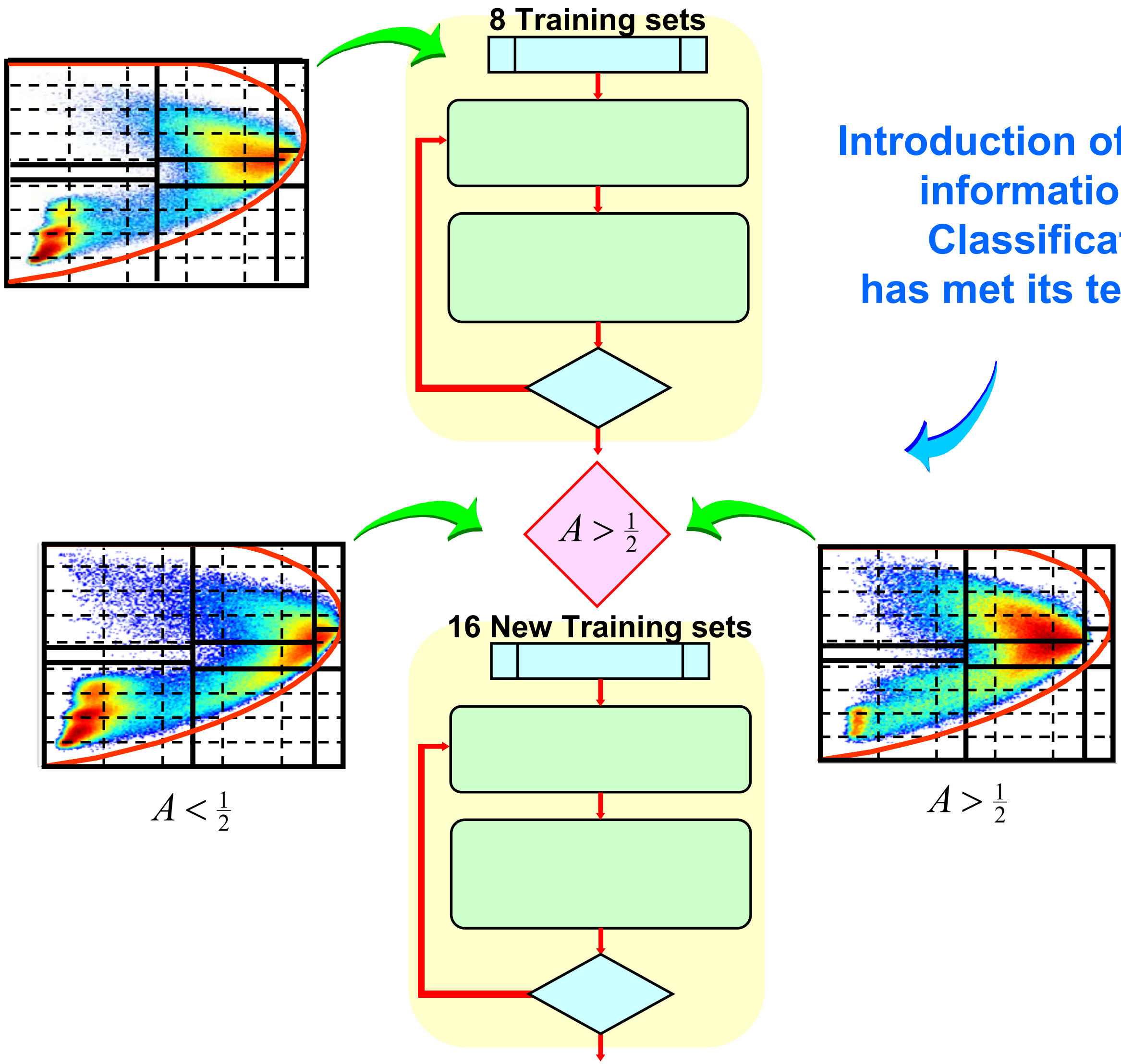

H / A / α - WISHART CLASSIFIER

SAN FRANCISCO BAY JPL - AIRSAR L-band 1988

4th ITERATION

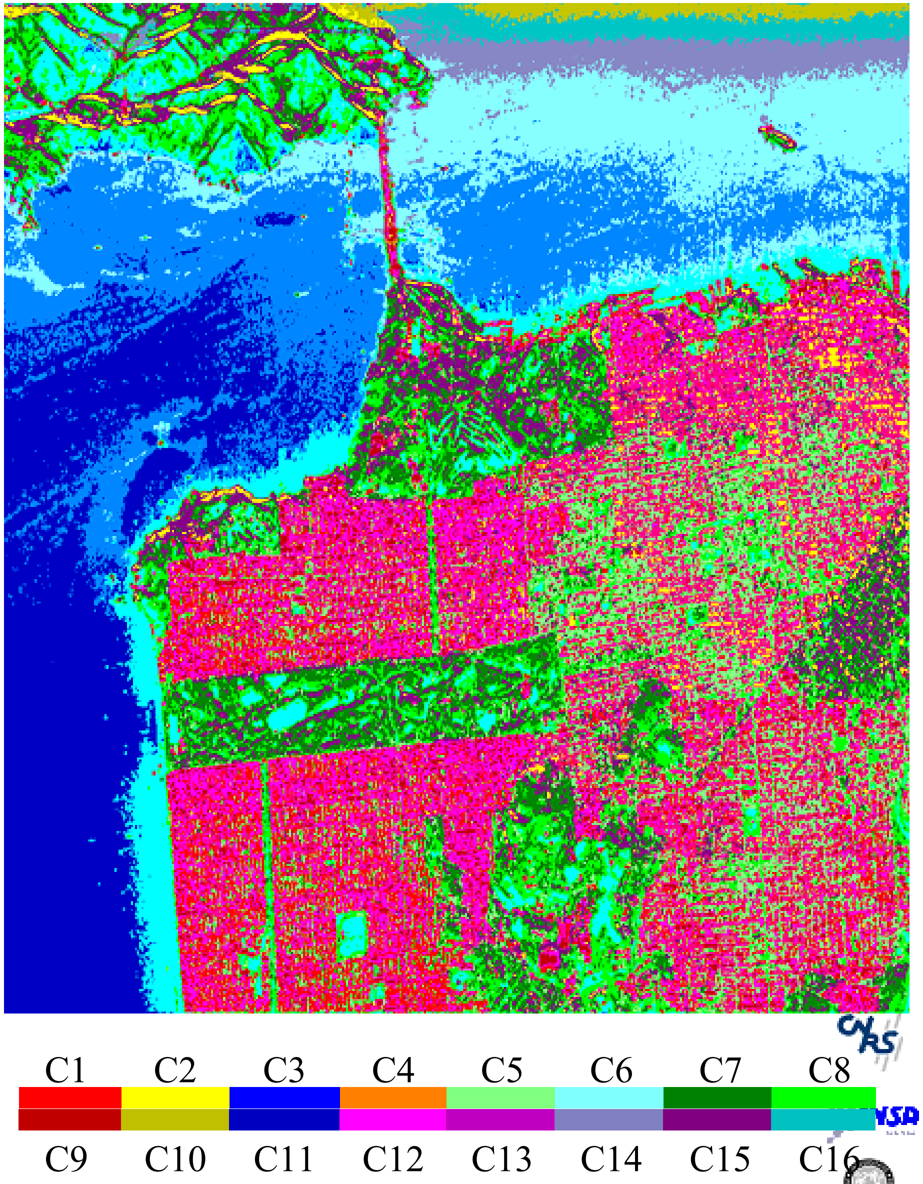

$2A_0$ $\quad B_0 + B$ $\quad B_0 - B$

H / A / α - WISHART CLASSIFIER

SAN FRANCISCO BAY JPL - AIRSAR L-band 1988

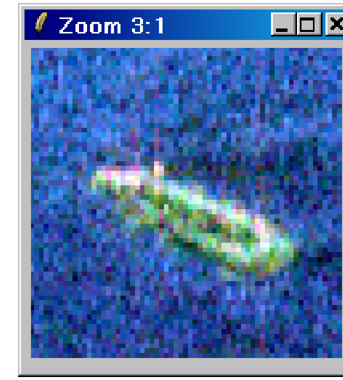

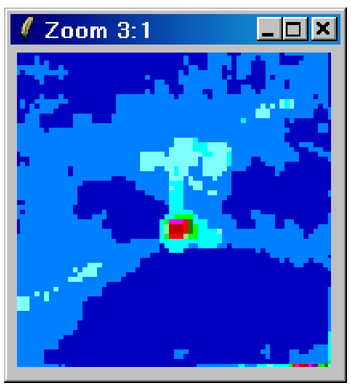

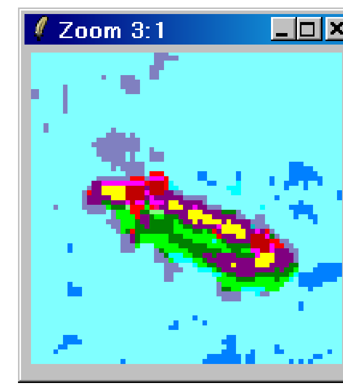

$2A_0$ $\quad B_0 + B$ $\quad B_0 - B$

H / A / $\underline{\alpha}$ - WISHART CLASSIFIER

ICE AREA JPL - AIRSAR L-band

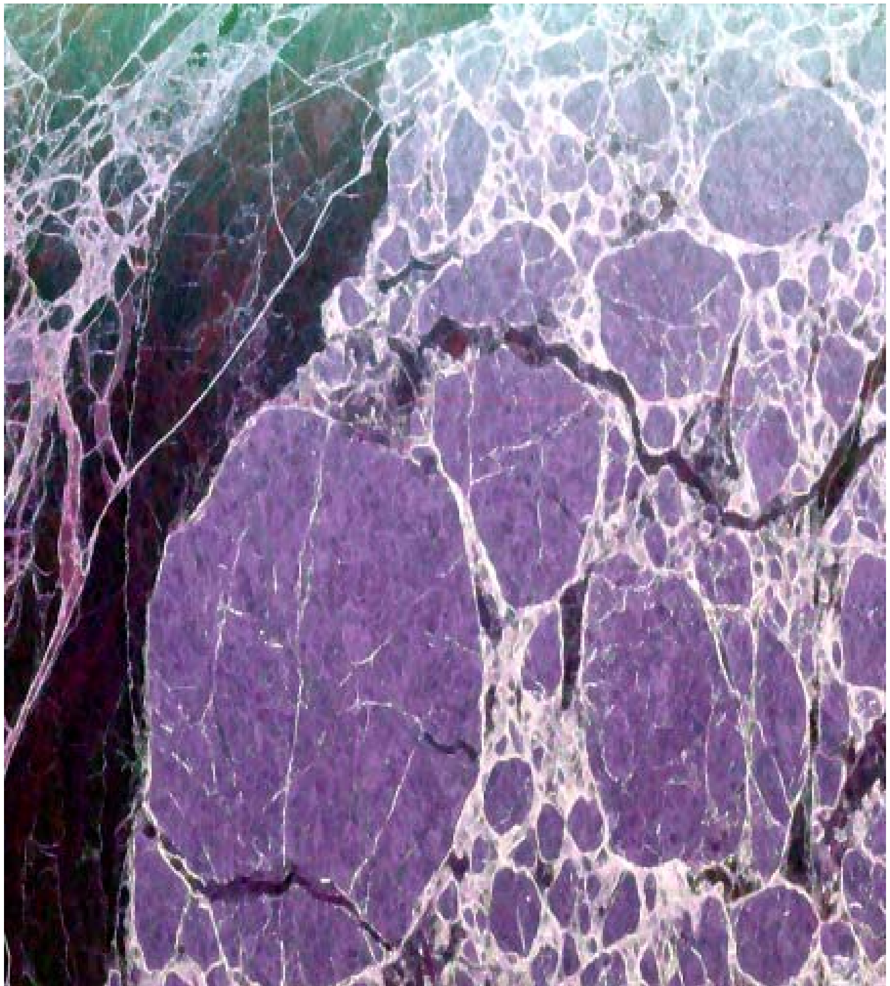

$2A_0$ $\qquad$ $B_0 + B$ $\qquad$ $B_0 - B$

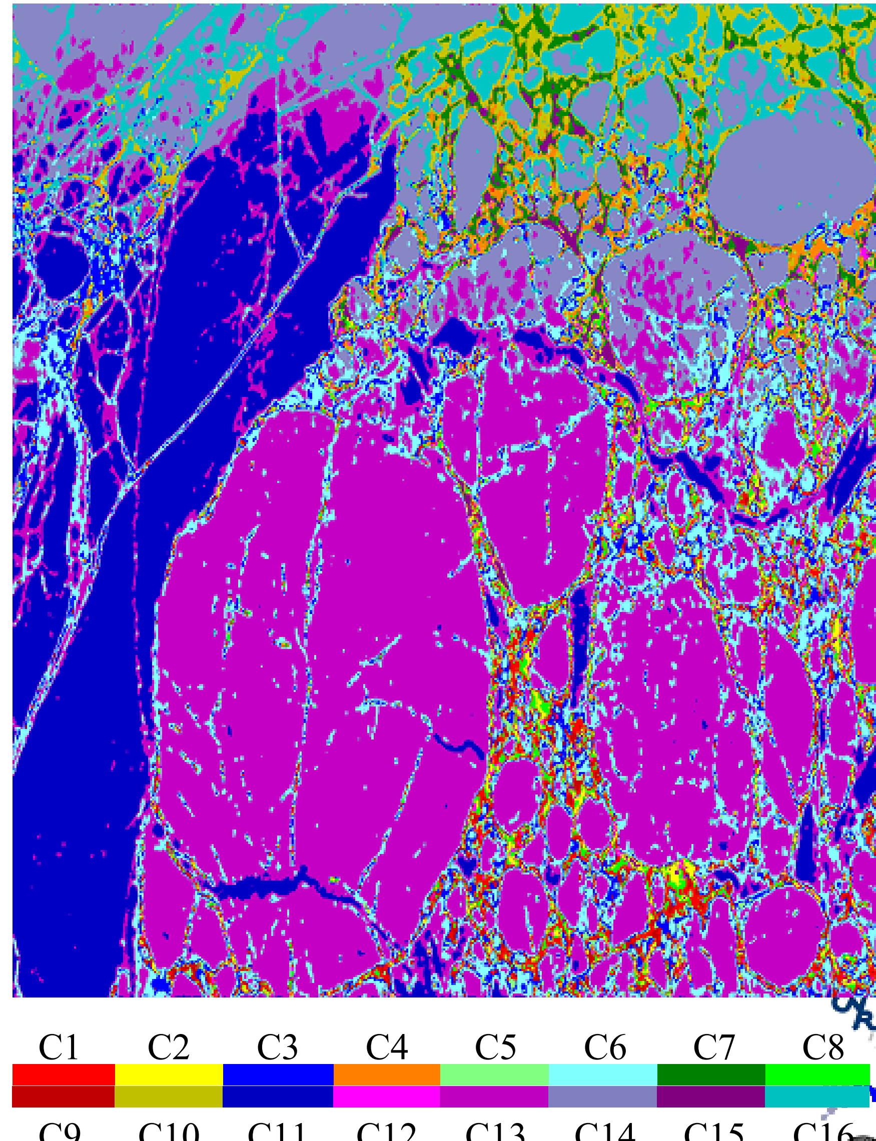

© E. Pottier, L. Ferro-Famil (01/2005)

H / A / $\underline{\alpha}$ - WISHART CLASSIFIER

DEATH VALLEY JPL - AIRSAR L-band

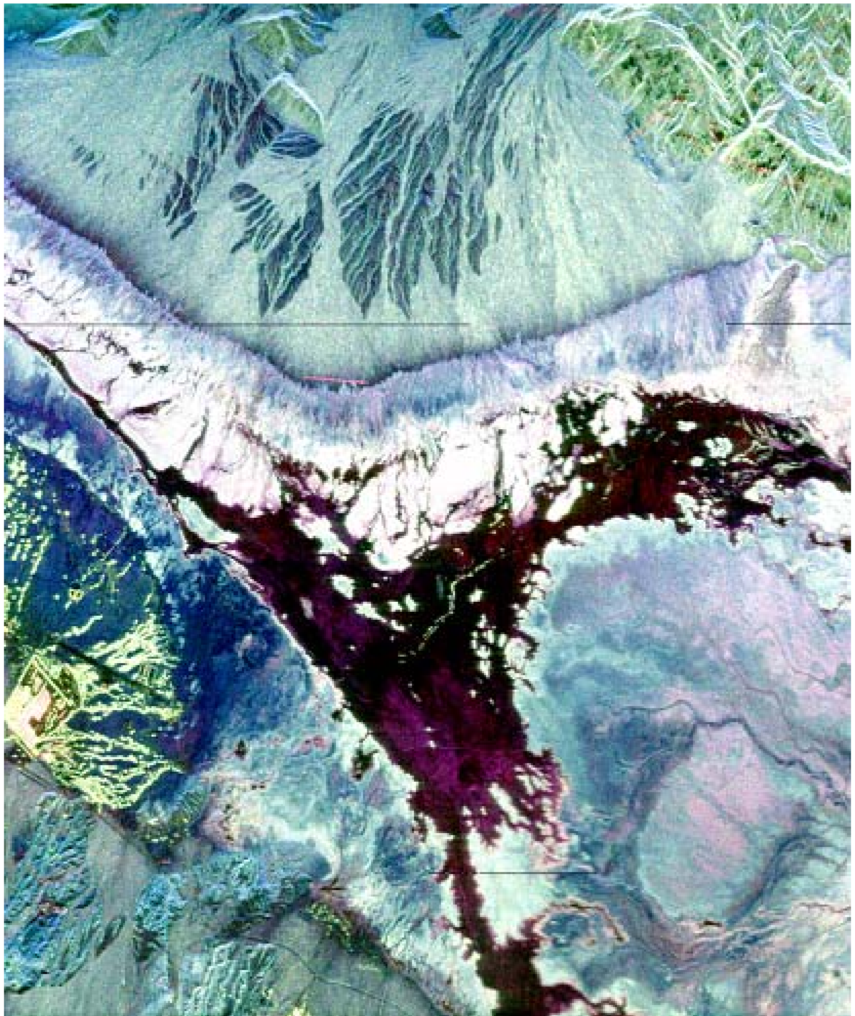

$2A_0$ $\quad B_0 + B$ $\quad B_0 - B$

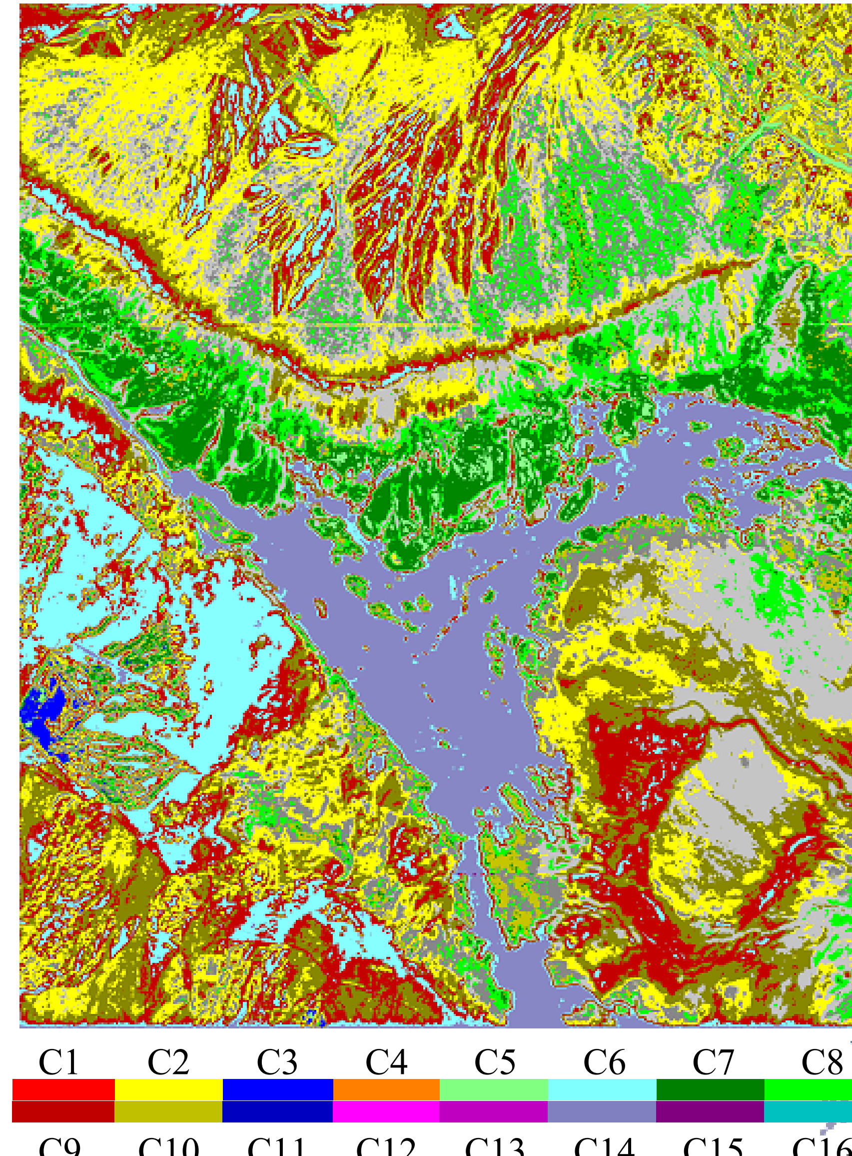

© E. Pottier, L. Ferro-Famil (01/2005)

H / A / $\underline{\alpha}$ - WISHART CLASSIFIER

OBERPFAFFENHOFEN - ESAR L-band

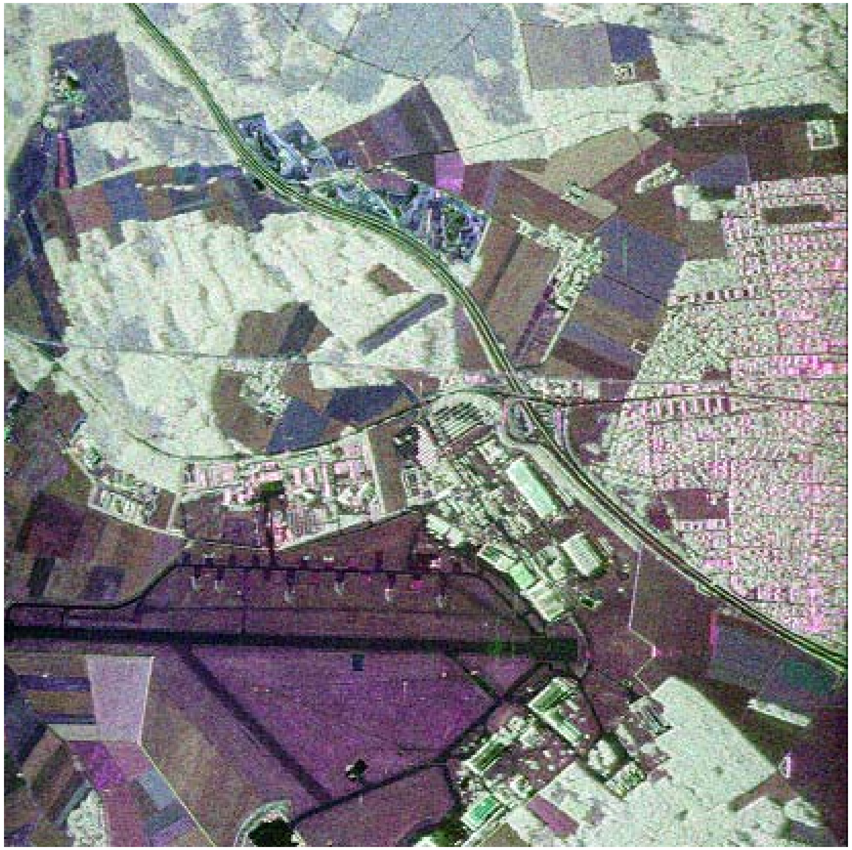

$2A_0$ $B_0 + B$ $B_0 - B$

H / A / $\underline{\alpha}$ and WISHART CLASSIFIER

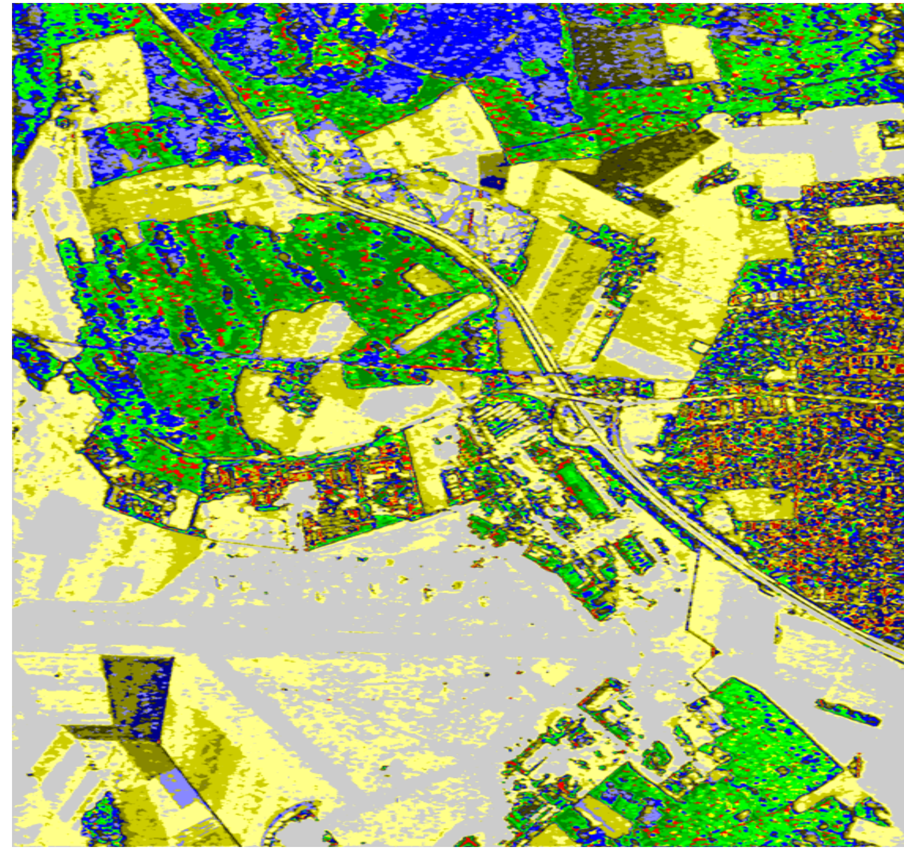

C1	C2	C3	C4	C5	C6	C7	C8
C9	C10	C11	C12	C13	C14	C15	C16

H / A / α - WISHART CLASSIFIER

SAPHIR

OBERPFAFFENHOFEN - ESAR L-band

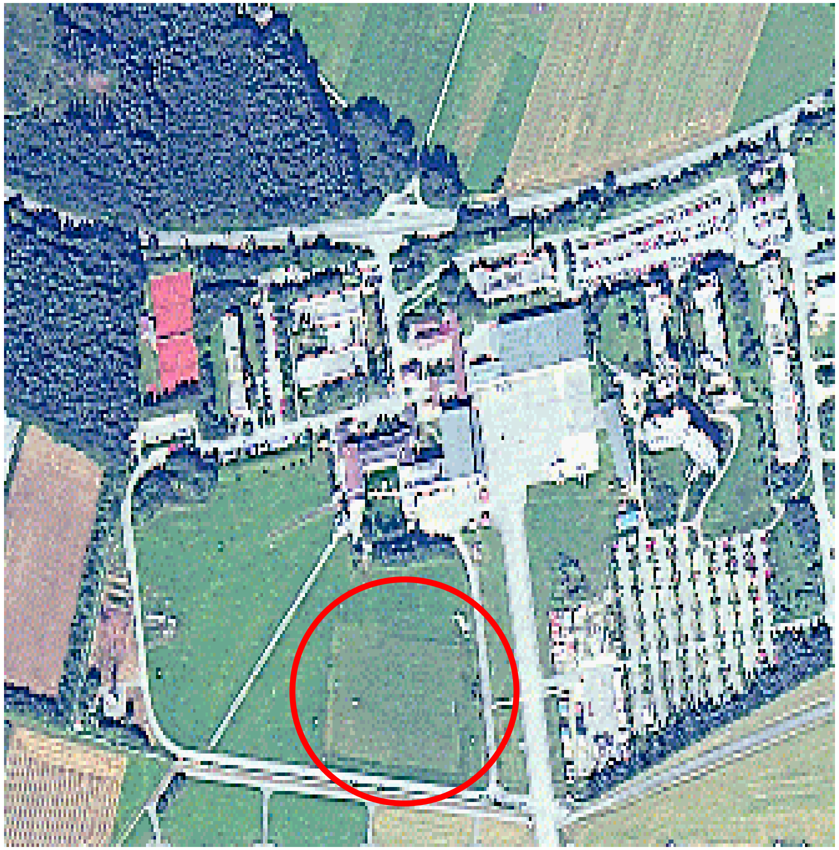

H / A / α and WISHART CLASSIFIER

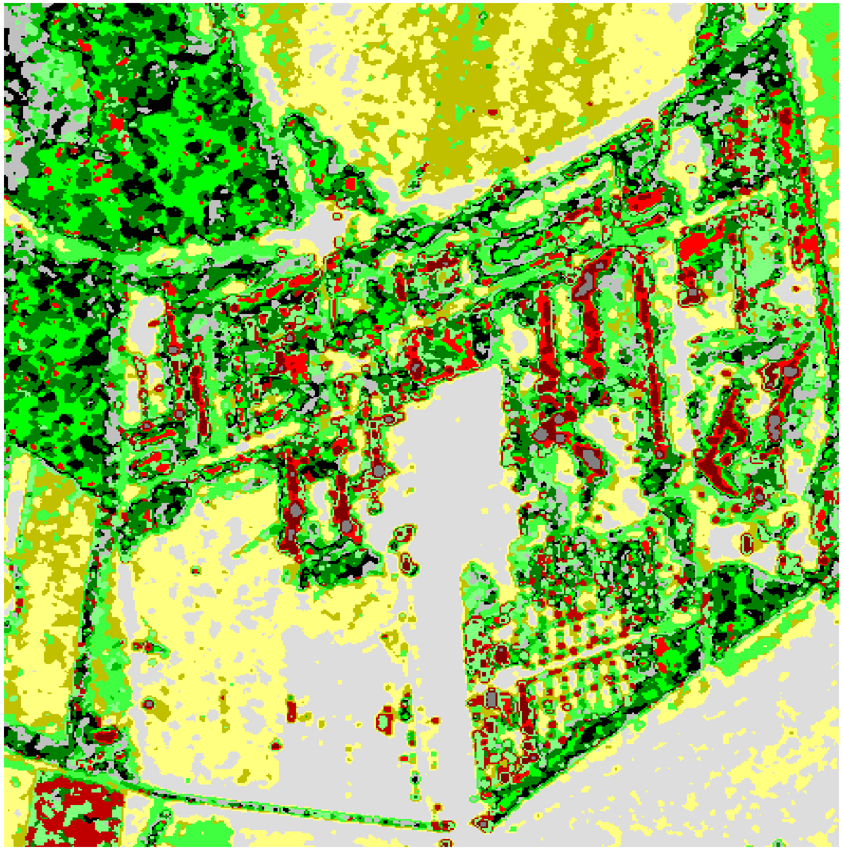

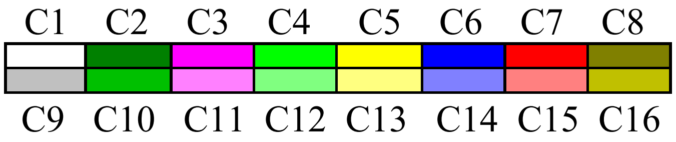

© IETR SAPHIR E. Pottier, L. Ferro-Famil (01/2005)

H / A / $\underline{\alpha}$ - WISHART CLASSIFIER

esa POLinSAR Project

TRAUNSTEIN - ESAR L-band

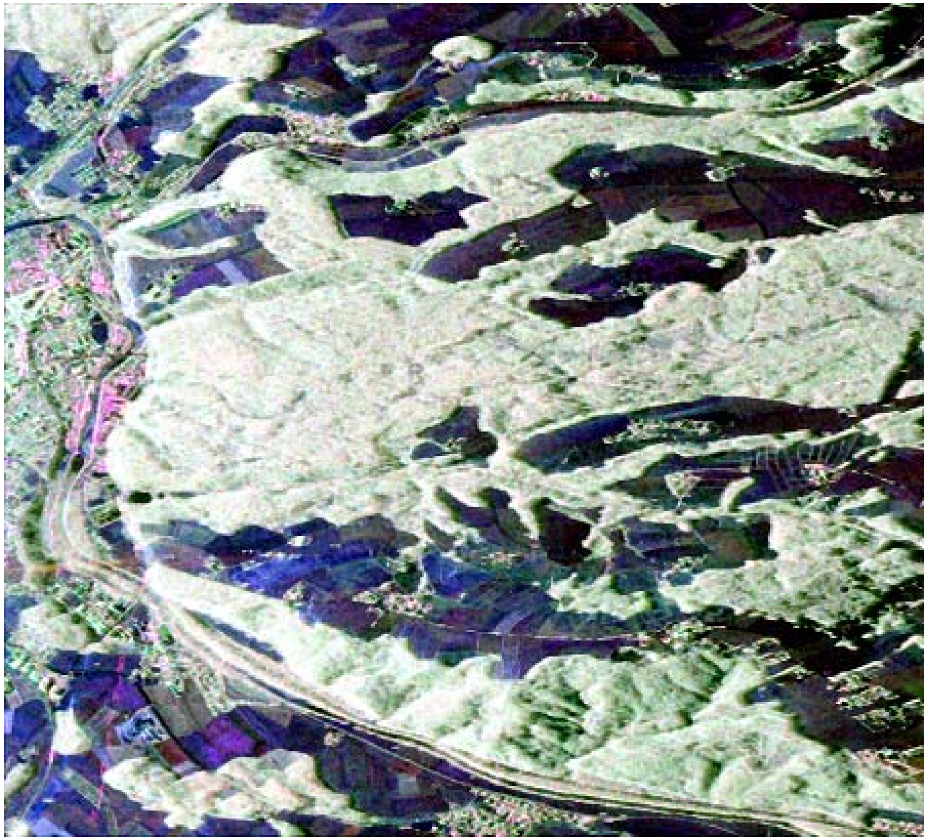

$2A_0$ $B_0 + B$ $B_0 - B$

H / A / $\underline{\alpha}$ and WISHART CLASSIFIER

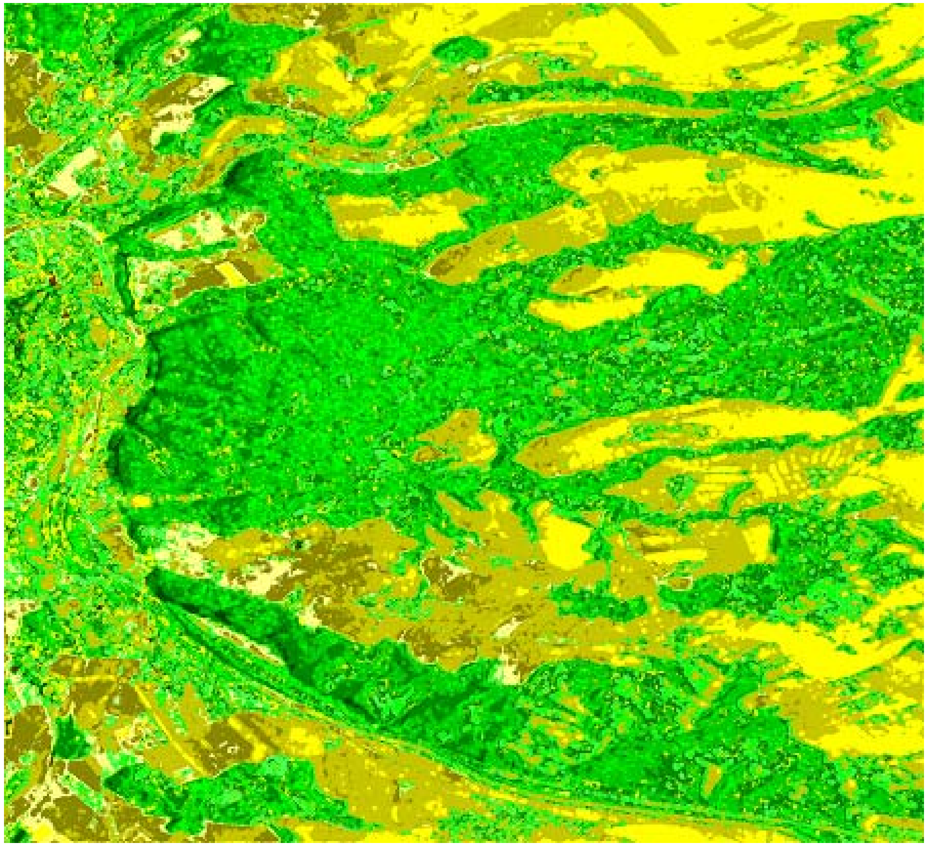

C1	C2	C3	C4	C5	C6	C7	C8
C9	C10	C11	C12	C13	C14	C15	C16

© IETR SAPHIR E. Pottier, L. Ferro-Famil (01/2005)

WISHART PDF

$$P(\langle[T]\rangle/[T_m]) = \frac{L^{Lp}\left|\langle[T]\rangle\right|^{L-p} e^{-LTr\left([T_m]^{-1}\langle[T]\rangle\right)}}{\pi^{\frac{p(p-1)}{2}}\Gamma(L)\ldots\Gamma(L-p+1)\left|[T_m]\right|^{L}}$$

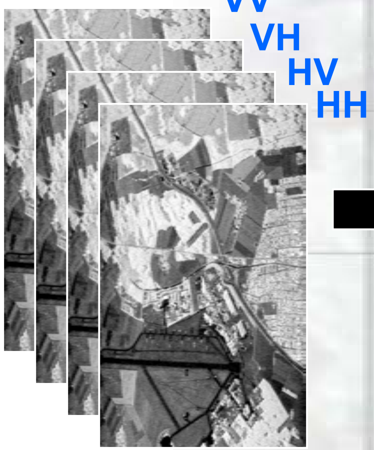

UNSUPERVISED POLSAR CLASSIFICATION

E.POTTIER, J.S LEE (2000)

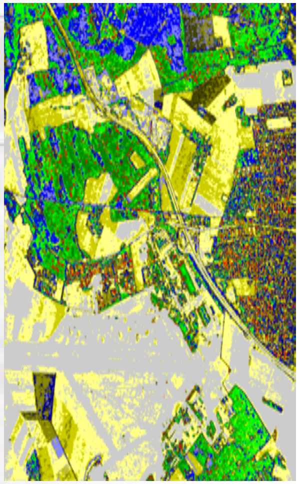

Unsupervised Classification Preserving Scattering Mechanisms

J.S. Lee, M. R. Grunes, E. Pottier, L. Ferro-Famil, "Unsupervised Terrain Classification Preserving Polarimetric Scattering Characteristics," IEEE TGRS, April 2004

FREEMAN DECOMPOSITION

Courtesy of Dr J.S Lee

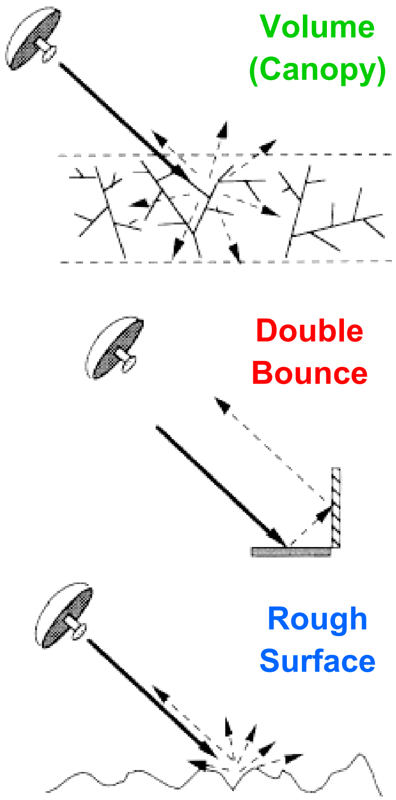

|HH-VV|, |HV|, |HH+VV|

Freeman and Durden

A. Freeman and S.L. Durden, "A Three-Component Scattering Model for Polarimetric SAR Data" IEEE TGRS, vol. 36, no. 3, May 1998

PROCEDURE – FLOW CHART

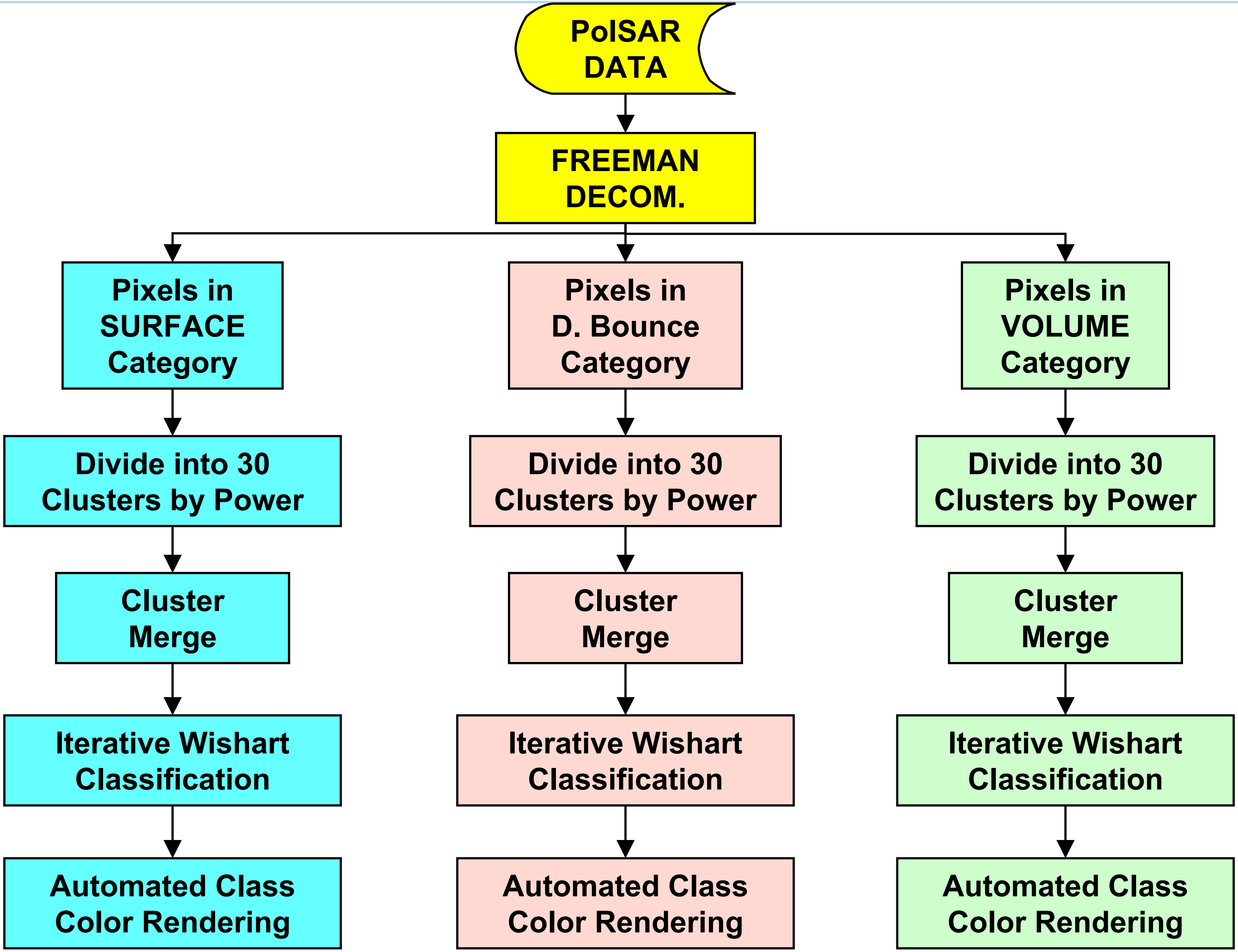

FREEMAN - WISHART CLASSIFIER

Courtesy of Dr J.S Lee

|HH-VV|, |HV|, |HH+VV|

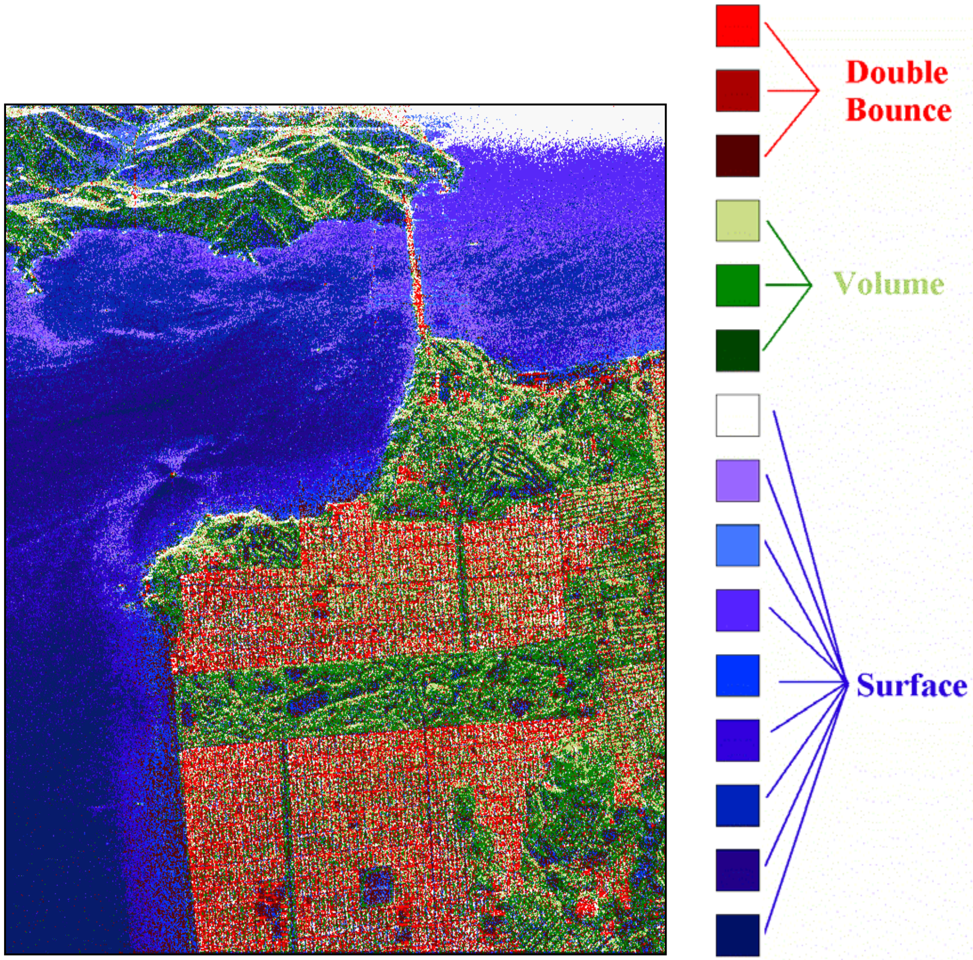

4th Iteration (15 classes)

Courtesy of Dr J.S Lee

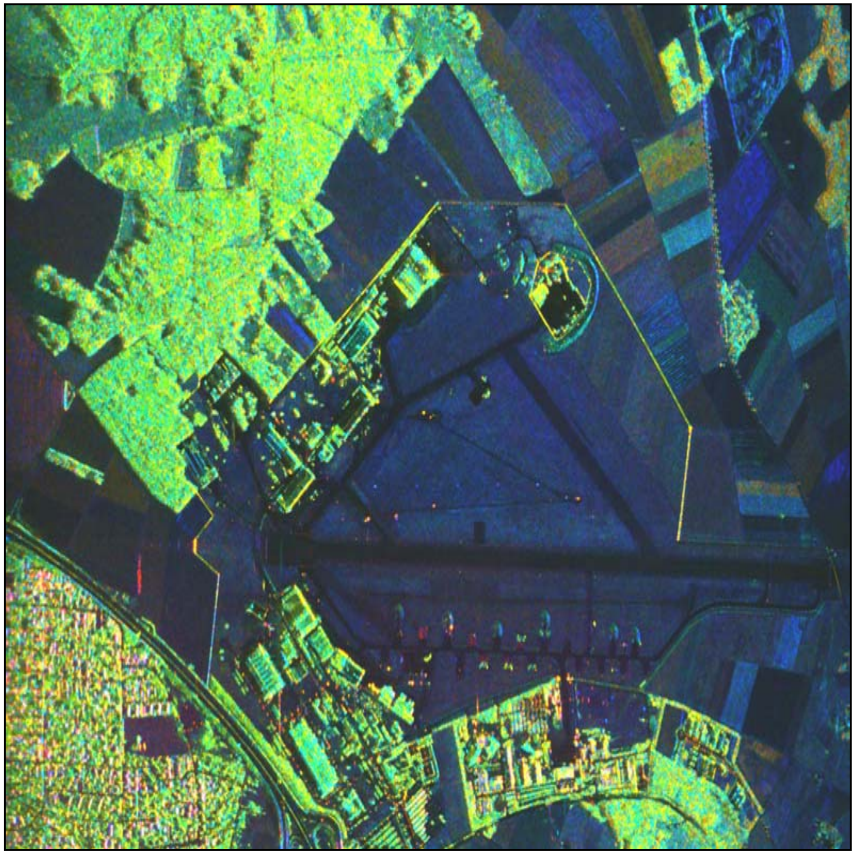

$2A_0$ $B_0 + B$ $B_0 - B$

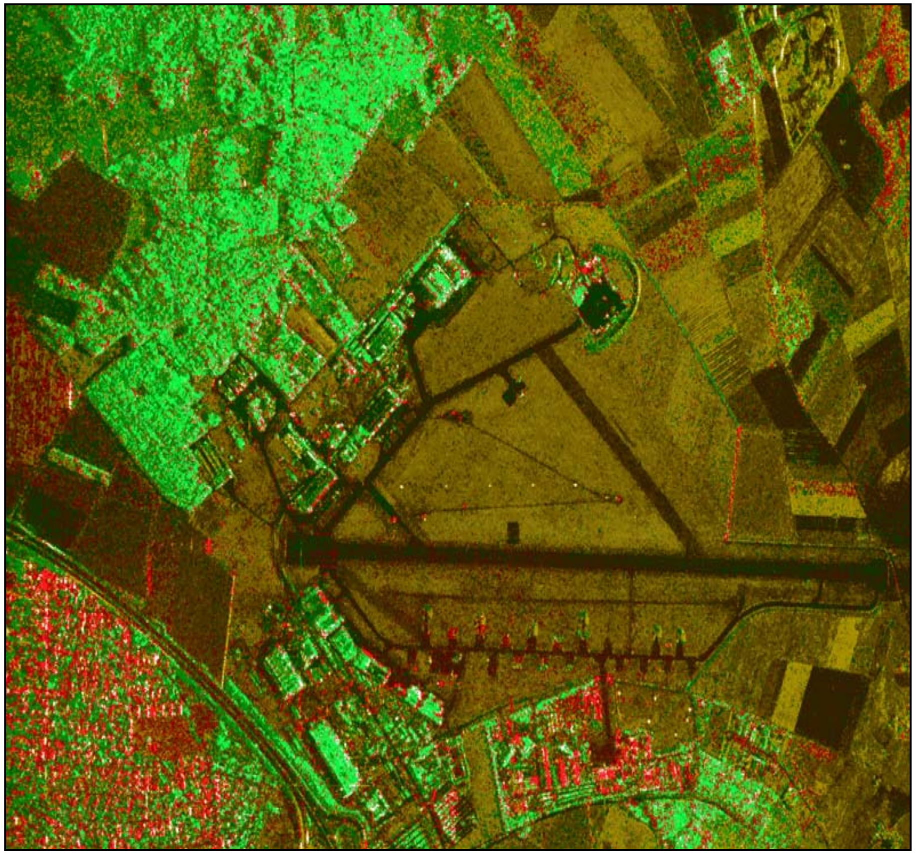

4th Iteration (15 classes)

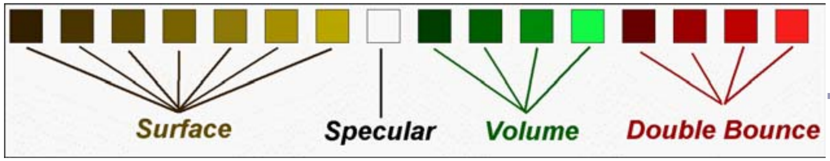

POLARIMETRIC REMOTE SENSING

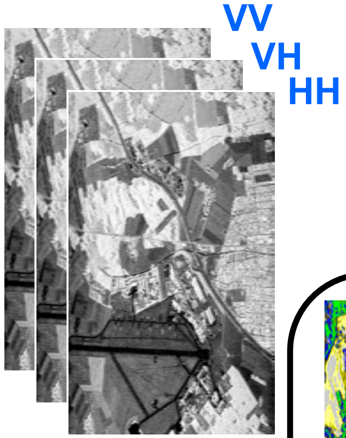

WISHART PDF

$$P(\langle[T]\rangle/[T_m]) = \frac{L^{Lp}\left|\langle[T]\rangle\right|^{L-p} e^{-LTr\left([T_m]^{-1}\langle[T]\rangle\right)}}{\pi^{\frac{p(p-1)}{2}}\Gamma(L)\ldots\Gamma(L-p+1)\left|[T_m]\right|^{L}}$$

POLINSAR CLASSIFICATION

L. FERRO-FAMIL, E.POTTIER, J.S LEE (2002)

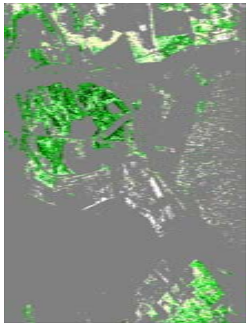

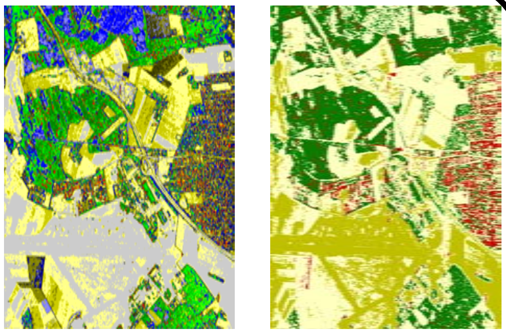

POLSAR CLASSIFICATION

OPTIMUM INTERFEROMETRIC COHERENCES SPECTRUM

POLARIMETRY AND INTERFEROMETRY

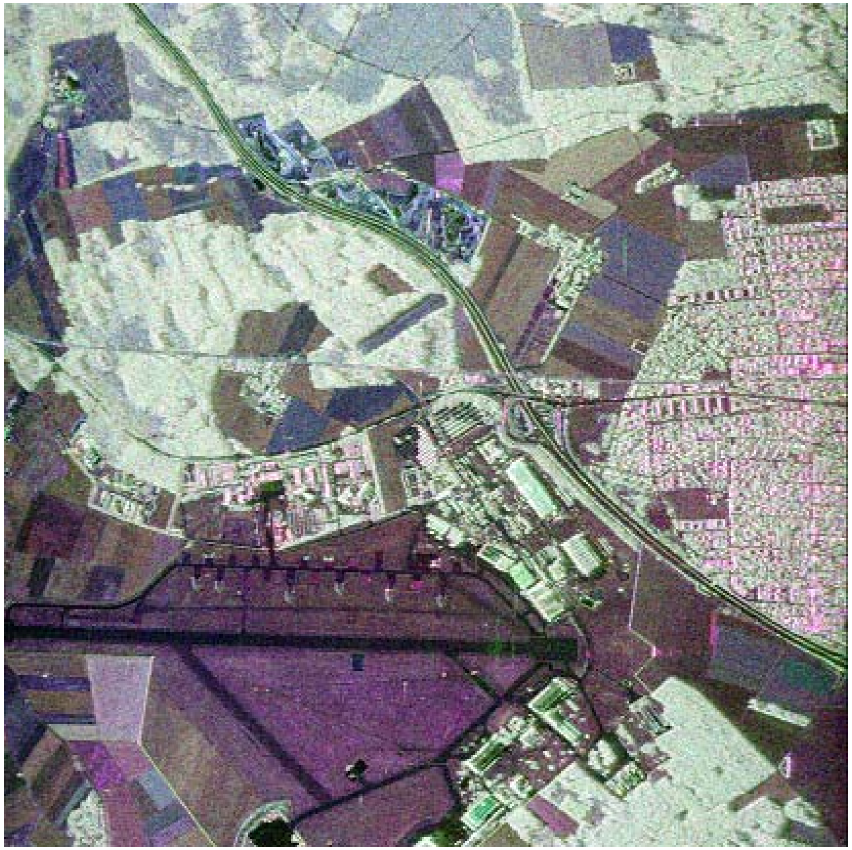

DLR E-SAR L Band
In-Pol SAR (1.5m x 3m) – Baseline 5m

POL-SAR INFORMATION

IN-SAR INFORMATION γ

COMPLEMENTARY INFORMATION

POLARIMETRY AND INTERFEROMETRY

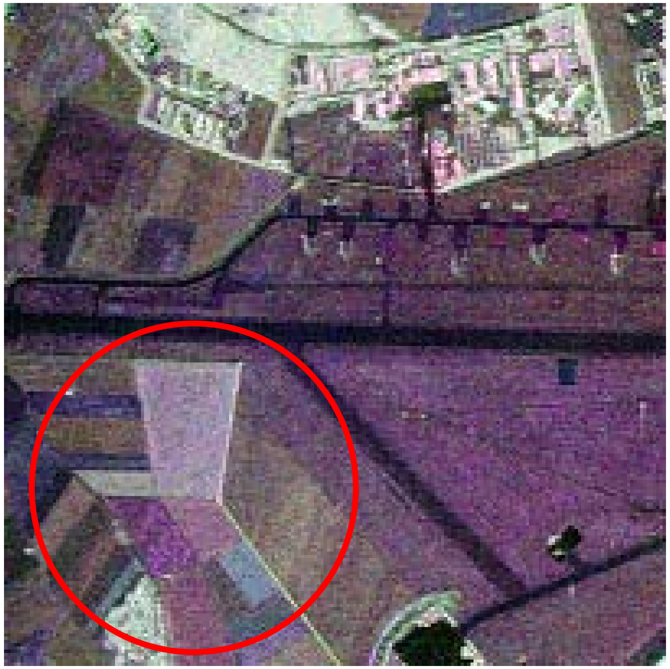

HETEROGENEOUS AREA

DIFFERENT POLARIMETRIC SCATTERING MECHANISMS

HOMOGENEOUS AREA

CONSTANT INTERFEROMETRIC COHERENCE

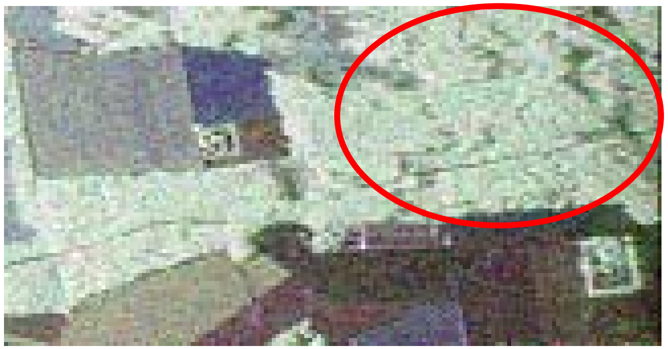

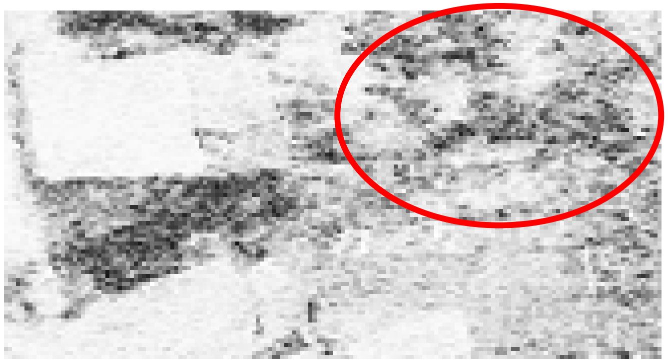

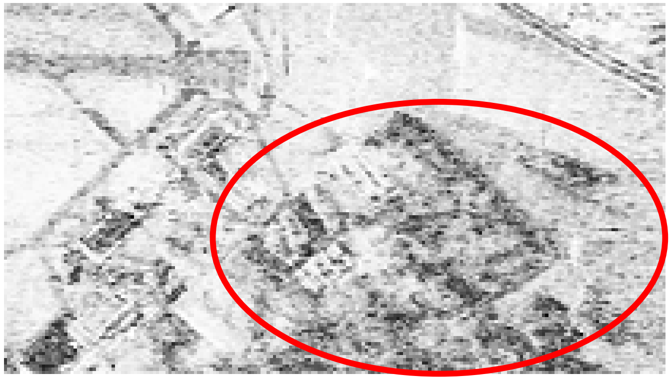

HOMOGENEOUS AREA

HETEROGENEOUS AREA

SAME POLARIMETRIC SCATTERING MECHANISMS

DIFFERENT INTERFEROMETRIC COHERENCE

POLARIMETRY AND INTERFEROMETRY

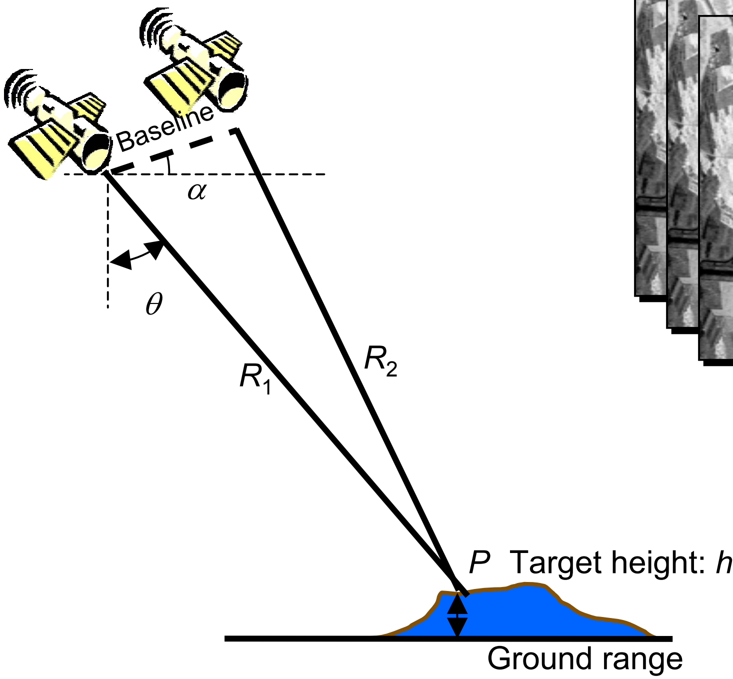

$$\underline{k}_1 = \frac{1}{\sqrt{2}}\begin{bmatrix} S_{XX_1} + S_{YY_1} \\ S_{XX_1} - S_{YY_1} \\ 2S_{XY_1} \end{bmatrix}$$

$$\underline{\underline{k}} = \begin{bmatrix} \underline{k}_1 \\ \underline{k}_2 \end{bmatrix}$$

POLARIMETRIC INTERFEROMETRIC TARGET VECTOR

$$\underline{k}_2 = \frac{1}{\sqrt{2}}\begin{bmatrix} S_{XX_2} + S_{YY_2} \\ S_{XX_2} - S_{YY_2} \\ 2S_{XY_2} \end{bmatrix}$$

POLARIMETRY AND INTERFEROMETRY

$$\underline{\underline{k}} = \begin{bmatrix} \underline{k}_1 \\ \underline{k}_2 \end{bmatrix}$$

POLARIMETRIC INTERFEROMETRIC TARGET VECTOR

$$\langle [T_6] \rangle = \langle \underline{\underline{k}} \cdot \underline{\underline{k}}^{T*} \rangle = \begin{bmatrix} \langle \underline{k}_1 \cdot \underline{k}_1^{T*} \rangle & \langle \underline{k}_1 \cdot \underline{k}_2^{T*} \rangle \\ \langle \underline{k}_2 \cdot \underline{k}_1^{T*} \rangle & \langle \underline{k}_2 \cdot \underline{k}_2^{T*} \rangle \end{bmatrix} = \begin{bmatrix} \langle [T_1] \rangle & \langle [\Omega_{12}] \rangle \\ \langle [\Omega_{12}]^{T*} \rangle & \langle [T_2] \rangle \end{bmatrix}$$

POLARIMETRIC INTERFEROMETRIC COHERENCY MATRIX (6x6)

$\langle [T_1] \rangle$ HERMITIAN POLARIMETRIC COHERENCY MATRIX (3x3)

$\langle [T_2] \rangle$ HERMITIAN POLARIMETRIC COHERENCY MATRIX (3x3)

$\langle [\Omega_{12}] \rangle$ NON HERMITIAN POLARIMETRIC INTER-COHERENCY MATRIX (3x3)

© IETR SAPHIR E. Pottier, L. Ferro-Famil (01/2005)

COMPLEX WISHART DISTRIBUTION

DUAL CHANNELS POLINSAR UNSUPERVISED SEGMENTATION

$$\langle [T_6] \rangle = \langle \underline{\underline{k}} \cdot \underline{\underline{k}}^{T*} \rangle = \begin{bmatrix} \langle \underline{k}_1 \cdot \underline{k}_1^{T*} \rangle & \langle \underline{k}_1 \cdot \underline{k}_2^{T*} \rangle \\ \langle \underline{k}_2 \cdot \underline{k}_1^{T*} \rangle & \langle \underline{k}_2 \cdot \underline{k}_2^{T*} \rangle \end{bmatrix} = \begin{bmatrix} \langle [T_1] \rangle & \langle [\Omega_{12}] \rangle \\ \langle [\Omega_{12}]^{T*} \rangle & \langle [T_2] \rangle \end{bmatrix}$$

POLARIMETRIC INTERFEROMETRIC COHERENCY MATRIX (6x6)

$\langle [T_6] \rangle$ FOLLOWS A WISHART DISTRIBUTION

$$P(\langle [T_6] \rangle / [\Sigma_m]) = \frac{|\langle [T_6] \rangle|^{L-p} \exp\left(-tr\left([\Sigma_m]^{-1} \langle [T_6] \rangle\right)\right)}{K(L,p)|[\Sigma_m]|^L} = W_C(L,[\Sigma_m])$$

L: Number of Look
p: Polarimetric Dimension

With: $K(L,p) = \frac{\pi^{\frac{p(p-1)}{2}}}{L^{Lp}} \Gamma(L) \ldots \Gamma(L-p+1)$

$[\Sigma m]$: Cluster Center of the class *m*

POLINSAR CLASSIFICATION PROCEDURE

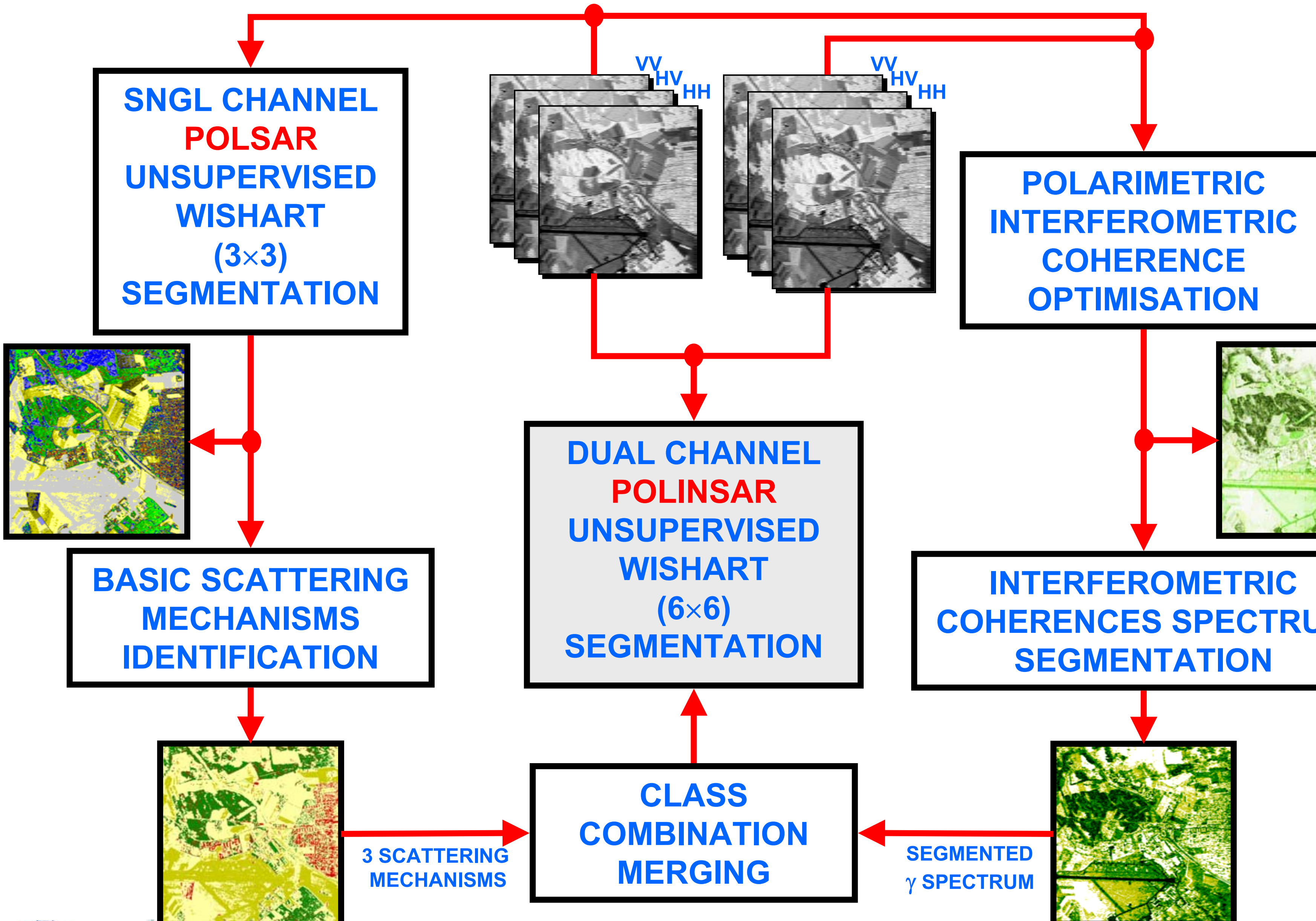

© *E. Pottier, L. Ferro-Famil (01/2005)*

CLASSIFICATION DETAILS: BUILDINGS AREAS

Optical Image

POLSAR Image

POLSAR Segmentation

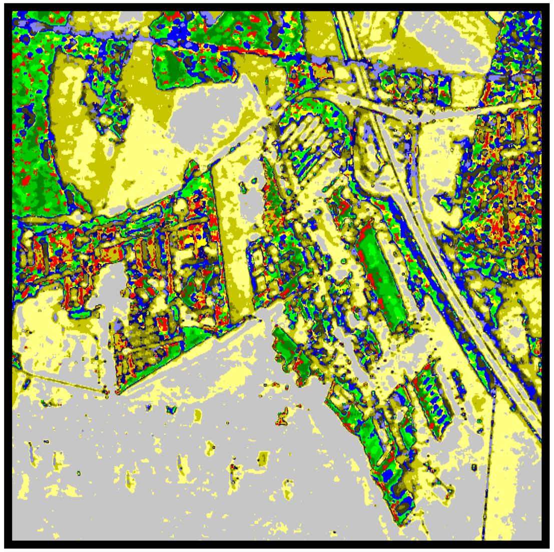

INSAR Image

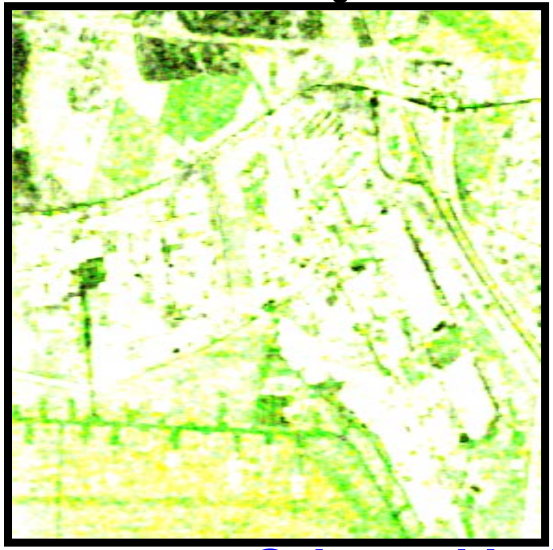

VOL POLINSAR Segmentation

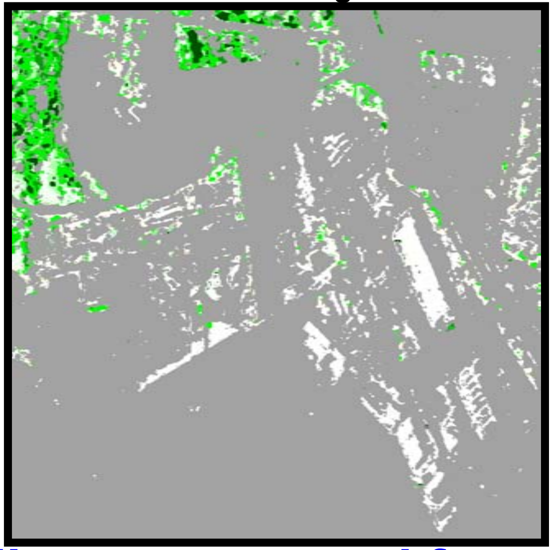

POLINSAR Segmentation

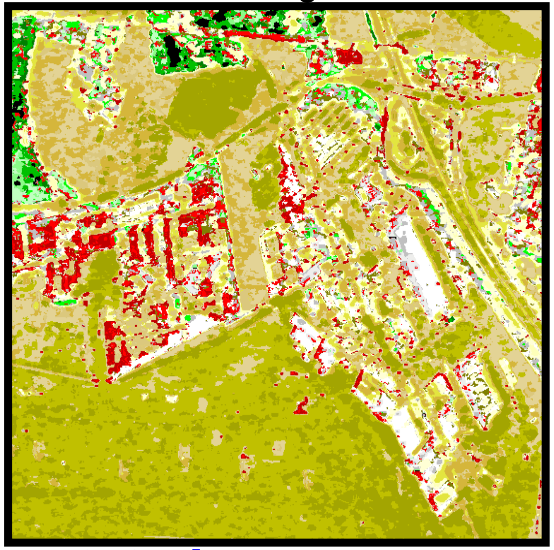

Oriented buildings segmented from vegetated areas

POLINSAR CLASSIFICATION PROCEDURE

esa POLinSAR Project

TRAUNSTEIN – ESAR – L-BAND

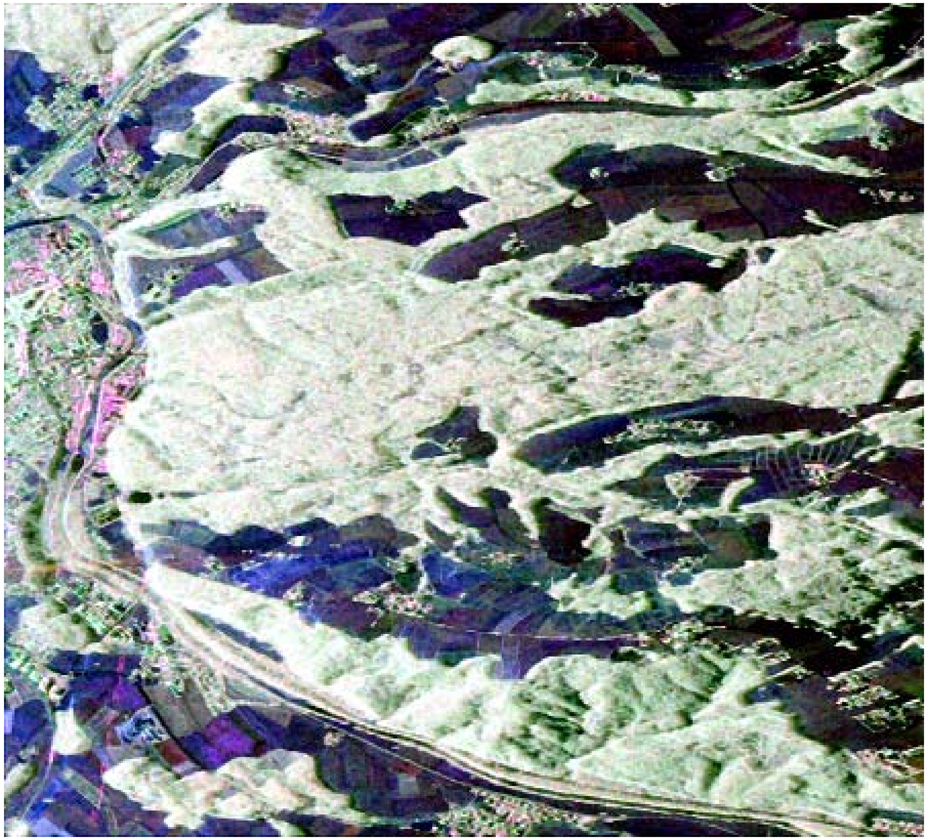

$2A_0$ $B_0 + B$ $B_0 - B$

TRAUNSTEIN – GROUND TRUTH

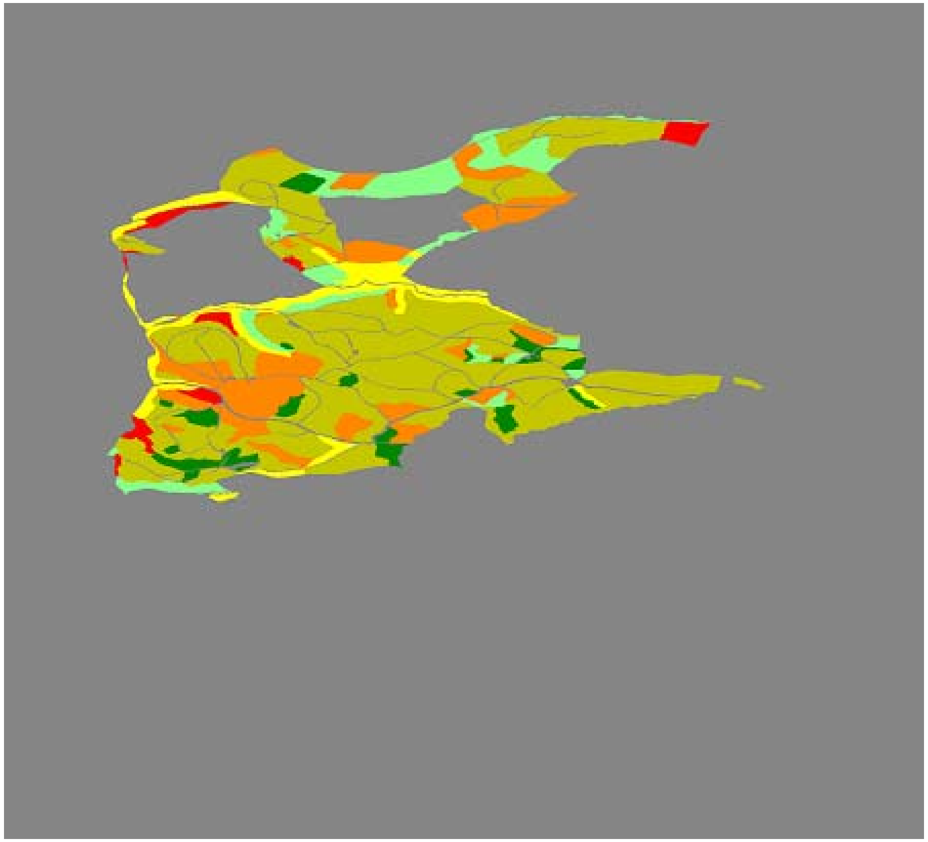

- Mature broadleaves
- Growth broadleaves
- Youth
- Mature conifer
- Growth conifer
- Plenter (heterogeneous)

DLR

© IETR SAPHIR *E. Pottier, L. Ferro-Famil (01/2005)*

POLINSAR CLASSIFICATION PROCEDURE

Ground Truth

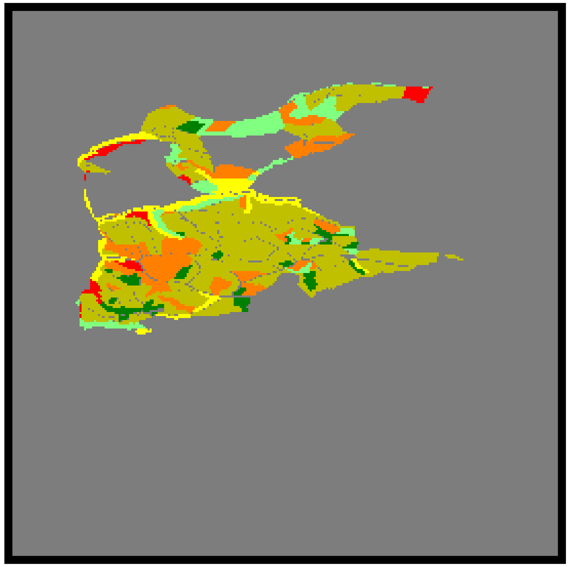

POLSAR Image

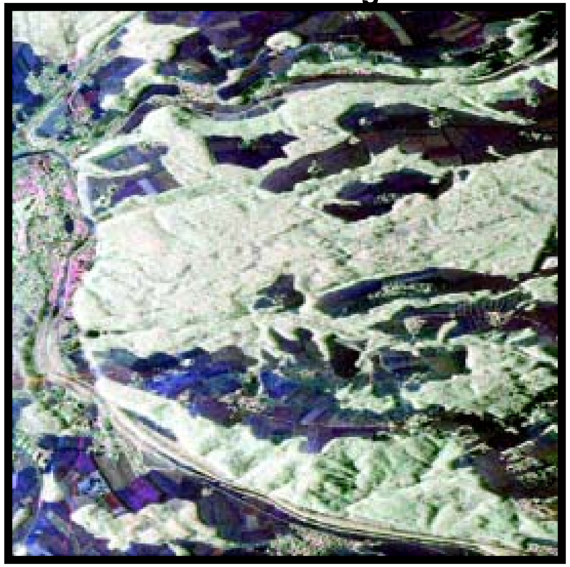

POLSAR Segmentation

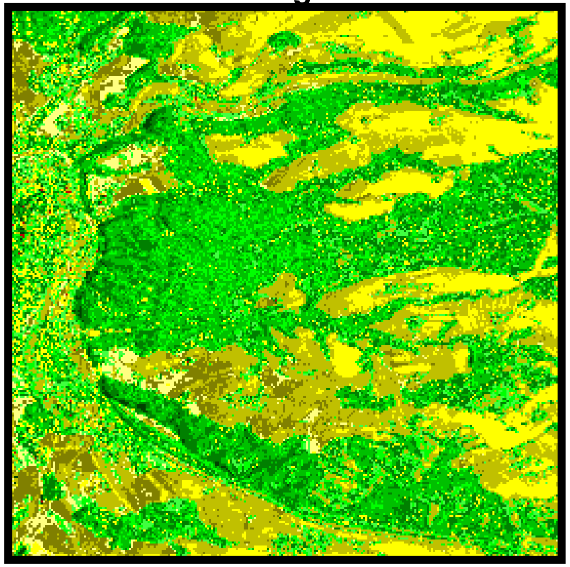

INSAR Image

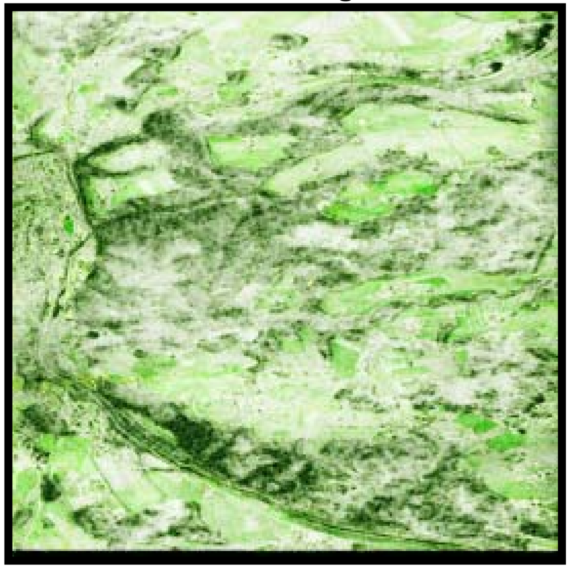

VOL POLINSAR Segmentation

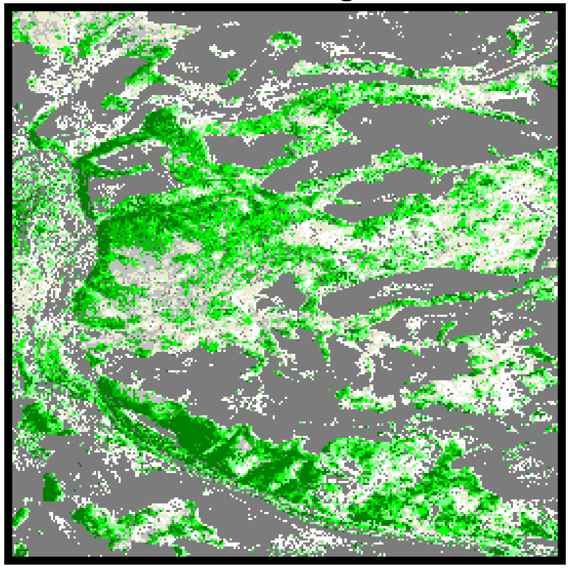

POLINSAR Segmentation

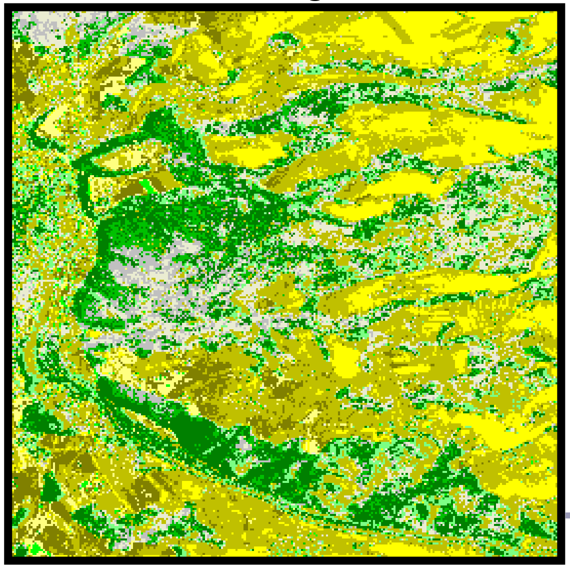

DATA INVERSION - APPROACH

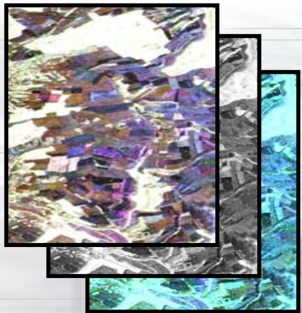

POLARIMETRIC
SAR DATA SET(S)

POLSAR - POLINSAR
DATA
PROCESSING

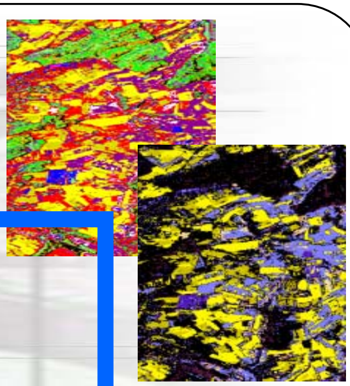

QUALITATIVE ANALYSIS

POLARIMETRIC
DESCRIPTORS
EXTRACTION

TWO-STEP INVERSION PROCEDURE

MODEL-BASED
PHYSICAL PARAMETER
INVERSION

BIO and GEO PHYSICAL
PARAMETERS

QUANTITATIVE ANALYSIS

© E. Pottier, L. Ferro-Famil (01/2005)

QUANTITATIVE ANALYSIS

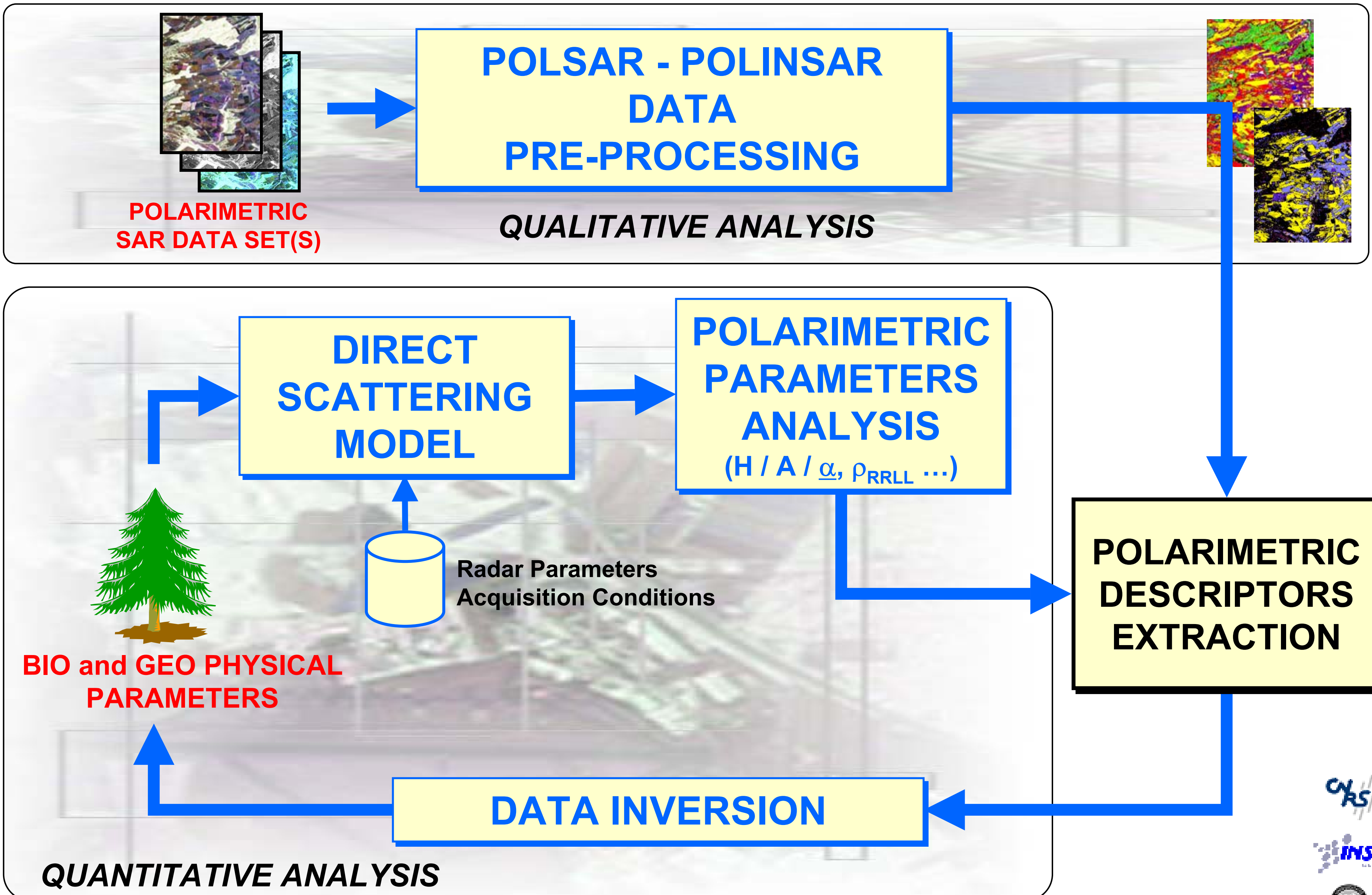

QUANTITATIVE ANALYSIS

DATA INVERSION

Nonlinear Parameter Estimation via Neural Nets (Learning - Training Phase)

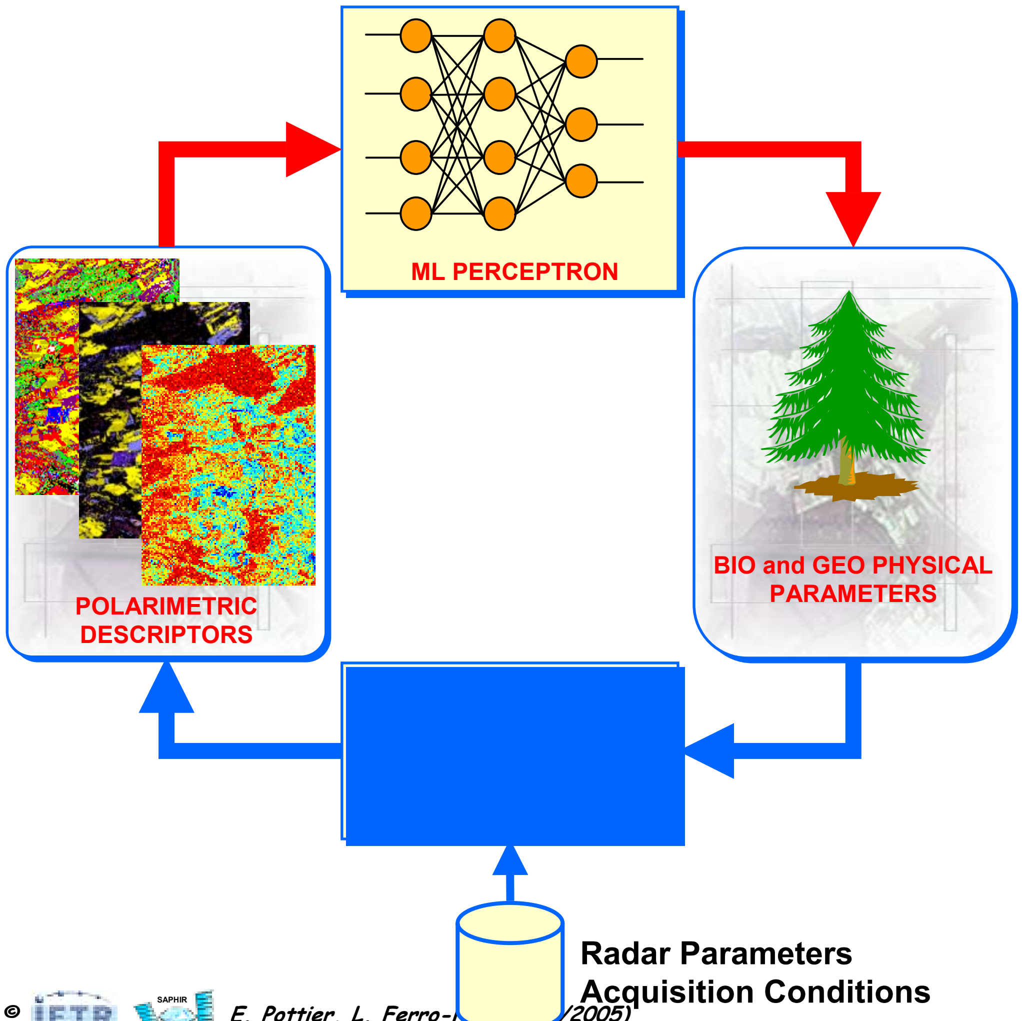

Look Up Table

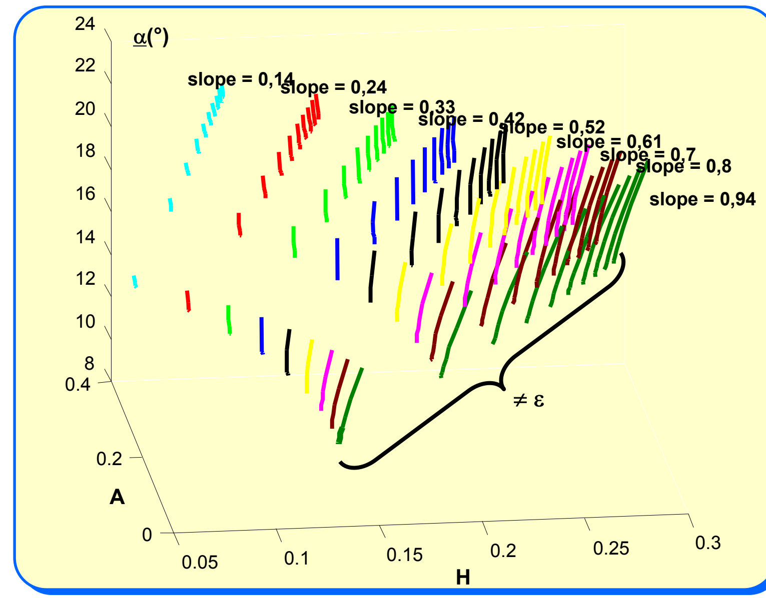

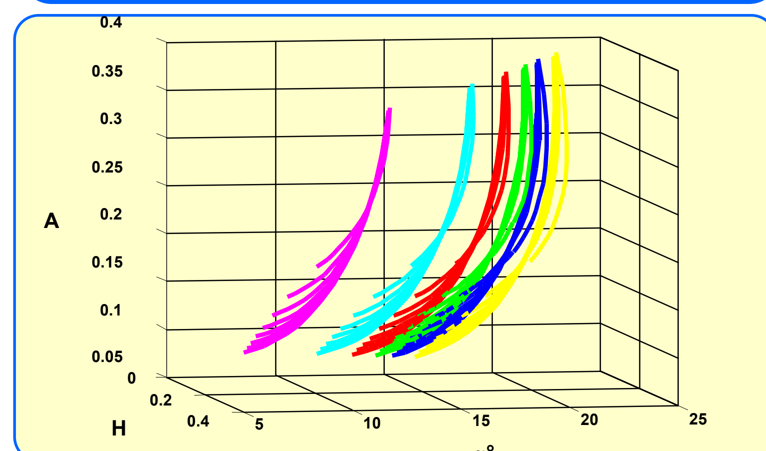

SNOW MONITORING – DRY SNOW MAPPING

SIR-C DATA - FRENCH ALPS – RISOUL –1994

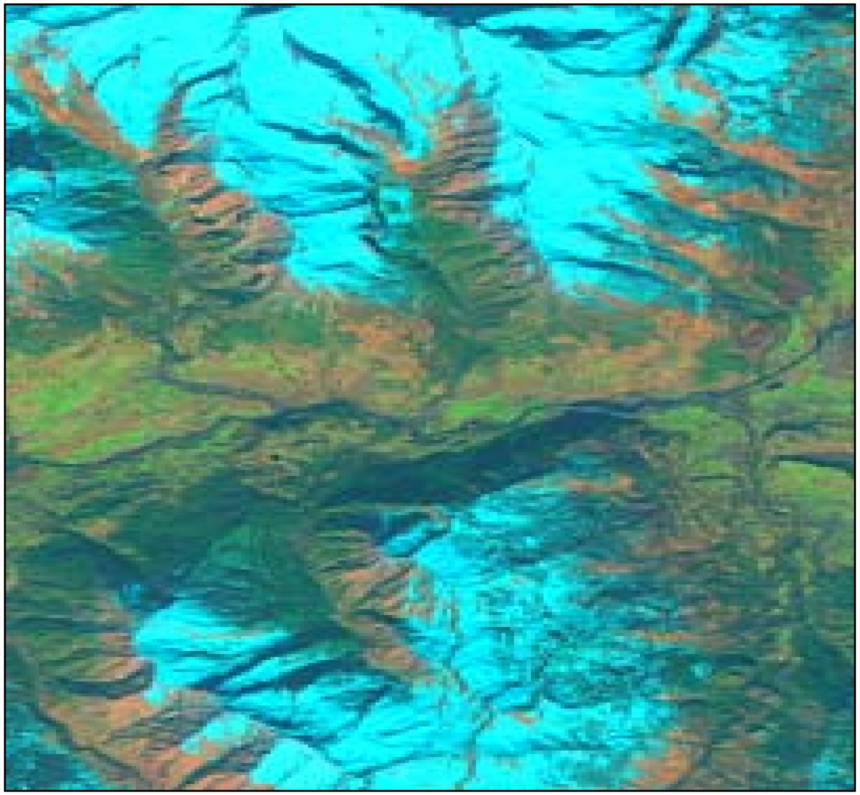

LANDSAT OPTICAL IMAGE

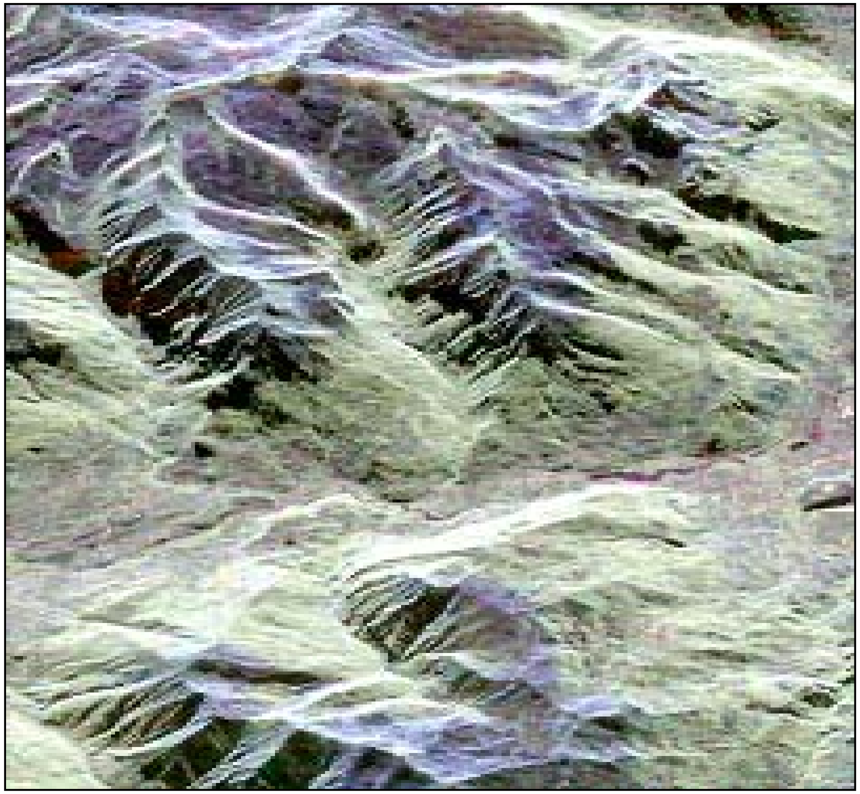

PAULI – RGB IMAGE

- Bare Soil
- Agricultural Fields
- Pasture Fields
- Dense Forest
- Snow

SNOW MONITORING – DRY SNOW MAPPING

SIR-C DATA - FRENCH ALPS – RISOUL –1994

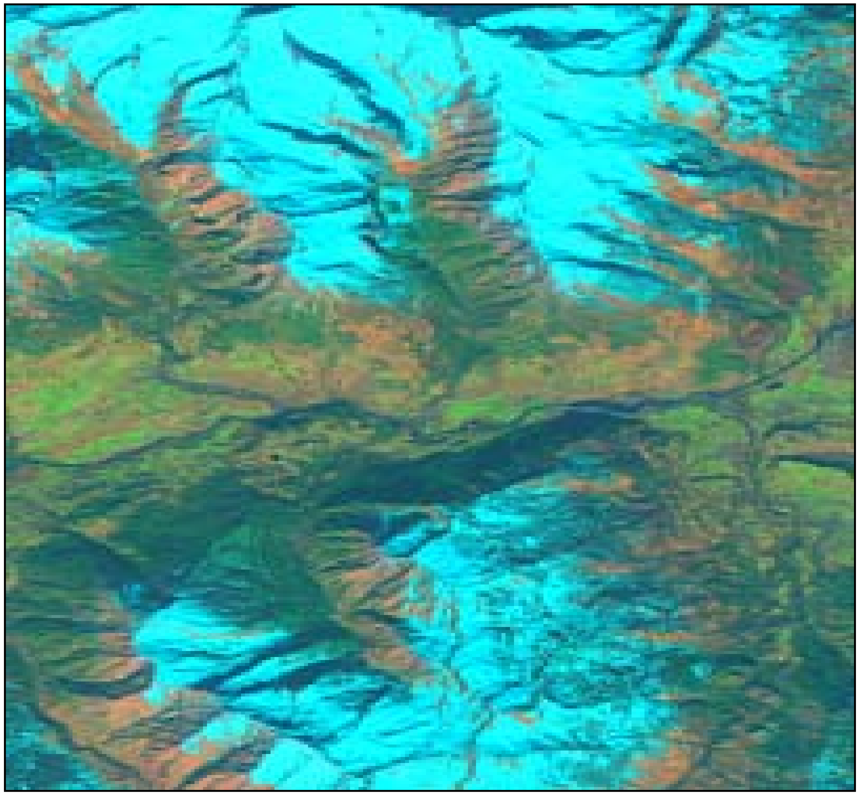

LANDSAT OPTICAL IMAGE

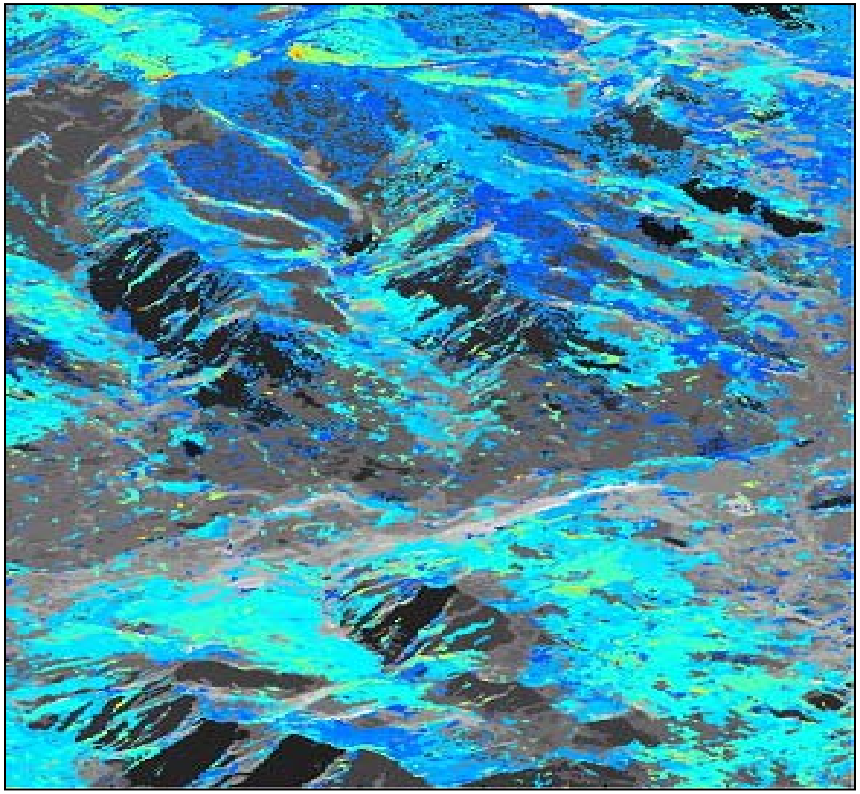

DRY SNOW MAPPING

Bare Soil
Agricultural Fields
Pasture Fields
Dense Forest
Snow

Polarimetric Contrast Variation Enhancement (PVCE) over surfaces $\Delta\underline{\alpha}$ from summer to winter over forests

Audrey Martini – POLinSAR 05 / Wednesday - AM

LAND – AGRICULTURE APPLICATIONS

Soil Moisture & Biomass Estimation using Polarimetric Scattering Theory

- Oh
- Shi
- Dubois
- Francesco Mattia
- X-Bragg (I. Hajnsek - 2000)
- E.R.D (S. Allain - 2003)

QUANTITATIVE ANALYSIS

LAND – AGRICULTURE APPLICATIONS

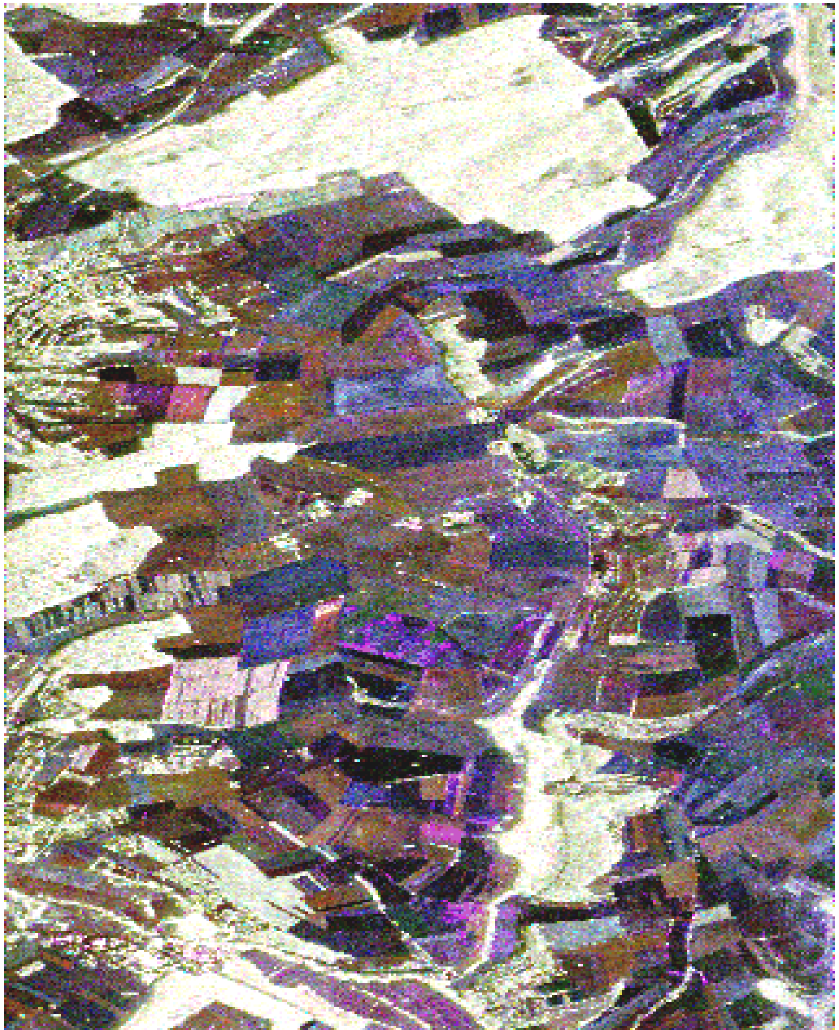

WEIHERBACHTAL   DLR - ESAR   L-band

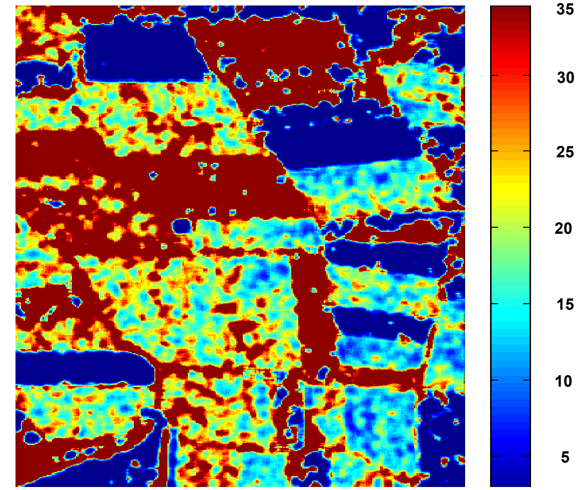

X-Bragg Model (H, $\underline{\alpha}$)

Estimated Volumetric Moisture (mv/vol%)

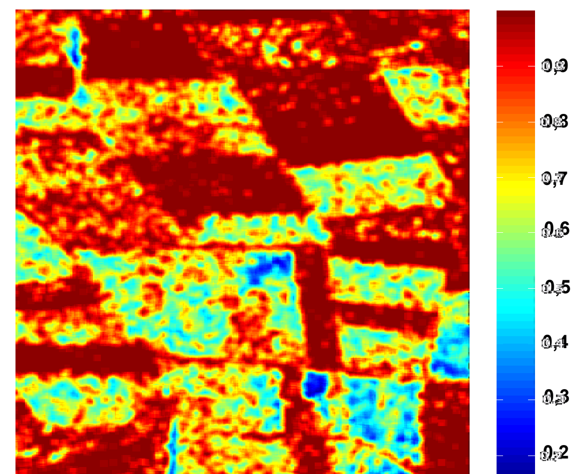

Anisotropy (A)

Soil Surface Roughness (*ks*)

© E. Pottier, L. Ferro-Famil (01/2005)

QUANTITATIVE ANALYSIS

LAND – AGRICULTURE APPLICATIONS

E.R.D : Eigenvalue Relative Difference

ALLING Site
DLR – ESAR
L-band

LAND – AGRICULTURE APPLICATIONS

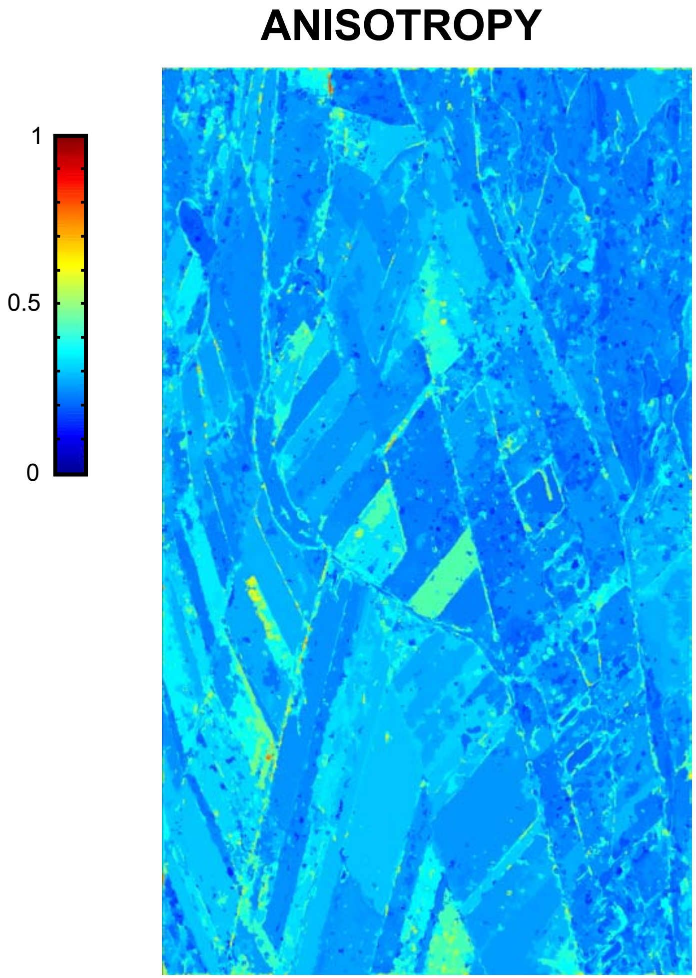

homogenous value
less information

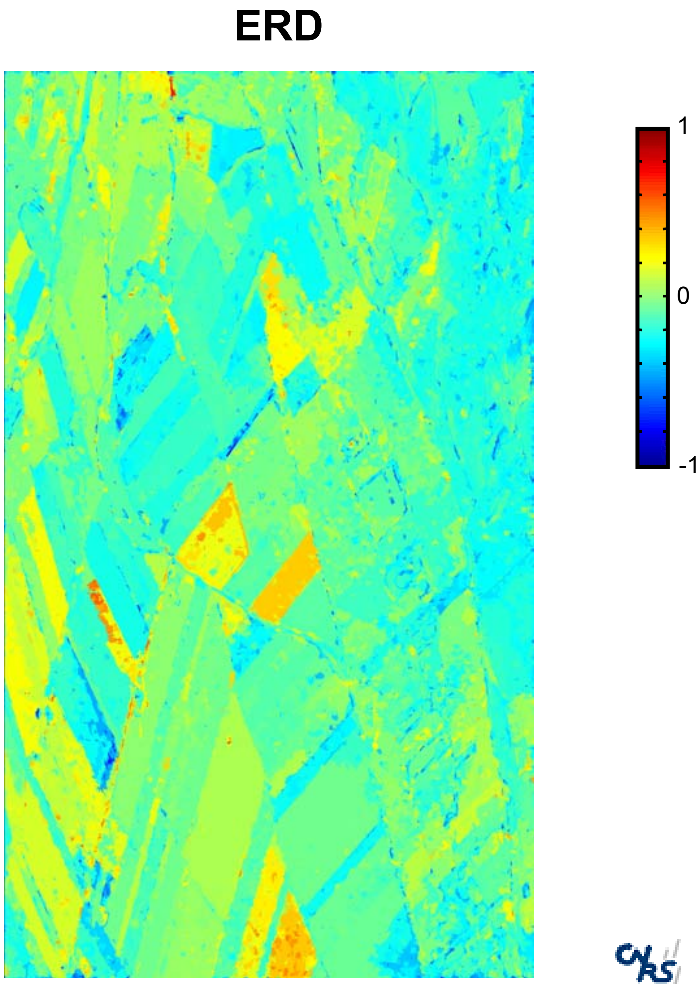

better discrimination

QUANTITATIVE ANALYSIS

LAND – AGRICULTURE APPLICATIONS

ANISOTROPY

ERD

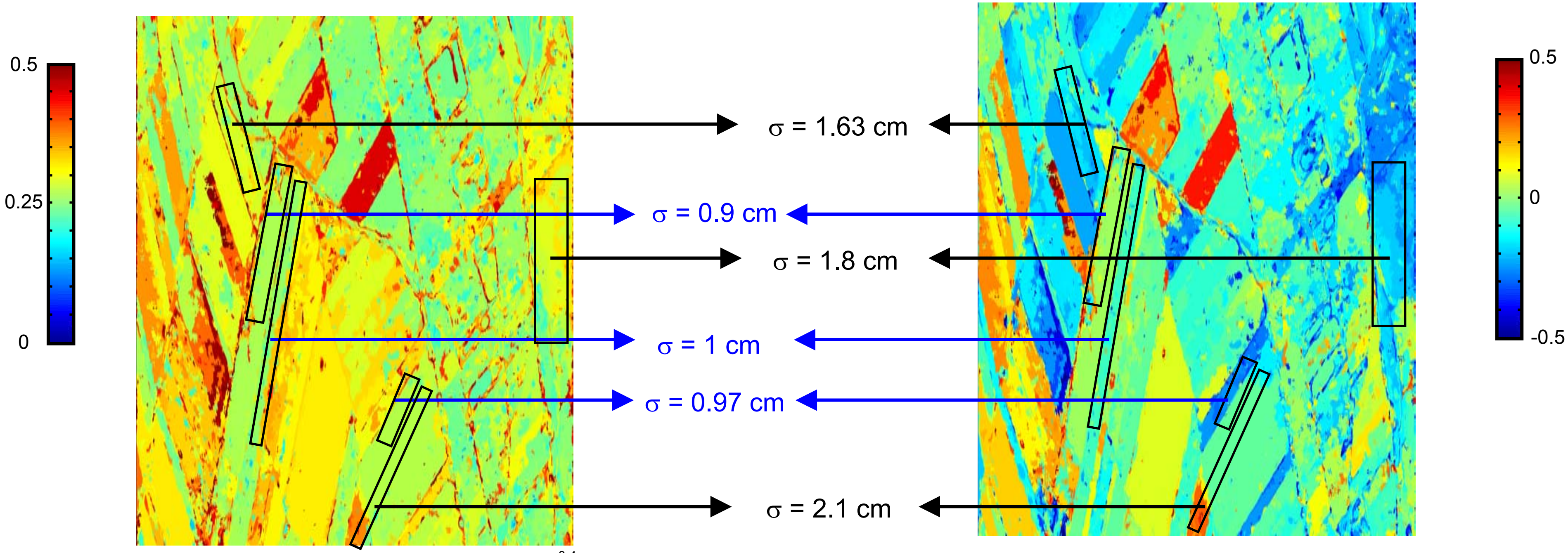

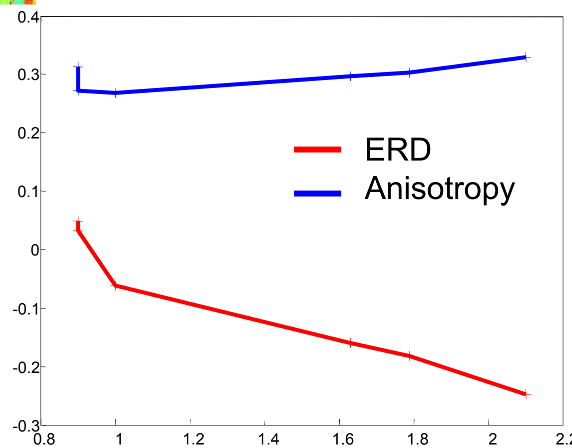

Better roughness discrimination with ERD

© E. Pottier, L. Ferro-Famil (01/2005)

QUANTITATIVE ANALYSIS

LAND – AGRICULTURE APPLICATIONS

ANISOTROPY

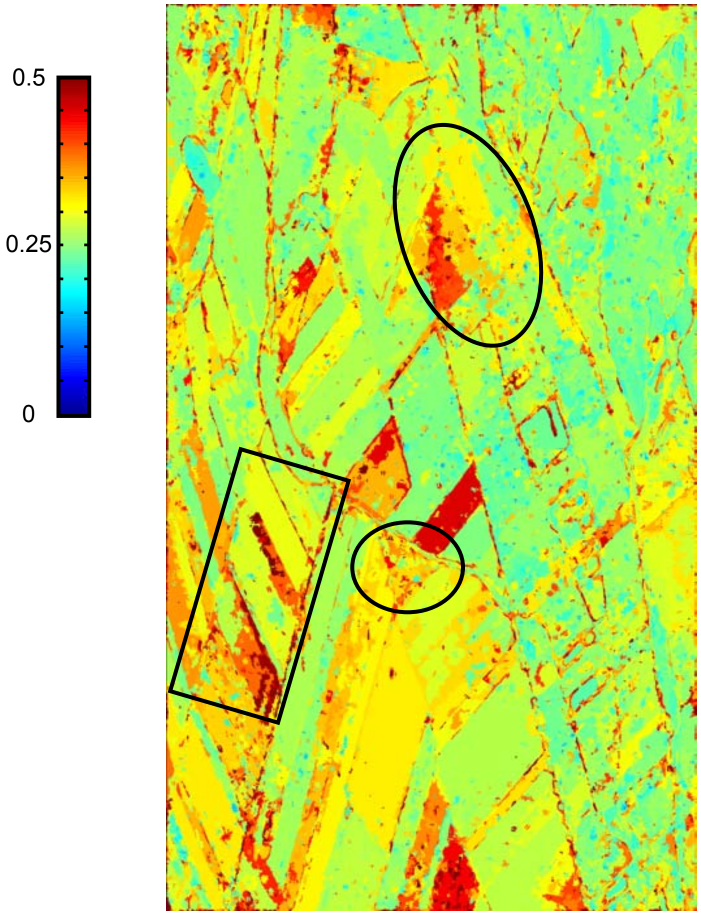

ERD

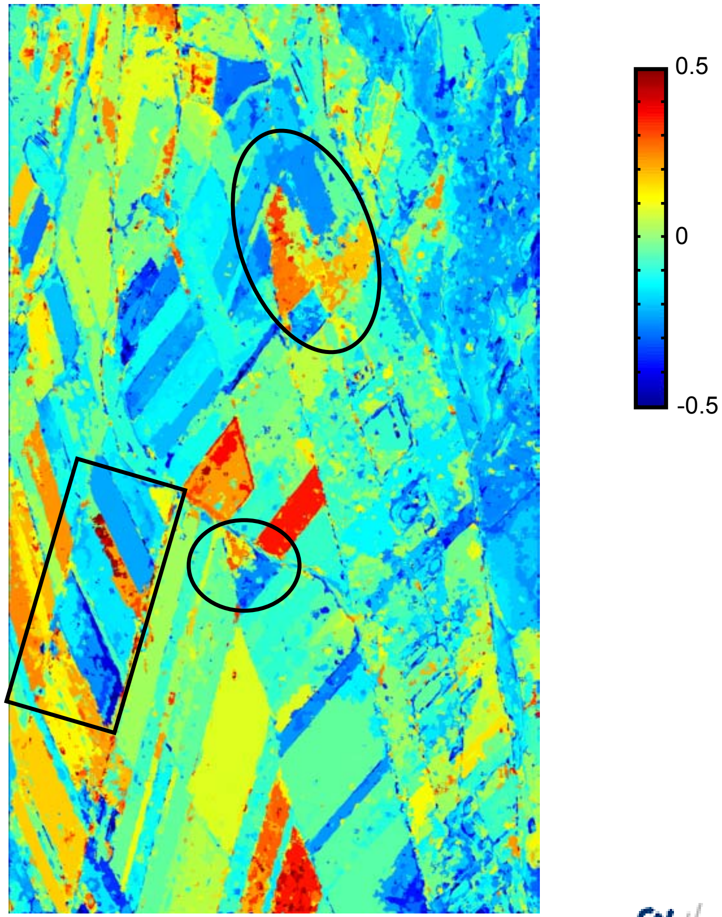

better field / surface separation

QUANTITATIVE ANALYSIS

LAND – AGRICULTURE APPLICATIONS

Ground truth measurements **Retrieved dielectric constant**

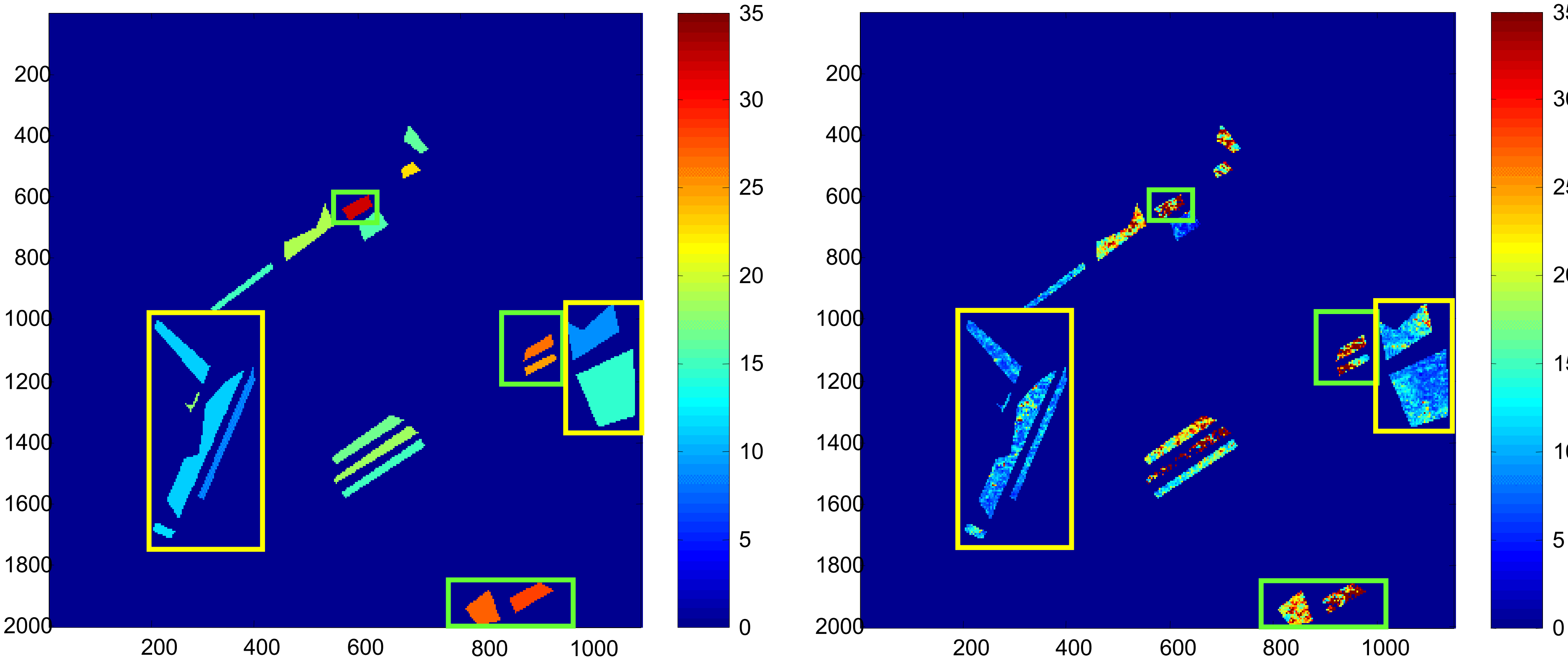

High ε values **Low ε values**

Good agreement between ground truth and estimated moisture

QUANTITATIVE ANALYSIS

ALLING - ESAR L-band

1 : Seedbed winter cereals
2 : Seedbed winter cereals (80%,15 cm)
3 : Harrowed
4 : Harrowed
5 : Pasture, grassland (95%,10 cm)
6 : Seedbed winter cereals (30%,4 cm)
7 : Seedbed
8 : Seedbed winter cereals (30%)
9 : Harrowed
10 : Pasture, grassland

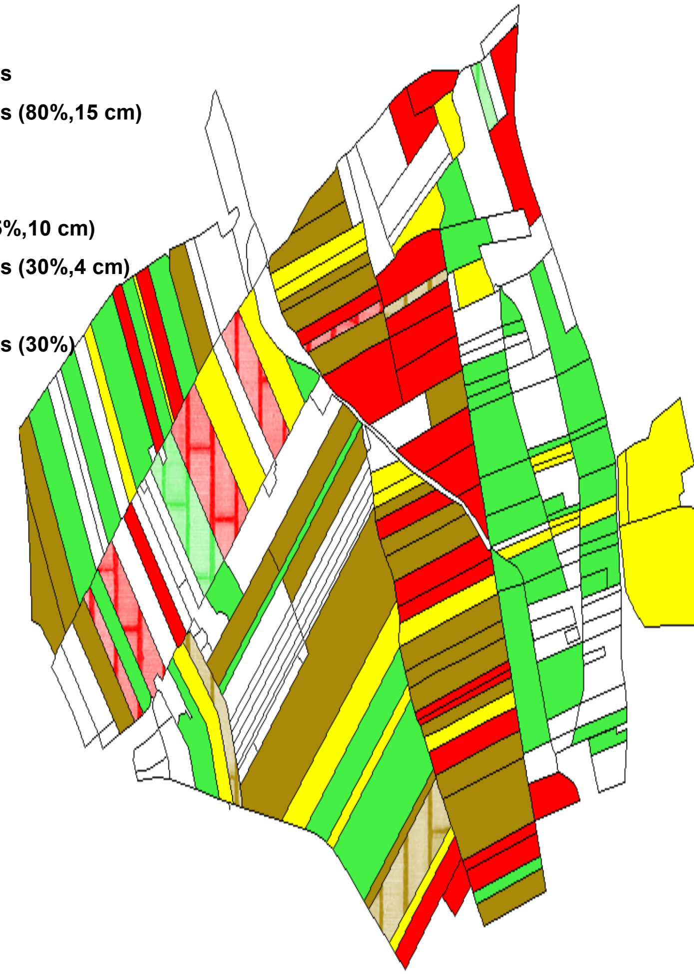

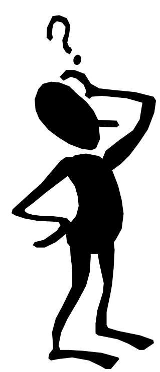

May I invert ?
Where can I invert ?

DLR QinetiQ

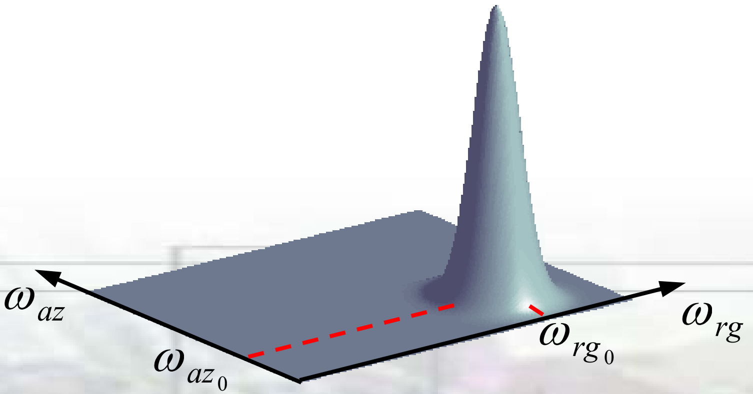

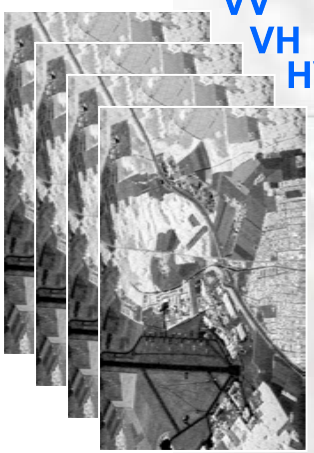

NON STATIONARY SCATTERING ANALYSIS

L. FERRO-FAMIL, A. REIGBER (2003)

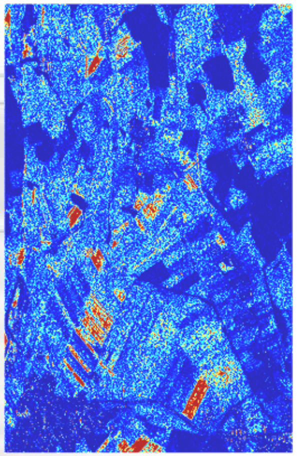

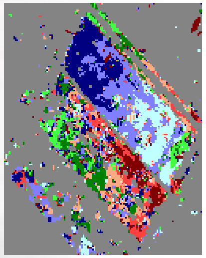

L. Ferro-Famil, A. Reigber, E. Pottier, W.M. Boerner"Scene Characterization Using Subaperture Polarimetric SAR Data" IEEE Transactions on Geoscience and Remote Sensing, Vol 41, n° 10, October 2003.

QUALITATIVE ANALYSIS

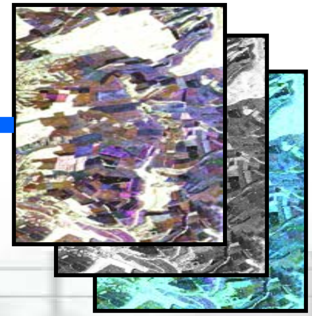

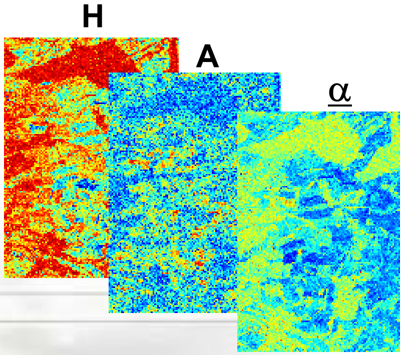

SUB-APERTURE POLSAR DATA ANALYSIS → SPECKLE FILTERING → POLARIMETRIC TARGET DECOMPOSITION

↓

WISHART POLARIMETRIC SEGMENTATION
MONO/DUAL FREQUENCY INTERFEROMETRY

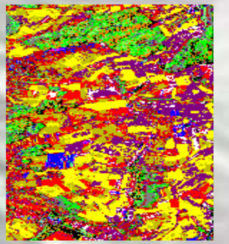

→ CLUSTER POLARIMETRIC IDENTIFICATION

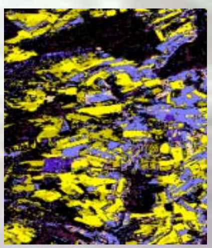

→ POLARIMETRIC DESCRIPTORS EXTRACTION

RANGE - AZIMUTH ANALYSIS

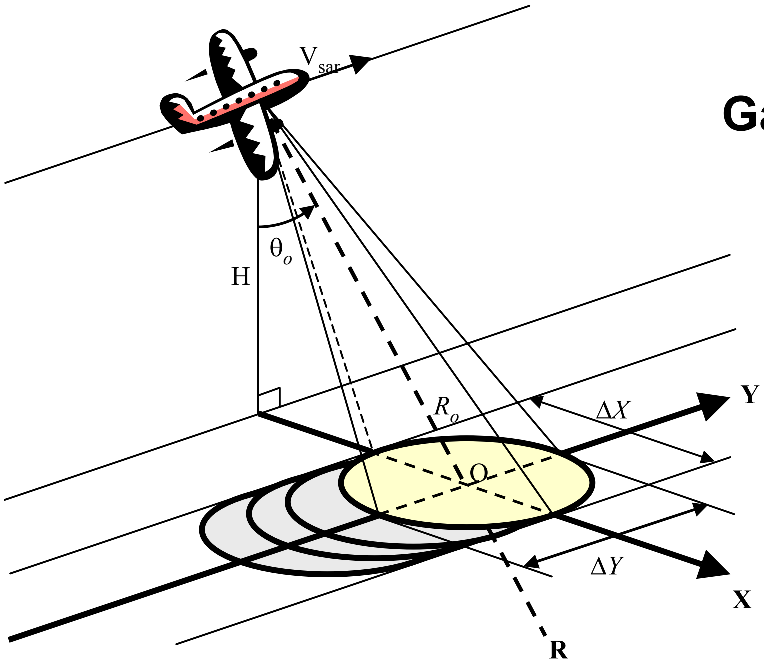

Gabor Transform

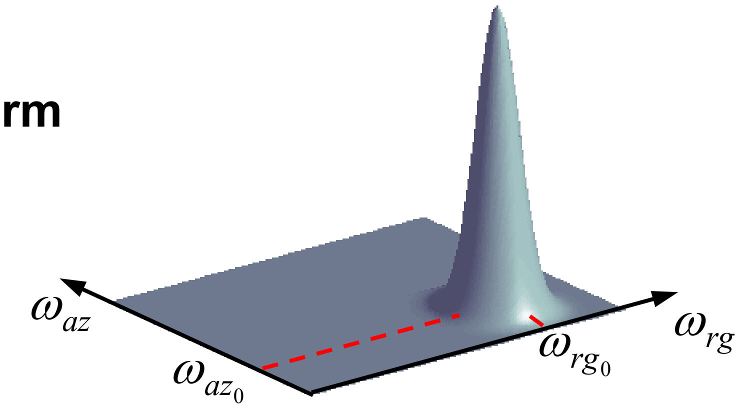

Range-Azimuth frequency domain

Azimuth

$$\omega_{az_0} = 2\omega_c \frac{V_{SAR}}{c} \sin\phi_0$$

$d_{SAR}(\mathbf{l}, \omega_{az}) \Rightarrow$ **Anisotropic Scattering Behavior**

Range

$$\omega_{rg_0} \in \left[\omega_c - \frac{B_\omega}{2}, \omega_c + \frac{B_\omega}{2}\right]$$

$d_{SAR}(\mathbf{l}, \omega_{rg}) \Rightarrow$ **Frequency Sensitivity**

AZIMUTH ANALYSIS

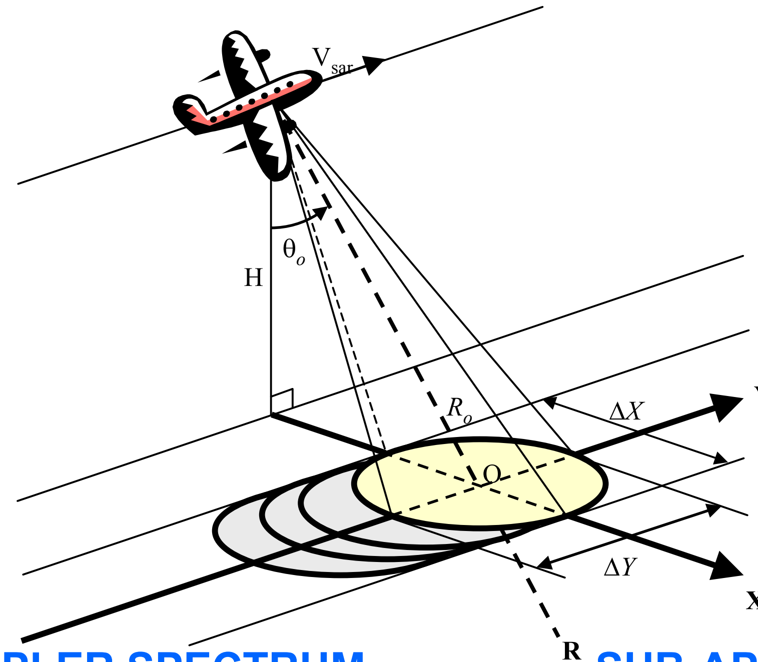

AZIMUT AVERAGE DOPPLER SPECTRUM

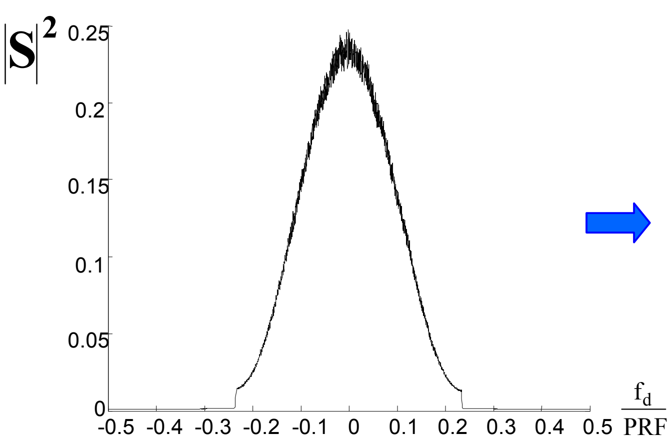

Side-lobes weighting / Antenna pattern

Amplitude correction

SUB-APERTURE DECOMPOSITION

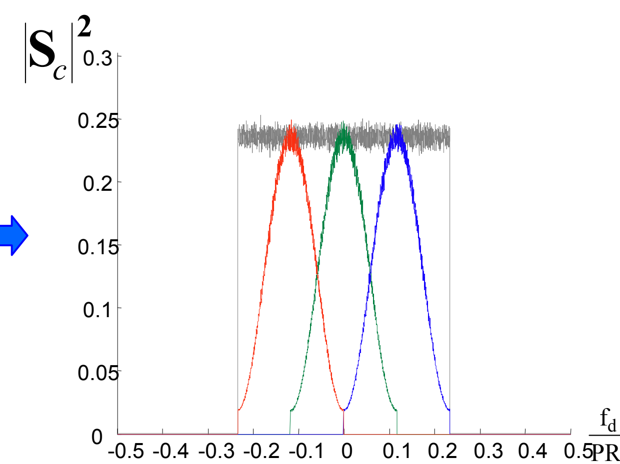

- Reduced azimuth resolution

- Varying center look angle ϕ_d

© E. Pottier, L. Ferro-Famil (01/2005)

AZIMUTH ANALYSIS

Pauli basis

$$|S_{HH} + S_{VV}|^2$$

$$|S_{HH} - S_{VV}|^2$$

$$2|S_{HV}|^2$$

ALLING Site
DLR – ESAR
L-band

DLR

QinetiQ

Visualization of polarimetric variations

AZIMUTH ANALYSIS

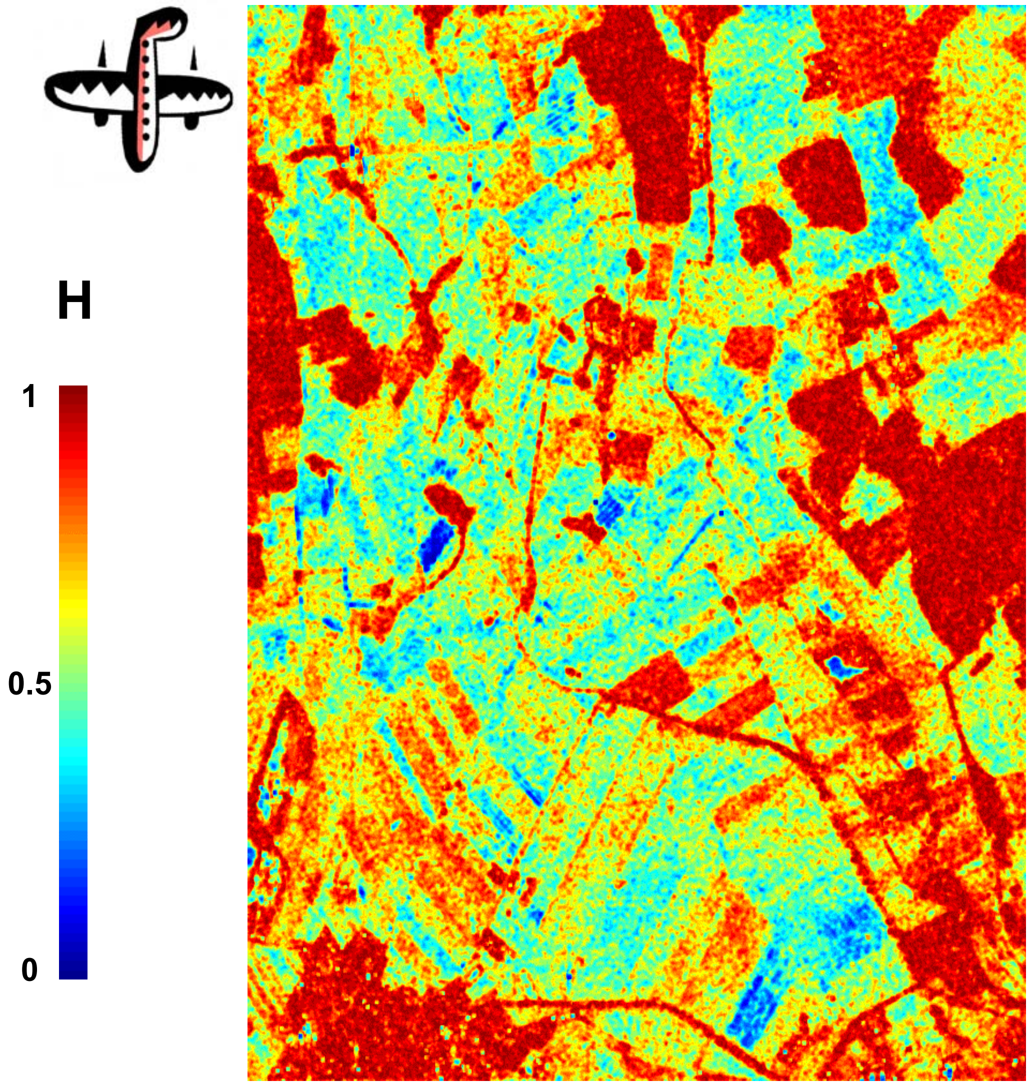

ALLING Site
DLR – ESAR
L-band

DLR

QinetiQ

Visualization of polarimetric variations

AZIMUTH ANALYSIS

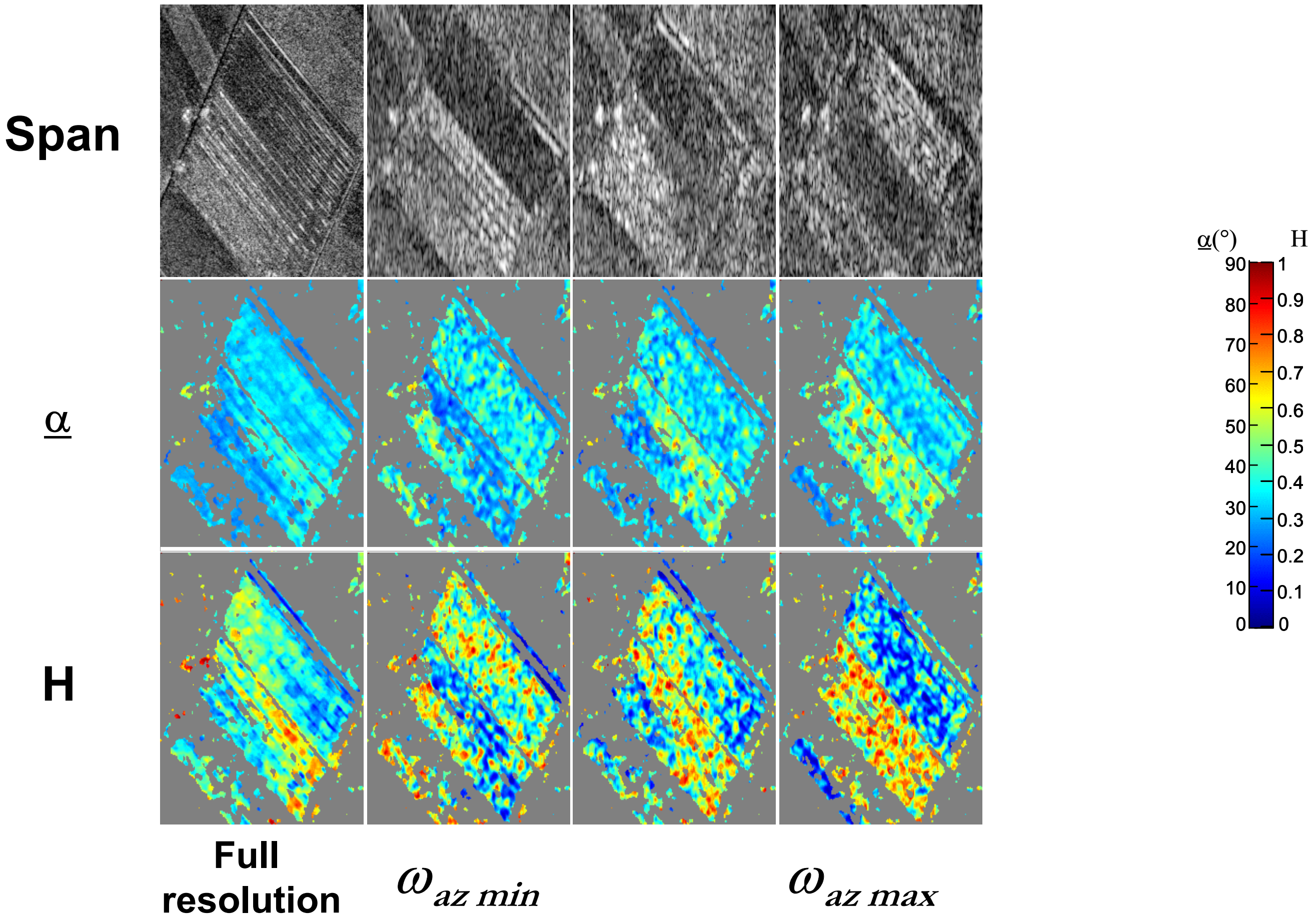

Polarimetric variations with the azimuth aspect angle, ϕ_d

Full resolution parameters are affected

Resonant surface backscattering

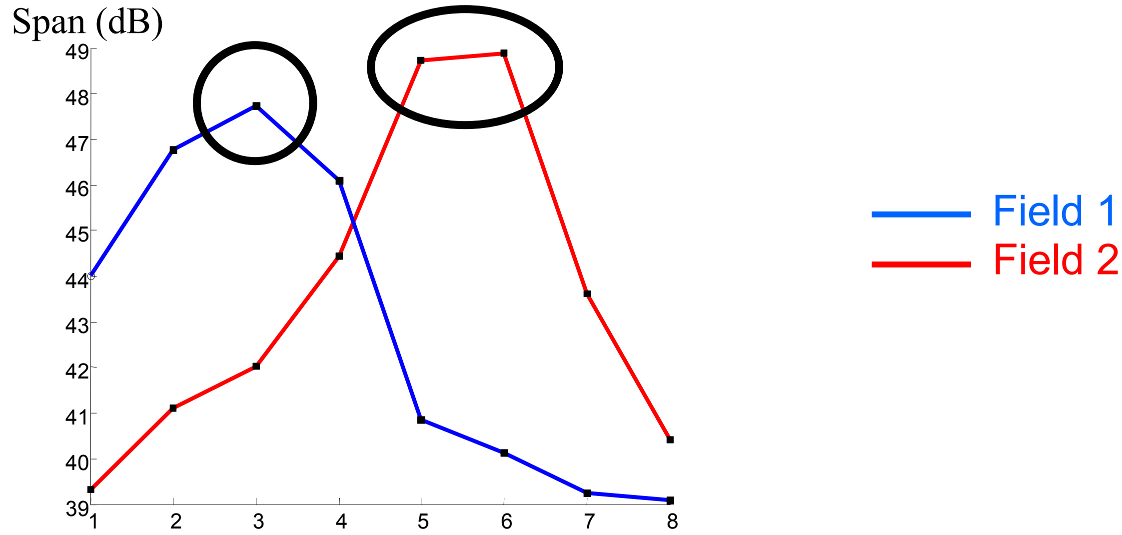

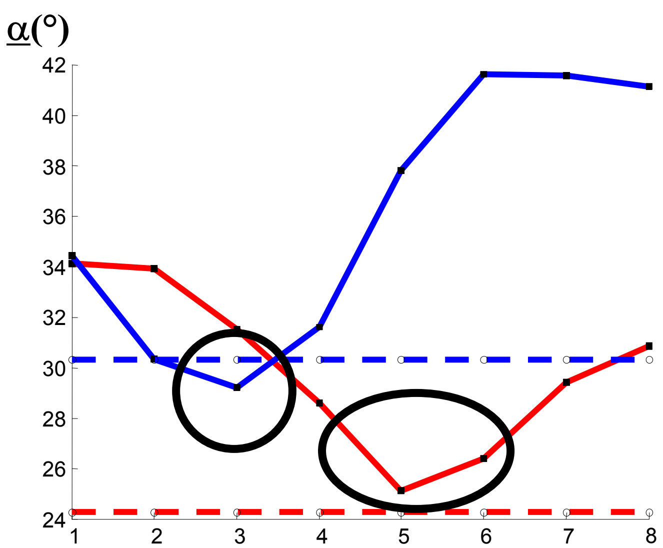

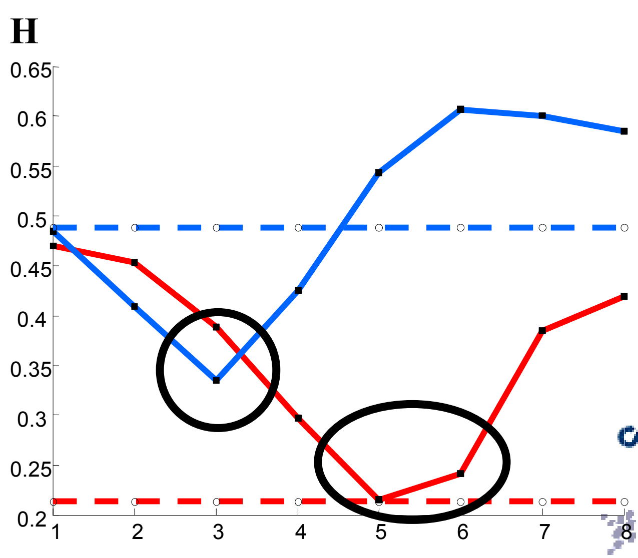

RANGE - AZIMUTH ANALYSIS

Span

$\omega_{az\,\min}$

$\omega_{az\,\max}$

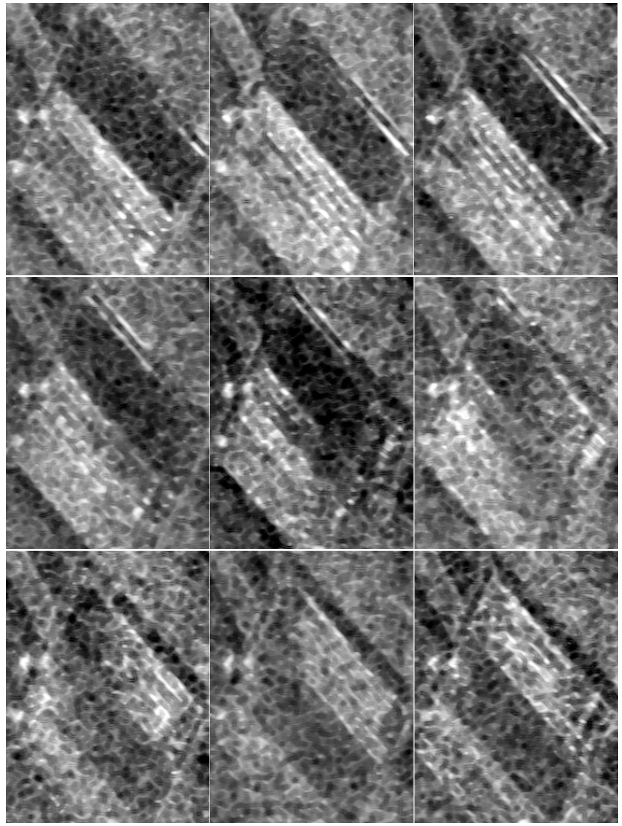

$\omega_{rg\,\min}$ $\omega_{rg\,\max}$

H

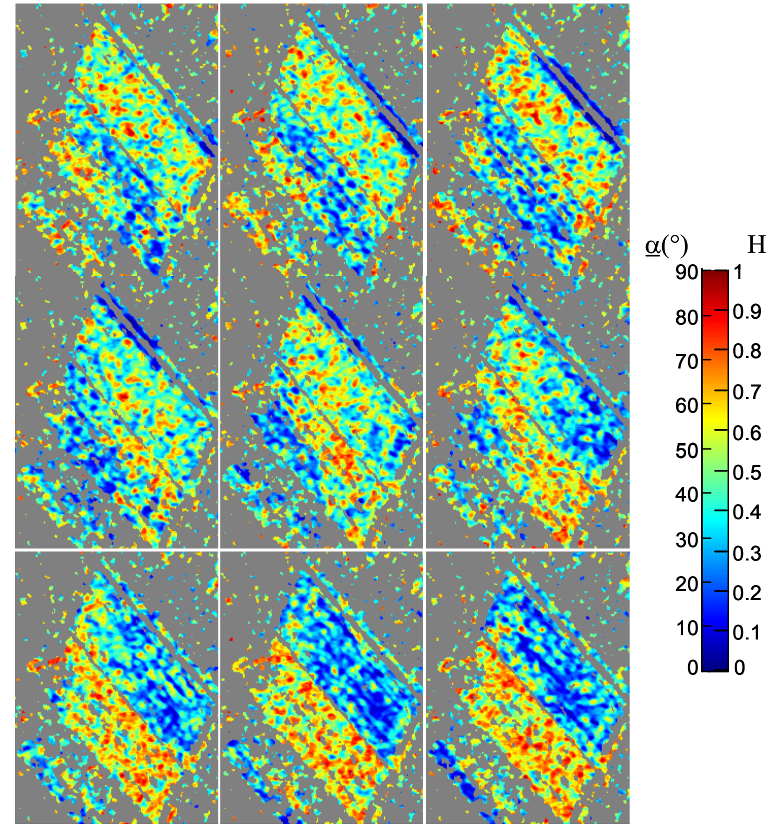

$\omega_{rg\,\min}$ $\omega_{rg\,\max}$

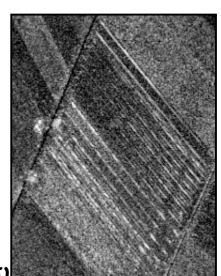

Full resolution

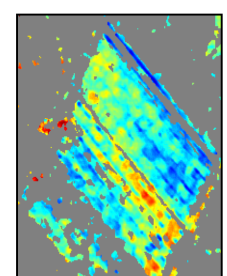

AZIMUTH ANALYSIS

Non-stationary media discrimination

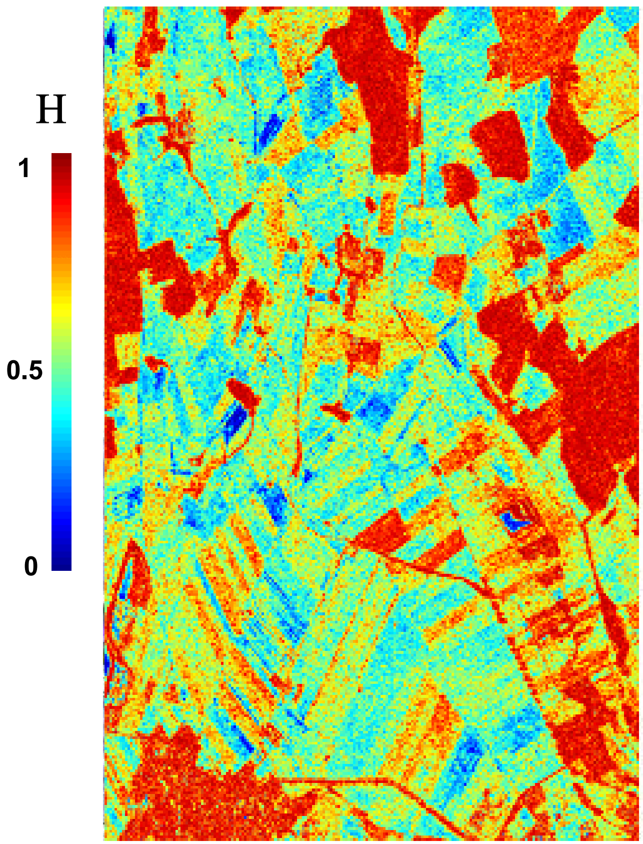

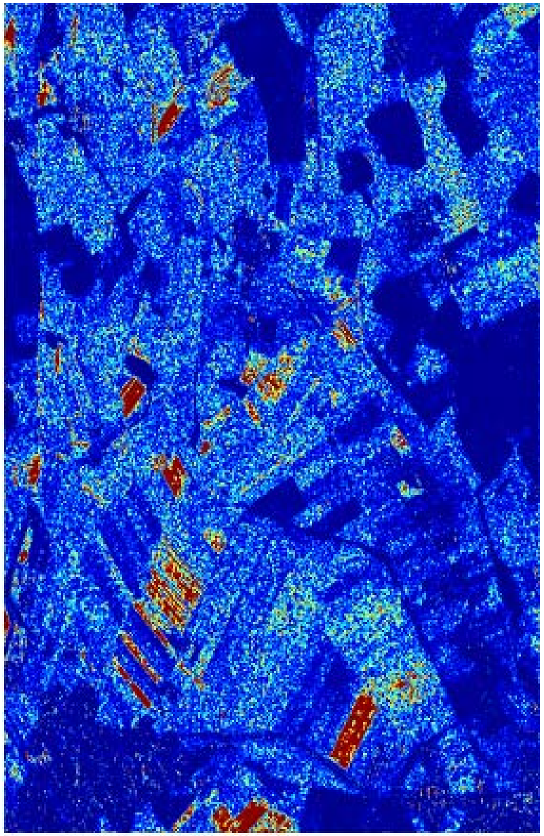

CV(H)

POLINSAR - AZIMUTH ANALYSIS

Full resolution

$|\gamma_{opt1}|$

$|\gamma_{opt2}|$

$|\gamma_{opt3}|$

Azimuth analysis

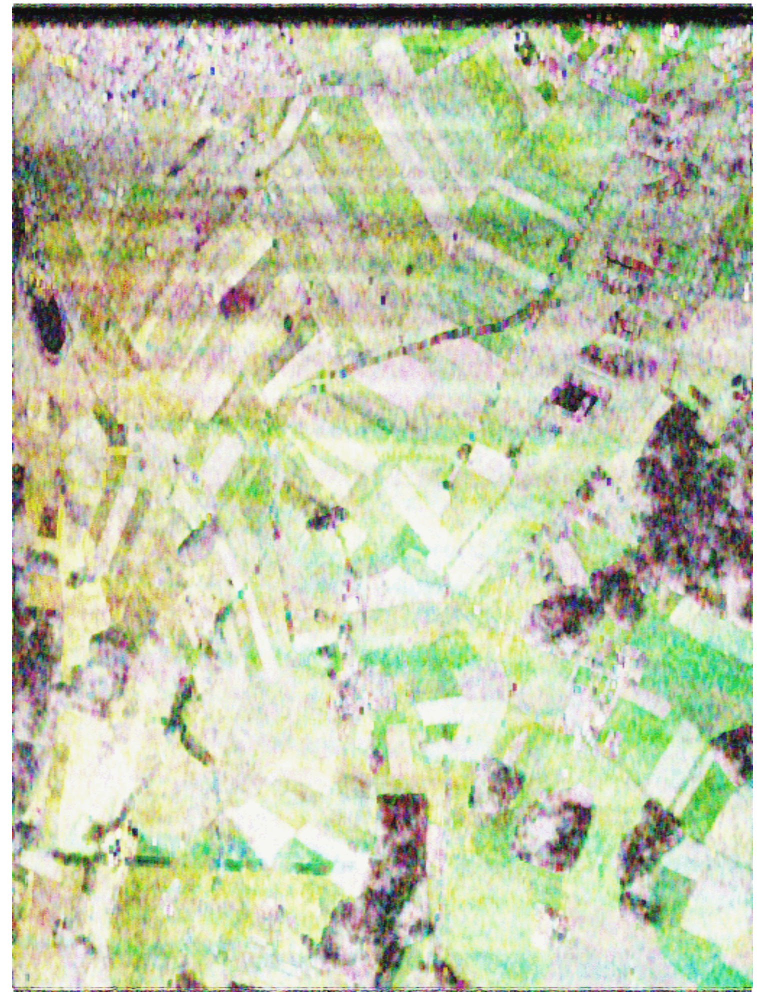

Interferences & residual motion compensation errors

Stronger perturbating effects in sub-spectra

© E. Pottier, L. Ferro-Famil (01/2005)

DATA INVERSION - APPROACH

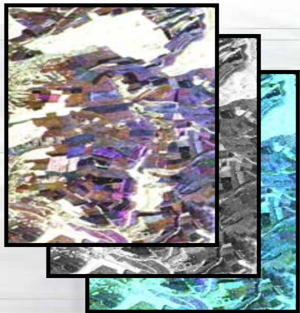

POLARIMETRIC
SAR DATA SET(S)

POLSAR - POLINSAR
DATA
PROCESSING

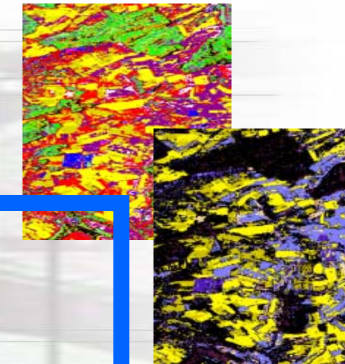

QUALITATIVE ANALYSIS

POLARIMETRIC
DESCRIPTORS
EXTRACTION

TWO-STEP INVERSION PROCEDURE

MODEL-BASED
PHYSICAL PARAMETER
INVERSION

BIO and GEO PHYSICAL
PARAMETERS

QUANTITATIVE ANALYSIS

© E. Pottier, L. Ferro-Famil (01/2005)

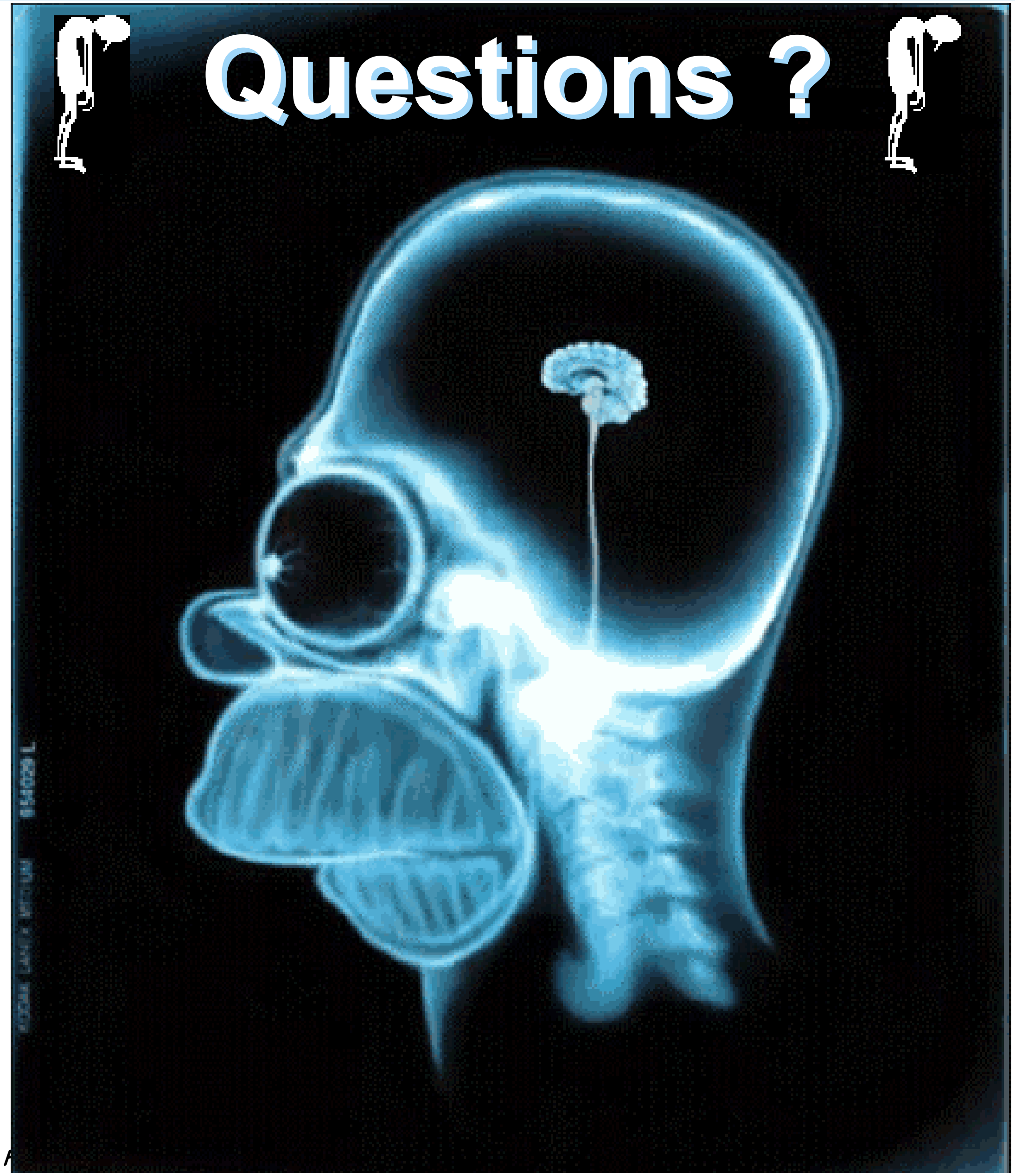
Questions ?